8-2020

The Role of Carbonate Minerals in Arsenic Mobility in a Shallow Aquifer Influenced by a Seasonally Fluctuating Groundwater Table

Jeremy Jensen
Utah State University

THE ROLE OF CARBONATE MINERALS IN ARSENIC MOBILITY IN A SHALLOW AQUIFER INFLUENCED BY A SEASONALLY FLUCTUATING GROUNDWATER TABLE

by

Jeremy Jensen

A thesis submitted in partial fulfillment
of the requirements for the degree

of

MASTER OF SCIENCE

in

Civil and Environmental Engineering

Approved:

_____	_____
Joan E. McLean, M.S. Major Professor	Laurie S. McNeill, Ph.D. Committee Member
_____	_____
R. Ryan Dupont, Ph.D. Committee Member	Richard S. Inouye, Ph.D. Vice Provost for Graduate Studies

UTAH STATE UNIVERSITY
Logan, Utah

2020

ABSTRACT

THE ROLE OF CARBONATE MINERALS IN ARSENIC MOBILITY IN A SHALLOW AQUIFER INFLUENCED BY A SEASONALLY FLUCTUATING GROUNDWATER TABLE

by

Jeremy Jensen, Master of Science

Utah State University, 2020

Major Professor: Joan E. McLean
Department: Civil and Environmental Engineering

Arsenic (As) threatens human health through contaminated groundwater used as drinking water. Groundwater in the Cache Valley Basin, Utah, USA, has elevated As concentrations; the source is geogenic. Soils in this semi-arid region have high carbonate concentrations. The influence of fluctuating groundwater on As solubility has been studied in Fe oxide rich sediments; the role of carbonate minerals in controlling As solubility has not been addressed.

Groundwater samples were collected from three monitoring wells located in the center of Cache Valley and analyzed for 2 years to track the effects of water level changes on As concentration and speciation. Laboratory columns were constructed using carbonate-rich soil and groundwater from the site. Biotic, abiotic, and carbon-enhanced treatments were subjected to alternating water levels and redox conditions. Columns were sacrificed at the end of each redox step and water and soil samples were analyzed to determine changes in geochemistry and associated As concentrations.

Arsenic concentrations in the field were influenced by fluctuating water levels. During a year with high precipitation (60cm), As levels were lower (27.8 ± 9.3 μg/L) compared to a year of low precipitation (36.8 ± 7.0 μg/L, 26cm). Arsenic groundwater concentration was not correlated with Fe or S, as expected if Fe and S minerals are controlling As solubility; other factors that influence As biogeochemistry, including carbonate minerals, were explored using laboratory columns.

Arsenic leached from laboratory columns yielded a cumulative mass in the aqueous phase of 73.5 ± 1.3 μg for biotic columns and 27.6 ± 0.9 μg for abiotic columns. The initial source of As in the leachate was from amorphous Fe and Mn oxides. As(III) continued to be released from these oxides, though the release was not influenced by Fe redox cycling; As behavior was independent of Fe as observed in the field study. Ligand exchangeable As was the consistent source (reducing conditions) and sink (oxidizing conditions) of As leached from the column. Arsenic concentrations associated with carbonate minerals remained constant for all redox conditions and cycles. Carbonate minerals provided a stable and secure sink for As unaffected by alternating redox conditions.

(156 pages)

PUBLIC ABSTRACT

THE ROLE OF CARBONATE MINERALS IN ARSENIC MOBILITY IN A SHALLOW AQUIFER INFLUENCED BY A SEASONALLY FLUCTUATING GROUNDWATER TABLE

Jeremy Carl Jensen

Arsenic (As) is a poison historically used to great effect before modern detection methods rendered it obsolete. However, the largest mass poisoning in human history occurred due to groundwater in the Bengal Basin contaminated by natural sources of As. Since that time, research has determined that As is found in groundwater worldwide. This includes aquifers located in basin-filled valleys of the western United States. One of these valleys is the Cache Valley Basin located in Northern Utah. This semi-arid region contains carbonate-rich soils and is heavily influenced by snowmelt and seasonal runoff. Previous studies have found that 15% of private wells in the valley have As concentrations above the USEPA Maximum Contamination Level (MCL) of 10 μg/L.

This study used groundwater samples collected over a 2-year period from three adjacent wells in the Cache Valley Basin, in conjunction with laboratory columns, to determine the effects of temporal and redox changes on As concentrations and associated carbonate minerals. Although it was determined that As concentrations fluctuated due to changes in water levels and seasonal runoff, column experiments determined that As associated with carbonate minerals remained constant. This indicates the potential for using carbonates as a means of preventing As contamination in groundwater.

ACKNOWLEDGMENTS

I would like to take a moment to thank all those who helped me to complete this thesis. Undertaking a project this large is not a one-man job and would not have been possible without everyone's help.

I would first like to thank Joan McLean, my advisor, employer, and major professor, for her help, support, insight, and review of my work from the day she asked me to take over this project through to the final completion of this paper. I would also like to thank my committee members, Dr. Laurie McNeill and Dr. Ryan Dupont for their help, reviews, and suggestions to make my experiments better. Additionally, I would like to thank those professors, including but not limited to Dr. Dennis Newell and Dr. Bill Doucette, whose classes gave me insight into problems that I was facing with my experiments and helped me appreciate the benefits of computer modeling.

Next, I would like to express my gratitude to the Utah Water Research Laboratory and the Utah Mineral Lease Fund for funding my research and providing all the instruments and services necessary to complete this project. I would also like to thank the many students who assisted with sample collection and analysis, including Dakota Sparks, Nikki Thornhill, Josh Hortin, Connor Tyson, Kaisa Patterson, and many more too numerous to list. Your help with the little things made this thesis possible.

I would like to thank my family for their support and encouragement. They have always been there for me through the good and bad times making it possible for me to come in day after day to work on this project. I couldn't have done this without your love

and support. Finally, I am grateful for my Faith which has given me strength beyond myself and inspiration when everything seemed impossible.

Jeremy Carl Jensen

CONTENTS

Page

LIST OF TABLES

Table Page

LIST OF FIGURES

Figure Page

Figure Page

Figure Page

CHAPTER 1

INTRODUCTION

Arsenic (As) is a known threat to human health through contaminated drinking water. Exposure at levels as low as 50 µg/L can cause keratosis, hypertension, and cardiovascular diseases. Arsenic is also a human carcinogen linked to skin, lung, and bladder cancers even at levels below 50 µg/L (Smith et al. 2002, Ng et al. 2003, Koutros et al. 2018). As a result, the United States Environmental Protection Agency (EPA) lowered its Maximum Contamination Level (MCL) for drinking water from 50 µg/L to 10 µg/L in 2001. Consumption of As-contaminated groundwater in the Bengal Basin, located in India and Bangladesh, resulted in the largest mass poisoning in human history. In total more than 40 million people were exposed to drinking water containing excessive As concentrations (Smedley and Kinniburgh 2002). As a result, sources and environmental conditions leading to As contamination in groundwater have been extensively studied in Southern Asia.

Arsenic contamination has also been discovered worldwide including in the Southwestern United States (Islam et al. 2004, Benner et al. 2008, Kocar et al. 2008, Larsen et al. 2008, Anning et al. 2012). The As contamination found in Southern Asia and the Southwestern United States was determined to be natural, resulting from the weathering of metamorphic and sedimentary As-bearing rocks. The studies also identified groundwater residence time and bio-geochemical characteristics as important influences on the occurrence, transport, and fate of As in the environment (Mandal and Suzuki 2002, Anning et al. 2012).

The emphasis of research efforts over several decades has been to identify the processes that lead to the release of As from mineral phases in the affected aquifers. Arsenic is found in the natural environment primarily as arsenate (As(V)) and arsenite (As(III)). Arsenic(V) will readily sorb to minerals like iron (Fe(III)) oxides. Arsenic(III) has been shown to have a lower affinity for sorption to minerals compared to As(V) (Ahmann et al. 1997, Ohtsuka et al.2013, Tufano et al. 2008) although the relative affinity of As(V) and As(III) sorption is mineral and pH dependent (Dixit and Hering 2003). Microbes are the primary catalysts for reduction of As(V) to As(III) as well as the reductive dissolution of host Fe(III) oxides. When microbes use As(V) or Fe(III) as electron acceptors, As(III) and As(V) (through dissolution of Fe(III) oxides) are released into the surrounding groundwater (Huang 2014); this is the primary mechanism for As contamination of groundwater identified in Southeast Asia.

In aquifers with low Fe oxide mineral concentrations, other processes may contribute to As retention and dissolution. Carbonate minerals have been found to host sorbed As(V) and structural As(III) at varying concentrations (Goldberg 2002, So et al. 2008, Bardelli et al. 2011, Costagliola et al. 2013). Studies of soil profiles in Northern Utah were found to contain a shallow (80 to 120 cm) layer with high carbonate concentrations. This layer was associated with the highest concentrations of labile As in the soil profile (Meng et al. 2017). These carbonated minerals may serve as the major sink/source for As retention/release in these systems (Meng et al. 2016). Smith et al. (2019) found that As(III) released during bioremediation under reduced conditions was naturally attenuated through association with carbonate minerals. Arsenic associated with

carbonates would be stable against changes in redox potential, unlike Fe(III) minerals, but would be susceptible to changes in wetting and drying patterns and changes in water quality components such as pH and concentrations of cations and anions. Batch studies of these high carbonate soils found that As was released to solution regardless of redox condition, indicating that dissolution/precipitation of carbonates may be the controlling factor for aqueous As concentrations in these aquifers (Abu-Ramaileh 2015, Meng et al. 2016).

Rising and lowering groundwater tables in shallow aquifers will alter redox potential and influence As solubility. Alternating water levels may also cause precipitation and dissolution of carbonates. In arid regions of the world, including the Southwestern United States, carbonate minerals are abundant in shallow aquifers and have been identified as deposits high in As concentration (Anning et al. 2012, Meng et al. 2017). The Cache Valley Basin, located in northern Utah, United States is a semi-arid region with high soil carbonate concentrations. Previous studies have identified As contamination in groundwater and associated soils in Cache Valley (Lowe et al. 2003, Abu-Ramaileh 2015, Meng et al. 2016, 2017).

Although the influence of fluctuating groundwater on altering redox conditions has been studied in Fe oxide rich sediments, the role of carbonate minerals in semi-arid regions has not been addressed. Dissolution and precipitation of carbonates resulting from a fluctuating water table may cause As to be sorbed/released in these aquifers while biological redox-sensitive processes may influence As species and mobility. The purpose of this study was to investigate how fluctuating groundwater levels alter the association

of As with carbonate minerals using a laboratory column study in association with real-time field observation.

CHAPTER 2

HYPOTHESIS AND OBJECTIVES

Hypothesis: Carbonate minerals located in a seasonally fluctuating water table retain and release As through dissolution and precipitation in conjunction with biological redox-sensitive processes, influencing As concentrations and mobility in a shallow subsurface aquifer.

The following objectives where used to test this hypothesis:

Objective 1: Determine the frequency of alternating wet-dry and oxidation-reduction (redox) cycles at a field study site using analysis of groundwater data indicative of dissolution/precipitation (Ca, Mg, bicarbonate, and pH) and redox conditions (Eh, DO, and Fe and As speciation) along with water level data at different temporal scales (annual, seasonal, and monthly).

Objective 2: Determine the effects of wet-dry and variable redox conditions within the carbonate enrichment zone on As mobilization and speciation using a laboratory column study. Columns were subjected to wet-dry cycles and sacrificed over time with analysis of pore water for carbonate dissolution and redox indicators (Eh, DO, and Fe and As speciation) along with sequential extraction of solids for As-mineral associations.

CHAPTER 3

LITERATURE REVIEW

3.1 Sources of Arsenic

Arsenic (As) is the 20th most abundant element in the earth's crust (Mandal and Suzuki 2002). Arsenic is commonly concentrated in sulfide-bearing mineral deposits including primary minerals arsenopyrite (FeAsS), realgar (AsS), and orpiment (As_2S_3) (Nordstrom 2002, Smedley and Kinniburgh 2002). Oxidation of these minerals forms secondary minerals such as arsenolite (As_4O_6), claudetite (As_2O_3), and pharmacosiderite ($Fe_3(AsO_4)_2(OH)_3$) (Smedley and Kinniburgh 2002). Weathering of these deposits allows for dissolution of As in rainwater, rivers, or groundwater (Mandal and Suzuki 2002).

Anthropogenic activities involving As can also contaminate water sources. These can include mineral extraction and processing wastes, poultry and swine feed additives, pesticides, and wood preservatives (Nordstrom 2002). Post-process leaching of As into soil from treated wood utility poles and fences has also been observed (Cao and Ma 2004).

Arsenic has been found in groundwater worldwide, with most of the sources of As being attributed to the native geology. Well known high-arsenic groundwater areas have been found in West Bengal (India), Bangladesh, and Vietnam. Other areas include Argentina, Chile, Mexico, China, Pakistan, and Hungary (Smedley and Kinniburgh 2002, Guo et al. 2003, Ali et al. 2019, Zhang et al. 2019). Anning et al. (2012) conducted research in the Southwestern United States and using statistical models predicted that

42.7 percent of basin-fill aquifers would equal or exceed the MCL of 10 µg/L for As concentration.

3.2 Arsenic Toxicity

Arsenic was one of the first chemicals recognized to cause cancer in humans. High rates of lung cancer in miners in Saxony were attributed to inhaled As in 1879. Years later, skin cancers and internal cancers were linked to As-contaminated drinking water in Argentina (Smith 2002). Arsenicosis, the effect of arsenic poisoning over long periods of time, has been reported in India, Bangladesh, China, Taiwan, Vietnam, and Nepal (Chen et al. 1999, Wang et al. 2018, Ahmad 2001, Berg et al. 2001, Guo et al. 2001, Ng 2003, Thakur et al. 2011).

The cancer risk of As at its previous MCL of 50 µg/L was more than 100 times greater than any other drinking water contaminant with an MCL (Table 1). Reports

Table 1. Carcinogens in Drinking Water, adapted from Smith (2002)

Chemical	**MCL (µg/L)**	**Lifetime Cancer risk at MCL per 100,000 people**
Arsenic	10 50 (old standard)	65.5 1300 (old standard)
Benzene	5	0.2-0.8
Carbon tetrachloride	5	1.9
Dichloromethane	5	0.1
Ethylene dibromide	0.05	12.5
Heptachlor	0.4	5.2
Hexachlorobenzene	1	4.6
Polychlorinated biphenyls (PCB's)	0.5	0.5
Pentachlorophenol	1	0.3
Vinyl chloride	2	8.4

indicate that cancer mortality risk can be as high as 1 in 100 for people drinking water containing 50 µg/L of As (Smith 2002). In response, the EPA lowered the drinking water standard from 50 µg/L to 10 µg/L on January 22, 2001 (USEPA 2017). Even at this lower standard, the cancer risk of As is 5 times greater than the next contaminant.

3.3 Arsenic Speciation

Arsenic exists in the environment in four oxidation states that are denoted -III, 0, +III, and +V. In groundwater, the most common inorganic forms are arsenite (As(III)) and arsenate (As(V)). The oxidation state is important due to As(III) being more toxic than As(V) (Lievremont et al. 2009, Sharma and Sohn 2009). In reducing conditions, As(III) will dominate while As(V) will dominate in oxidizing conditions. At normal environmental pH (5-9) the dominant species of As(III) will be H_3AsO_3, while As(V) species will be $HAsO_4^{2-}$ and $H_2AsO_4^-$. Redox potential (Eh) and pH are the most important factors affecting the speciation of As (Smedley and Kinniburgh 2002).

Arsenic can also exist in organic forms in the environment. These are usually due to anthropogenic sources such as pesticides and are associated with reducing conditions that favor the formation of methylated As species. However, Meng et al. (2016) conducted studies on biologically active, highly reducing condition microcosms using Cache Valley Basin soils. The reactors resulted in no detectable levels of organic As.

3.4 Abiotic Controls on Arsenic Behavior

The fate and behavior of As in the natural environment is dependent on multiple abiotic hydrogeological processes. However, the primary focus of this study was on sorption and co-precipitation due to their influence on As mineral association. Sorption is

an important process that removes arsenic from solution through interactions with mineral surfaces, but is reversible depending on environmental factors. Co-precipitation also removes arsenic from solution; however, the process is usually irreversible without physical or chemical destruction of the mineral precipitate. Both of these processes are influenced by pH and competition with other ligands in a system. In addition, sorption of As is further complicated by the occurrence of As(V) in reducing conditions and As(III) in oxidizing conditions. This results in natural systems that contain combinations of both species, implying that arsenic is rarely in thermodynamic equilibrium in nature (Cullen and Reimer 1989, Johnston et al. 2015).

The relative sorption of As species to various minerals over a range of pH values has been measured in multiple studies (Manning and Goldberg 1997, Jain et al. 1999, Goldberg 2002, Dixit and Hering 2003). In these various studies contrasting results have been reported due to different experimental conditions such as As concentrations, solution ionic strength, and sorbent mineral types and concentrations. Dixit and Hering (2003) studied sorption of various concentrations of As to amorphous iron oxide and found that generally As(V) sorption decreased with increasing pH while As(III) sorption peaked between pH 6 to 9. Additionally, Dixit and Hering (2003) reported a decrease in As sorption associated with increasing iron mineral crystallization. Goldberg (2002), using lower As concentrations, found that As(V) sorption to iron oxides decreased only above pH 7 while As(III) sorption was highest in the same range of pH 6 to 9 with only slight decreases at lower and higher values.

In addition to Fe minerals, As has been found to associate with clay minerals, aluminum hydroxides, manganese oxides, natural organic matter, and carbonate minerals (Manning and Goldberg 1996, O'Day 2006, Alexandratos et al. 2007, Bardelli et al. 2011, Yokoyama et al. 2012, Winkel et al. 2013, Simon et al. 2014, Catelani et al. 2018). Manning and Goldberg (1996) found that As(V) sorption to kaolinite peaks at pH 5.0, montmorillonite at pH 6.0, and illite at pH 6.5. Goldberg (2002) reported that, similar to findings with iron oxide, As(V) sorption to clays only decreases above pH 5 and to aluminum oxide above pH 9. Additionally, As(III) sorption to all materials peaked around pH 8.5. Winkel et al (2013) found that calcite was able to sequester at least 25% of naturally occurring aqueous As particularly when Fe concentrations were low. Alexandratos (2007) found that As(V) ions show a great affinity for calcite at pH 8.3. Other studies have found conflicting evidence of associations between As(III) and calcite with So et al. (2008) finding no sorption of As(III) to calcite and Yokoyama et al. (2009) finding a preference for As(V) over As(III) in calcite while other studies concluded As(III) has a higher affinity to calcite than As(V) (Roman-Ross et al. 2006, Bardelli et al. 2011, Catelani et al. 2018).

Certain compounds will also compete with As for sorption sites on soil minerals. In addition to competition between As(V) and As(III), studies have observed competition from phosphate, bicarbonate, and dissolved organic matter (Kim et al. 2000, Goldberg 2002, Kinniburgh 2002, Dixit and Hering 2003, Cao and Ma 2004, O'Day 2006, Smedley and So et al. 2008, 2012, Bardelli et al. 2011, Gonzalez et al. 2012). Phosphate has been observed to be highly competitive for sorption sites on iron oxide and carbonate minerals,

likely due to the similar tetrahedron structures of the arsenate oxyanion (AsO_4^{3-}) and orthophosphate anion (PO_4^{3-}) (Dixit and Hering 2003, O'Day 2006, So et al. 2012). Dixit and Hering (2003) observed a general decrease in sorption to iron oxides for both forms of As in the presence of phosphate. Most notable was at pH 4.0 where As(III) sorption decreased from 75% to undetectable. So et al. (2012) found that phosphate strongly decreased the sorption of As(V) to calcite, but As(V) only moderately decreased the amount of phosphate sorption. Appelo et al. (2002) and So et al. (2008) found that increasing alkalinity decreased the sorption of As(V) to ferrihydrite, indicating that (bi)carbonates may also compete with As for sorption sites. Gonzalez et al. (2012) added marble sludge ($CaCO_3$), compost, and iron oxide amendments to metal-arsenic contaminated soil from sulfide-mine waste. They found that marble sludge decreased pore water concentrations of As compared to soil with no amendments. However, addition to soil of natural organic matter as compost or soil amended with the compost and marble sludge caused an increase in pore water As concentrations due to competitive sorption by the organic matter. In contrast, Cao and Ma (2004) studied uptake of As in carrots and lettuce using soil sampled from areas near chromated copper arsenate treated wood poles or fences. They found that the addition of biosolid compost significantly reduced As uptake while addition of phosphate fertilizer increased plant uptake suggesting sorption of As by the biosolid compost and competition between phosphate and As.

3.5 Biotic Control on Arsenic

Microorganisms have a significant influence on the environmental fate and transport of As, both directly and indirectly, and are considered the major driving force of the arsenic biogeochemical cycle. Microbial transformation of As, Fe, S, and Mn simultaneously affect the release and mobility of As in the natural environment (Huang 2014). These microbes can change the speciation of As through both reductive and oxidative processes. Chemoautotrophic arsenite-oxidizing bacteria (CAOs) and heterotrophic arsenite oxidizers (HAOs) oxidize As(III) to As(V) to gain energy. Dissimilatory arsenate-respiring prokaryotes (DARPs) utilize As for a terminal electron acceptor during respiration. This process reduces As(V) to As(III). Finally, other arsenate-resistant microbes (ARMs) reduce As(V) to As(III) as a means of coping with high As in their environment and do not gain energy from the process (Oremland 2003). A conserved functional gene, arrA, can be used to detect microbes that are capable of arsenate respiration (Malasarn et al. 2004, Mirza et al. 2014, 2017).

Metal-respiring bacteria (including DARPs) are able to reduce numerous compounds in addition to As(V), including iron oxides, manganese oxides, and sulfur compounds. Multiple studies have indicated that microbial dissolution of Fe oxides is the primary mechanism for As groundwater contamination in Southern Asia (Nordstrom 2002, Smedley and Kinniburgh 2002, Islam et al. 2004, O'Day 2006). Microbial reduction of amorphous iron oxides releases sorbed As into the groundwater. This As mobilization is compounded by the reduction of As(V) in solution to As(III). Other studies have observed a disassociation of these reactions with reduction of Fe and As

occurring at different times (Islam et al. 2004, Oremland and Stolz 2005, Huang 2014, Mirza et al. 2014, Abu-Ramaileh 2015, Meng et al. 2016).

Dissolved organic carbon (DOC) influences the reduction of As and associated minerals. Zhou et al. (2018) used stable carbon isotope ratios to determine the degradation of DOC to inorganic carbon and the link to As contamination in groundwater. In the study, high As concentrations corresponded to microbial degradation of DOC coupled with reduction of As and Fe oxides.

3.6 Wet-Dry Cycles and Precipitation/Dissolution

Groundwater is subject to level fluctuations from infiltration of precipitation and surface irrigation, lateral water flow, and groundwater withdrawls. These seasonal drawdowns and recharges potentially change groundwater quality (Schaefer et al. 2016). Seasonal groundwater table fluctuations create alternating redox cycles in the soil subsurface (Mackay et al. 2014, Schaefer et al. 2016). During wetting cycles, when groundwater tables rise, reducing conditions can occur when soil pores are filled with oxygen-depleted groundwater. Reducing conditions are further enhanced with increased levels of organic carbon. Microbes consume this carbon and deplete available oxygen through aerobic respiration. As groundwater levels recede, drying and oxidizing conditions will occur due to evacuated pore spaces, plant evapotranspiration, and possible influence from oxygen saturated surface water (Schaefer et al. 2016). When a groundwater system is not in a steady state hydrologically, As concentrations can be expected to change over time (Fendorf et al. 2010).

Groundwater changes are further influenced by regional irrigation practices. Large-scale agricultural irrigation pumping from groundwater lowers the water table below natural drying cycle levels. High groundwater pumping can also substantially alter natural flow patterns. This can cause low As zones to be vulnerable to invasion from high As zones. Shallow, low As zones are particularly vulnerable to this type of As invasion (Fendorf et al. 2010).

Fluctuations in groundwater can also indirectly influence As mobility through redox and precipitation/dissolution processes. Reductive dissolution of Fe oxides and direct reduction of sorbed As(V) can release As into solution (Polizzotto 2005, Meng et al. 2016). In addition, fluctuation of the water table causes formation and dissolution of carbonate minerals. Precipitation and dissolution of carbonates is not directly related to redox conditions; instead it is influenced by pH, partial pressure of CO_2, alkalinity, temperature, and solution ionic strength (Morse and Arvidson 2002, Boggs 2009, 2012). Precipitation and dissolution kinetics of carbonates are further complicated by diffusion and surface controlling processes as well as environmental changes in pH and CO_2 from plant root or microbial activity (Morse and Arvidson 2002).

3.7 Carbonates and Arsenic

The molecular structures of As species appear to influence sorption to carbonates. However, different studies have produced varying results (Goldberg 2002, So et al. 2008, Bardelli et al. 2011, Costagliola et al. 2013). So et al. (2008) found that As(V) rapidly sorbed onto and desorbed from calcite, but that little to no As(III) associated with calcite. However, Bardelli et al. (2011) found that As(III) substitutes for carbonate more readily

than As(V) in calcite lattices. This discrepancy was attributed to the molecular structure of As(III) that allows it to substitute for the planar carbonate molecule. Costagliola (2013) found natural calcite travertines containing As in amounts two orders of magnitude higher than normal crustal abundances. The study also identified As(III) associated with the calcite lattice, but concluded that As uptake mostly occurred in the As(V) form.

Arsenic association with calcite may not be due to only molecular structure. Hafeznezami et al. (2017) studied the effects of pH, Ca, and Fe levels on As(V) sorption to sediment particles. A consistent increase in adsorption capacity (26-37%) was observed with the addition of Ca. This increase was attributed to the increase in surface positive charges due to surface accumulation of Ca^{2+} ions on the sediment particles serving as a cation bridge for As sorption.

Soil depth appears to influence carbonates and associated As concentrations. Studies have found that high carbonate areas in soils tend to be concentrated in small horizontal profiles at a relatively shallow depth (Dietrich et al. 2016, Meng et al. 2017). Dietrich et al. (2016) studied As occurrence in carbonate-rich soils that also contained significant concentrations of crystalline iron oxyhydroxides. While the majority of As found was associated with silicates and the iron oxyhydroxides, the next significant amount of As was associated with carbonate-rich soils found at depths between 80-120 cm. Meng et al. (2017) studied soils in the Cache Valley that were also carbonate-rich, but contained significantly lower concentrations of iron oxyhydroxides. This study found

that the largest concentrations of As were associated with the carbonate-rich soils also found at a depth of 80-120 cm.

CHAPTER 4

STUDY BACKGROUND

4.1 Study Site

The site used in this study is located in the center of the Cache Valley Basin, an area with abundant carbonate minerals, known As contamination, and previous groundwater monitoring locations. The Cache Valley is an area of approximately 1710 km^2 located in Northern Utah and Southeast Idaho. It is a roughly oval shaped valley approximately 80 km long, north to south, and 24 km wide, east to west, at its widest point. The valley is bounded by the Bear River Range to the east and the Wellsville, Malad, and Bannock Ranges to the west (Inkenbrandt 2010, Meng 2016).

Tertiary rocks of the area consist of the Eocene Wasatch Formation and the Miocene-Pliocene Salt Lake Formation (Evans and Oaks 1996). Quaternary unconsolidated lacustrine and fluvial deposits (Alpine, Bonneville, and Provo Formations) overlay the Tertiary formations in the Cache Valley Basin. These deposits are associated with lake cycles within the Cache Valley Basin. Lake Bonneville filled the valley from about 30,000 to 16,400 years ago and was at an elevation of 1550 m above sea level for about 500 years. A catastrophic failure at Red Rock Pass, Idaho caused Lake Bonneville to retreat from Cache Valley about 14,000 years ago (Evans and Oaks 1996). The source of As in the lower elevations of the Cache Valley may be associated with weathering of the Salt Lake Formations (conglomerates, sandstone, siltstone, and limestone) that are exposed at high elevations in the Bear River and Wellsville Ranges as well as along the margins of the valley (Meng 2016).

The soils and rocks of Cache Valley have abundant levels of carbonate. The Salt Lake Formation has conglomerate layers ranging from 44% to 68% Paleozoic carbonates and chert with various persistent limestone layers (Smith et al. 1997). The high levels of carbonate, combined with relatively low iron levels in the soil, create a unique study area in the Cache Valley that is different from previously mentioned study areas in Asia or even other regions of the Southwestern United States.

A network of wells was installed to monitor leachate from the Logan City Landfill located near the center of the Cache Valley Basin (Fig. 1). An additional series of piezometers was installed to the north and east of the landfill in July 2009 as part of a study to evaluate sources of As observed in the monitoring wells. The site used in this study is one of 13 wells that were installed at the time and is labeled as New Piezometer 13 (NP13) (Meng et al. 2016). NP13 is located northeast of the Logan City Landfill, directly north of Logan City's firefighter training facility (41°44'03 N and 111°52'22 W) (Fig. 1). The surrounding site is an open area covered with native field grasses and is used by the training facility for storage/disposal of concrete slabs and non-toxic construction materials.

4.2 Previous Work

A survey of private domestic wells in Cache Valley found that 23 of the 157 wells tested (15%) had As concentrations greater than the MCL (Lowe et al. 2003, Meng et al. 2016). Building on this survey, both Abu-Ramaileh (2015) and Meng et al. (2016, 2017) performed studies on groundwater and soil cores collected from the previously mentioned study site.

Fig. 1. Cache Valley, Utah, location map adapted from Sanderson and Lowe (2002) and Meng et al. (2017). Red pin indicates the location of piezometer NP-13

Meng et al. (2017) collected core samples using a direct push technique until 1.5 m of low chroma, bluish/greenish sediment was obtained (indicating permanent reducing conditions). Near well NP13 the total depth averaged 4.6 m. Cores were sectioned at the Utah Water Research Lab (UWRL) according to observations of duplicate cores made in the field. These soil profiles were then classified into four zones: vadose, carbonate

enrichment, redox transition, and depletion. Concentrations of selected solutes from water extracts were measured and compared to these zones (Fig. 2). Water extractable As concentrations peaked in the carbonate enrichment zone. In addition, Na, Cl, bicarbonates, and sulfates were concentrated in the vadose zone near the top of the soil profile while phosphates were relatively low through the vadose and carbonate enrichment zones before increasing in the lower redox transition zone and depletion zone.

A seven-step chemical extraction procedure adapted from Huang and Kretzschmar (2010), Keon et al. (2001), and Amacher (1996) was performed on the core material to determine changes in As mineral association down the profile. The total As concentration associated with the NP13 core ranged between 3.8 to 15.9 mg/kg. These equaled or exceeded reported concentrations for sediments collected in Bangladesh, Cambodia, and Vietnam (Polizzotto et al. 2006, Rowland et al. 2008, Seddique et al. 2011, Meng 2017). Results from the sequential extractions showed the highest percentage of arsenic (60%) extracted in the first three steps was associated with the carbonate enrichment zone and only a slightly smaller percentage was associated with the redox transition zone (Fig. 3).

From this core study, Meng et al. (2017) concluded that As solubilization in the Cache Valley Basin involves a series of redox and non-redox processes occurring at different depths. A conceptual model was proposed wherein, below the vadose zone, As is associated with carbonate minerals in the carbonate enrichment zone and with Fe/Mn oxides in the redox transition zone. Further, it was proposed that these two zones are influenced by a seasonally rising and lowering water table. A lowering water table and

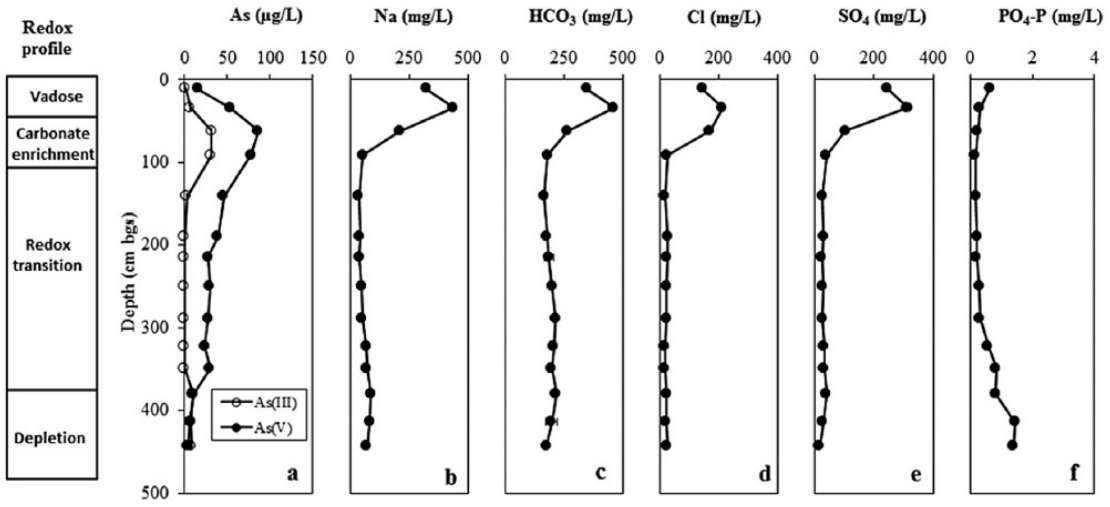

Fig. 2. Depth profile of the concentration of selected solutes in water extracts at NP13 with the redox profile on the left: (a) As speciation, (b) Na, (c) HCO_3, (d) Cl, (e) SO_4, (f) PO_4-P (Meng et al. 2017).

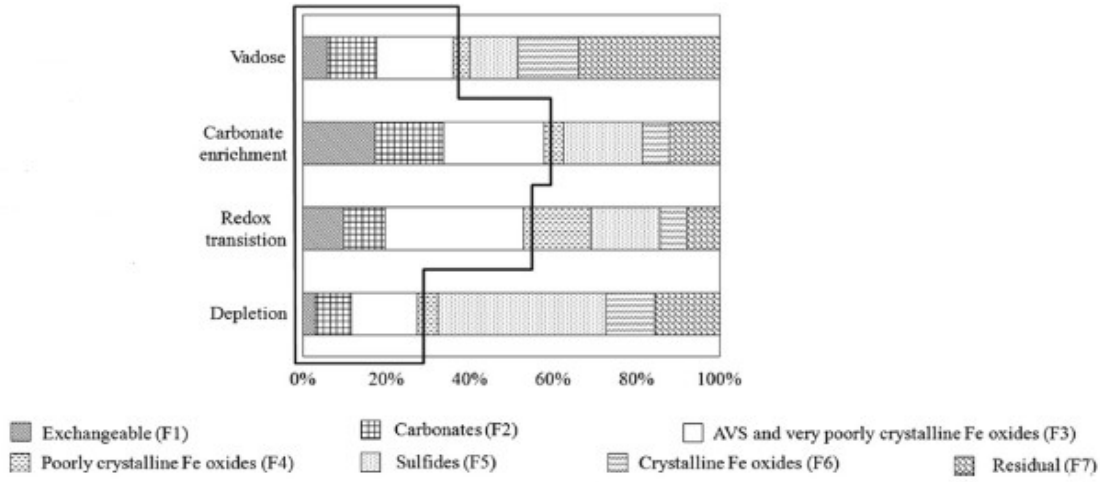

Fig. 3. Averaged percentage of As in each pool of the total As in NP13. The squared box indicates arsenic pools thought to be labile. Adapted from Meng et al. (2017).

evaporation causes the formation of carbonates as well as Fe(III) and Mn(III/IV) oxides that can sorb As species. A rising water table not only reduces these Fe and Mn

oxides releasing As, but also dissolves carbonate minerals releasing additional As into the groundwater.

In a related study, Meng et al. (2016) constructed microcosms using soils from the previously mentioned New Piezometer locations. The soil was saturated with groundwater from a well with general water quality properties similar to NP13, but with low background As concentrations. Microcosm treatments included groundwater, groundwater amended with glucose, and a control where the soil and groundwater were autoclaved to create an abiotic environment. The microcosms were placed in an anaerobic glove bag, then sacrificed at discrete time points over a 54-day period. The supernatant was decanted, filtered, and measured for aqueous As and Fe concentrations. The incubated solids were subjected to 0.5 M HCl extraction to determine As and Fe speciation. In addition, Day 0 and Day 54 samples were subjected to the same sequential extraction used for the previously mentioned field core studies (Meng et al. 2017).

The microcosm study (Meng et al. 2016) further supports this theory for dissolution of carbonate minerals releasing As into the groundwater. It was found that addition of groundwater to the sediments at Day 0 resulted in an immediate release of total As into solution equivalent in concentration to ionically (exchangeable) bound As defined by chemical extraction. It was theorized that this initial release of As was due to desorption of As or dissolution of As-containing non-Fe minerals, specifically carbonates. Carbon addition also dramatically increased the release of total As and As(III) supporting the previously mentioned link between redox and biological processes in the field core study.

Abu-Ramaileh (2015) investigated the effects of seasonally alternating redox conditions, due to fluctuating groundwater levels, on As mineralogy and mobility using NP13 soil in a microcosm study. Additionally, PHREEQC modeling using pore water chemistry reported by Meng et al. (2017) was used to predict precipitates, dissolved species, and Eh for each layer to understand which minerals affect arsenic release and retention. Finally, MINTEQ was used to model arsenic species distribution and sorption to Fe-oxides and $CaCO_3$.

In PHREEQC modeling, As(V) was not predicted to form any minerals throughout the soil profile of NP13. Additionally, As_2S_3 was predicted to be the controlling solid phase for As(III) solubility throughout most of the NP13 profile. Other important minerals predicted to form down the profile included calcite, dolomite, and various Fe and Mn oxides. MINTEQ predicted 59% and 19% of As(V) sorbed to calcite in the top two vadose zone layers. The proportion of As(V) associated with calcite decreased down the profile.

Further studies by Abu-Ramaileh (2015) consisted of laboratory microcosms using sediments from the layers located at the fluctuating water table elevation at NP13. The samples were inoculated with groundwater from a separate nearby monitoring well. Half of the samples were stored in an anaerobic, N_2 filled glove bag and flushed with N_2 filtered gas periodically to force reducing conditions while half of the samples were stored on a lab bench, flushed periodically with filtered ambient air to create oxidizing conditions. All samples were stored in a constant temperature room (16±1˚C) in the dark. Samples from each treatment were sacrificed at specific times and analyzed for As and Fe

redox species, major cations and anions, and trace elements. Control samples poisoned with mercuric chloride ($HgCl_2$) were also set up independent of the regular samples. However, due to material shortages, control sample sacrifices were only done twice during the experiment.

Abu-Ramaileh (2015) concluded that As release occurred under oxidized, reduced, and poisoned conditions. However, As reduction was biologically controlled as evidenced by the lack of As(III) in the poisoned samples. Abu-Ramaileh (2015) also concluded that, contrary to some literature, As solubilization/reduction and Fe reduction are decoupled and As(V) desorption from calcite is a major process controlling its release.

4.3 Focus of This Study

Previous studies (Abu-Ramaileh 2015, Meng et al. 2016, 2017) used microcosms to determine the importance of how the carbonate zone contributes to groundwater As chemistry. However, both these microcosms were only set up to compare these different conditions and did not directly study the effect of carbonate precipitation on As sorption, desorption, or mobility. Additionally, both studies used a small amount of soil compared to groundwater (10 g to 40 mL). Finally, neither of these studies focused on the effects of wetting and drying or redox cycles on soil mineralogy, As chemistry, and potentially related carbonate dissolution and precipitation.

The purpose of this study was to examine the influence of wetting and drying cycles and related reducing and oxidizing conditions on carbonate, As, and Fe species and behavior. This was conducted by simultaneous experiments with biotic, carbon-

supplemented biotic, and poisoned soil/groundwater columns. These columns allowed for wetting/drying and redox cycles that were not possible in the batch microcosms used by Abu-Ramaileh (2015) and Meng et al. (2016, 2017). To support laboratory findings, groundwater samples from NP13 were collected and tested approximately every 2 weeks over a 24-month period and used to determine initial experiment conditions and to compare with final experiment results. A 2-year groundwater monitoring scheme was used to capture annual and seasonal variations in water quality parameters due to variations in precipitation, groundwater levels, and time from drilling of wells. Monitoring for 2 years also allowed for comparison of these factors during similar time periods of different years.

Groundwater and column samples were analyzed for various parameters to determine redox conditions and dissolution of carbonate minerals. Redox parameters included dissolved oxygen (DO), electrical conductivity (EC), redox potential (Eh), and Fe(III)/Fe(II), As(V)/As(III), nitrite/nitrate, and sulfide/sulfate species. Parameters to determine dissolution of carbonate minerals included concentrations of Na, Ca, Mg, Mn, and bicarbonate ions as well as phosphate and dissolved organic carbon. All samples were also measured for pH.

CHAPTER 5

FIELD STUDY

5.1 Materials and Methods

Three piezometers (P-1, P-2, P-3) were installed on September 2, 2016 near NP13 and were used for collection of groundwater samples and monitoring of water levels (Fig.4). These piezometers were drilled to a depth of 5.1 m and screened for the top 3.5 m to provide a constant water column that facilitated sample collection and water level monitoring. A HOBO U20 Water Level Logger was placed in P-2 to collect real-time water level data throughout the study period.

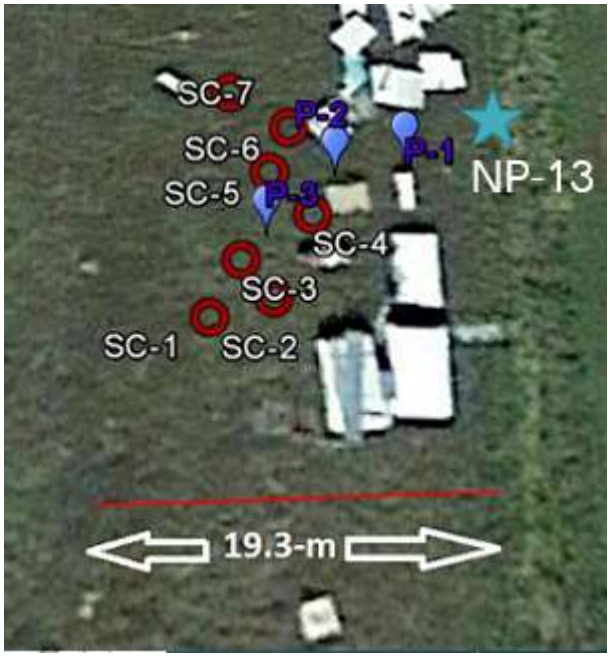

Fig. 4. Approximate locations of piezometers (P-1, P-2, P-3) and soil core samples (SC-1 to SC-7) relative to well NP13. Adapted from Kelsey Wagner (2017).

When each well was constructed, screening was installed to an approximate depth of 3.5 meters. This depth is greater than the estimated carbonate enrichment zone depth and reaches into the redox transition zone (Fig. 5). This may have caused samples taken when the water level was low to be influenced only by redox conditions and not high carbonate concentrations (Figure A-2). Samples collected at this time may have been in a more permanently reduced state and under less influence from precipitation and infiltration from surface water with high DO concentrations.

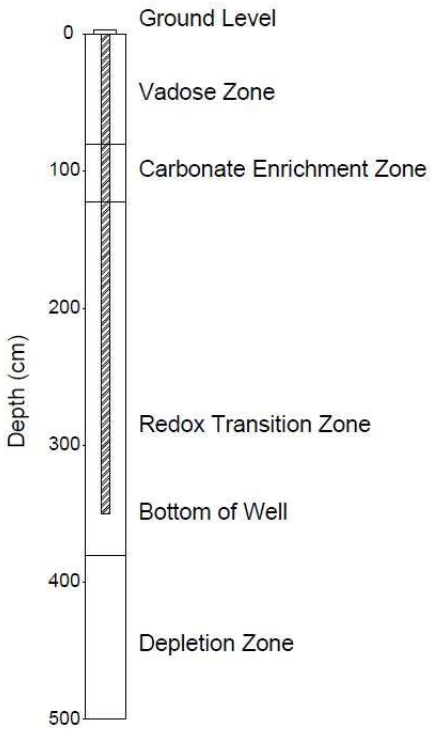

Fig. 5. Piezometer screening in relation to soil profiles.

Groundwater was collected and tested approximately every 2 weeks for 24 months. Groundwater was collected from all three piezometers due to statistically significant variations in each well. Water levels in P-2 were also continuously monitored using the HOBO U20 Water Level Logger to collect measurements every 10 minutes. Data downloaded from the Logger were corrected using average daily atmospheric pressure as measured by the Logan-Cache weather station (WU 2019). Additionally, any data collected when the logger was removed from the well, such as during sample collection or data downloading, were removed.

Groundwater properties measured included pH, EC, Eh, DO, As(V), As(III), Fe(III), Fe(II), sulfides, total alkalinity, major inorganic anions, major cations, and dissolved organic carbon (DOC). During collection, each well was pumped individually. Groundwater was allowed to flow through a plastic block holding probes from a portable Orion 5-star series meter in order to measure pH, EC, and DO. Water was also collected in a plastic cup holding a probe from a portable Corning 313 pH/Eh meter after flowing through the plastic block to measure Eh. Eh was measured against a saturated Ag/AgCl reference electrode and readings were corrected to standard hydrogen electrode using correction factors given in Striggow (2017). When all four measurements reached stable conditions, groundwater was collected. Groundwater was tested in the field for Fe(II) and sulfides using HACH field test kits and measured using a portable HACH DR 2800 spectrophotometer. Remaining samples were placed in a cooler and transported to the UWRL for testing of alkalinity, phosphates, DOC, anions, and cations (Table 2). Samples

not immediately tested at the UWRL were stored at 4˚ C and stabilized with acid as necessary.

Table 2. Groundwater testing methods and references

Groundwater Property	Method	MDL or MRL	Reference
pH	Gel-filled pH Electrode	N/A	Thermo Scientific 2007 Orion 5 Star Series Meter
EC	Conductivity Cell probe	N/A	Thermo Scientific 2007 Orion 5 Star Series Meter
Eh	Platinum tip Eh probe	N/A	Corning 313 pH meter
DO	RDO® Optical Dissolved Oxygen Sensor	1 mg/L	Thermo Scientific 2007 Orion 5 Star Series Meter
Alkalinity	Standard titration	10 mg $CaCO_3$/L	APHA et al. 2012 Method 2320
Phosphate	Ascorbic acid with Spectrophotometer	10 µg/L	APHA et al. 2012 Method 4500F
DOC	Standard combustion/IR	0.8 mg/L	APHA et al. 2012 Method 5310B
Anions (chloride, sulfate, nitrate, nitrate)	Ion chromatography (IC) Dionex ICS-3000	0.5 mg/L	Dionex Method 123
Major cations (Ca, Mg, Na, K) Trace elements (Fe, As, Mn)	Inductively Coupled Plasma Mass Spectrometry (ICP-MS) Agilent 7700x	Fe = 5.0 µg/L As = 0.25 µg/L	USEPA Method 6020
As(III)	Separation of As species using Dowex 1x8 anion exchange resin (100 mesh Bio-Rad) Analysis by ICP-MS	0.25 µg/L	Wilkie and Hering 1998
Fe(II)	1, 10 Phenanthroline with Spectrophotometer	200 µg/L	HACH Method 8146
Sulfides	USEPA Methylene Blue with Spectrophotometer	5 µg/L	HACH Method 8131

Arsenic species were separated in the field using columns packed with 2 g of Dowex 1x8, 100 mesh Bio-Rad anion exchange resin (Wilkie and Hering 1998). Filtered groundwater samples (20 mL) were acidified to pH 4 with H_2SO_4 before pouring into

resin columns. The first 5 mL filtered through the columns were discarded and the remaining amount collected for analysis. Collected samples were analyzed by ICP-MS to determine As(III) concentrations. As(V) concentrations were assumed to be the difference between total As and As(III) concentrations.

5.1.1 Quality Control

All analyses followed the standard EPA method for project quality assurance and control (USEPA SW-846). This included blanks, calibration curves, and matrix spikes. Various blank samples were used to determine any contamination from instruments, during sample collection, or from reagent materials as appropriate. Calibration curves were used to determine the correct range and response from specific instruments. Continuous calibration verification (CCV) samples were used to verify no drift in the instrumentation. Matrix spikes were used to indicate any interference within a particular method on instrument readings.

5.1.2 Geochemical Modeling

PHREEQC (USGS 2018) modeling was used to determine $CaCO_3$, $CaMgCO_3$, $MgCO_3$, and $MnCO_3$ saturation in groundwater samples. Additionally, As(III) concentrations were compared between modeling and sample measurements to determine if As was in thermodynamic equilibrium. Equilibrium for carbonate and As species was considered to be at a model generated Saturation Index value of 0 with an error of ±0.1 (Langmuir 1971). Stability constants in PHREEQC were from the Lawrence Livermore National Laboratory (llnl) database. Measured values included pH, alkalinity (as mg/L $CaCO_3$), major cations, and major anions. Temperature was measured in the field for

groundwater samples and assumed to equal the constant temperature room (16˚C) for column samples. Redox potential was calculated using Eh measurements for all samples. Total As concentration measurements were used to allow the modeling of As speciation. $CaCO_3$ saturation was assumed to equal calcite saturation in modeling output due to calcite being more thermodynamically favored to dissolve and precipitate compared to other forms of $CaCO_3$. Total dissolved Fe concentrations were used for PHREEQC modeling due to discrepancies in Fe(II) measurements.

5.1.3 Data and Statistical Analysis

Field measurements were made in triplicate except for those used to determine steady state conditions in the field (pH, EC, Eh, DO, and Temp). Data below the minimum detection limit (MDL) were imputed using regression on Rankits method (Berthouex and Brown 2002) using log-normal distribution of quantifiable data and assigning a value randomly based on an extrapolation of that log-normal distribution. The method was only applied if >60% of the data were reportable to define the distribution of known values. This was only necessary for field measurements of sulfides, Fe, and Fe(II). With the exception of pH and Eh, data were log transformed to achieve normal distributions prior to further statistical analysis.

JMP 8.0 statistical software by SAS was used for all statistical analyses. All data points were compared by one-way analysis of variance (ANOVA; independent factors were wells, seasons, and year) to determine variables influenced by these factors. Differences in means were determined by Student's t-test or Tukey's HSD as appropriate with $\alpha = 0.05$. Principle component analysis (PCA) was used to determine the underlying

relationships among parameters while a correlation matrix determined parameters correlated with each other and with As(III) and As. Positive correlation as defined by pairwise comparison by JMP (α=0.05) was expressed as $r>0.1$ and negative correlation was expressed as $r< -0.1$.

5.2 Results and Discussion

Groundwater collected from all three wells exceeded the MCL of 10 µg/L for As concentrations (Table 3, Fig. 6-A). Arsenic concentrations in Wells P-1 and P-3 were consistently above the MCL for the entirety of the study. Well P-2 contained the lowest average concentrations of total As (Table 3) and occasionally was below the standard during the first year of collection (Fig. 6-A). However, it still exceeded the MCL for a majority of sampling events and throughout the second year of the study. Arsenic concentrations in Well P-3 remained the most consistent throughout the study period with a range of 30.5 to 54.5 µg/L (Table 3). Well P-1 contained average As concentrations statistically the same as P-3 but with a wider range of 13.1 to 57.5 µg/L. Wells P-2 and P-3 contained significantly different average As(III) concentrations while P-1 was statistically the same as the other two wells (Fig. 6-B, Table 3). As(III) comprised 55% of As in P-2 compared to 30% in the other two wells.

Table 3. Distribution of As in groundwater samples by piezometer. Letters next to mean values represent statistical one-way ANOVA. Values not connected by same letter are significantly different (α=0.05) by Tukey's honestly significant difference

	Well P-1		Well P-2		Well P-3	
As (µg/L)						
Mean	36.3	a	21.6	b	39.7	a
Median	36.4		21.1		39.7	
Maximum	57.5		50.8		54.5	
Minimum	13.1		3.9		30.5	
SD (±)	9.2		11.8		6.2	
As(III) (µg/L)						
Mean	9.8	a,b	11.2	a	8.0	b
Median	7.5		7.9		6.3	
Maximum	26.8		42.2		26.7	
Minimum	0.4		0.7		0.3	
SD (±)	7.9		9.9		7.0	

5.2.1 Temporal Effects on Groundwater Levels and Associated Arsenic Concentrations

All three piezometers followed the same seasonal fluctuations in water levels (Fig. 7). Water levels were low during summer months when regional irrigation use is highest and precipitation is limited. Seasonal snowmelt and precipitation in winter and spring then replenished groundwater, increasing these water levels.

Two unique trends were observed in the groundwater levels. First, total yearly precipitation influenced groundwater levels, but infiltration from individual precipitation events did not have as significant of an impact (Fig. 7). Cache Valley has a typical semi-arid cold desert climate with the majority of precipitation occurring as snowfall in the winter and rain in the spring along with hot, dry summers. Therefore, aquifer recharge at the study site was influenced more by snowmelt and early spring runoff carried

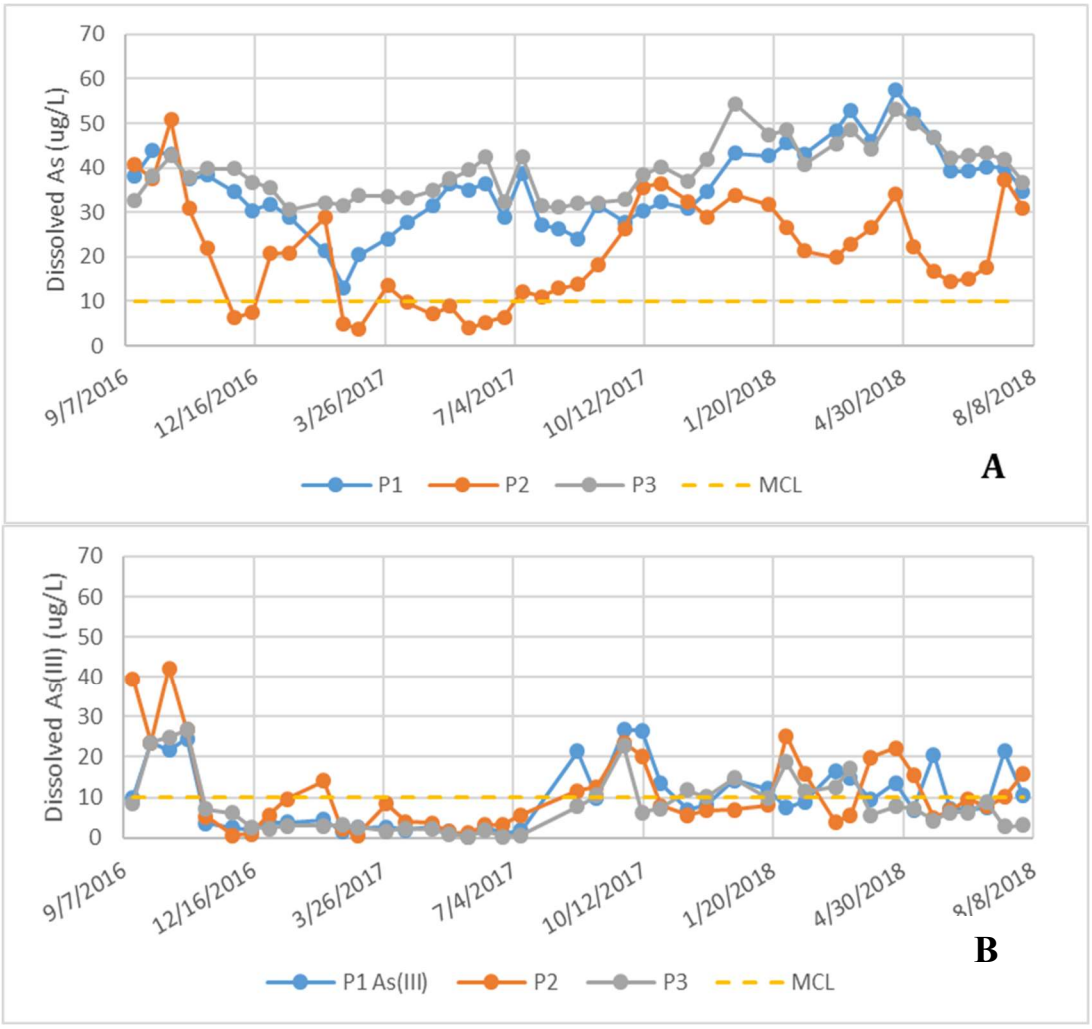

Fig. 6. Time series graph of As (A) and As(III) (B) concentration by piezometer. Yellow dashed line represents MCL of 10 µg/L.

from the surrounding mountains by the Logan River and other surface waters then by direct infiltration from local precipitation or non-seasonal fluctuation of nearby water bodies. Cache Valley receives an average of 47 cm of annual rainfall (USCD 2019). The first year of data collection (September 2016-August 2017) consisted of above average precipitation levels (60.4 cm) followed by a year (2017-2018) of low precipitation (26.3

cm) (WU 2019). This increased the time necessary for the wells to reach full saturation in winter 2018 compared to the previous year.

Second, irrigation practices only had an indirect impact on water levels. The study site was not directly irrigated and no water was pumped directly from the wells for irrigation purposes. However, yearly drawdown occurred in early spring to summer and a local high point was observed near the middle of October in each year that does not appear to be related to any precipitation event. The timing of these spikes correlates with the annual cessation of canal and irrigation water use in Cache Valley. Additionally, despite previously mentioned yearly precipitation amounts, groundwater levels were not as low in summer 2018 as those in summer 2017 and remained low in summer 2018 for a shorter period of time. One explanation for this discrepancy is the recent conversion of canal systems, located miles upstream from the study site, from open channel to a closed pipe system in the Cache Valley area that was finished in late 2017 (UPR 2013, CHWA 2014). This may have resulted in more water remaining in the Logan River that would have otherwise been lost in the canal system through evaporation or leakage.

Data from the U20 HOBO Water Level Logger, corrected for atmospheric pressure, in Well P-2 followed the same trends as data collected manually (Fig. A-1, A-2). Similar depth values and high and low peaks were observed. Additionally, due to the data logger remaining in the well until early November 2018, the same pattern was observed as the previous 2 years with a local high point occurring in the middle of October 2018.

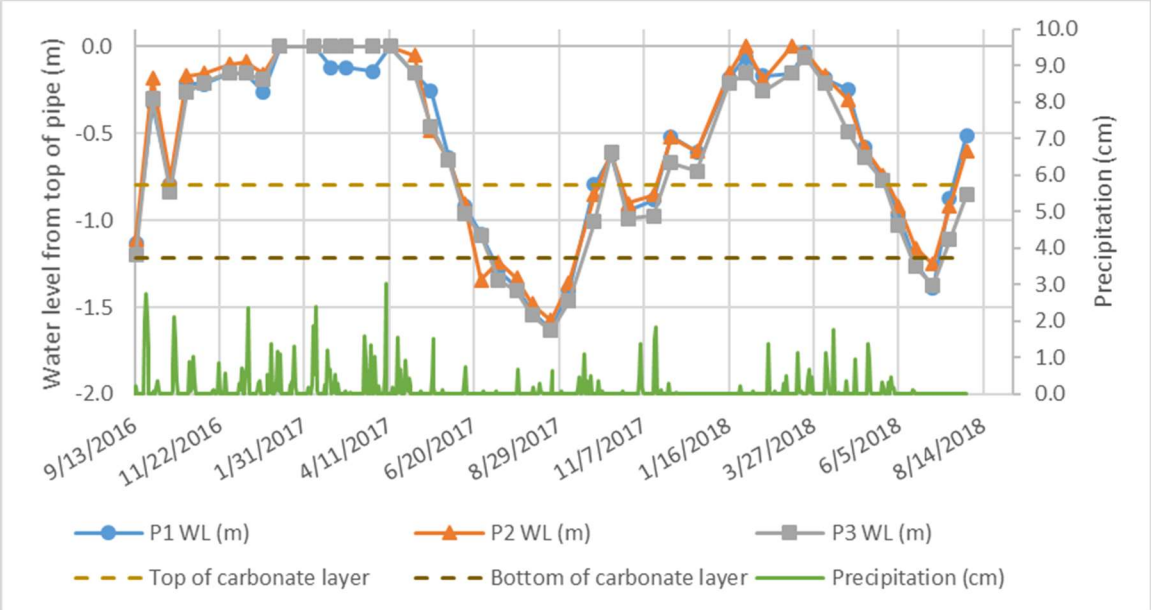

Fig. 7. Water level data for piezometers. Green lines are daily precipitation in cm as measured at the Logan-Cache weather station (WU 2019).

This annual variation of groundwater infiltration and depth influenced As concentration and speciation. In all three wells, As(III) and total As concentrations were higher during the second, dryer year (Sept. 2017 to Sept. 2018) compared to the first year (Sept. 2016 to Sept. 2017; Fig. 6, 8, Table A-1). The increase in As(III) was not exclusively due to higher As concentrations, as the percentage of As(III) is also higher during the second year.

Comparison of seasonal variations for both years further emphasizes the effect of this annual water infiltration variation on As concentrations and speciation (Fig. 9, Table A-1). Autumn, defined in this study as September through November, is the only season in both years with similar As(III) and As concentrations. Spring (March-May), summer

(June-August), and winter (December-February) of the first year were lower in As(III) and As compared to the same seasons in the second year.

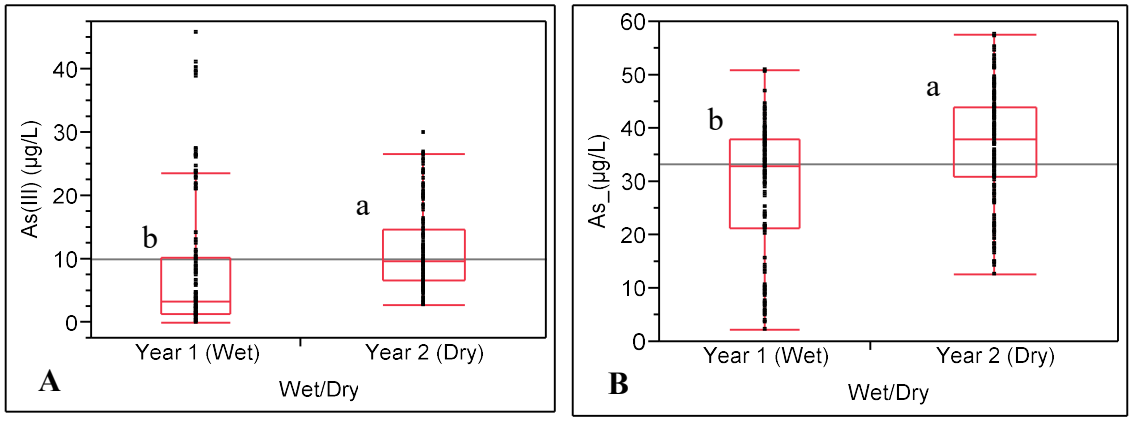

Fig. 8. Quantile box plots for As(III) (A) and total As (B) by year. Red line within the box is median value, box indicates 25th and 75th percentile, whiskers indicate 10th and 90th percentile, dots are data spread, and grey line is the global mean. Years are statistically different by student's t-test (α=0.05).

Schaefer et al. (2016) reported findings of seasonal groundwater fluctuations influencing As concentrations in a shallow aquifer within the Jianghan Plain, China. The study found that during periods of groundwater recharge, influx of oxidizing (high DO and nitrate) water resulted in lower concentrations of aqueous As, Fe(II), and sulfide. When the flow gradient reversed, groundwater levels declined with limited recharge from surface water and reducing conditions prevailed. This resulted in increased levels of aqueous As, Fe(II), and sulfide due to reductive dissolution of Fe oxides and sulfate reduction. These findings were supported by laboratory batch experiments performed by Duan et al. (2019) on sediments taken from the same Jianghan Plain.

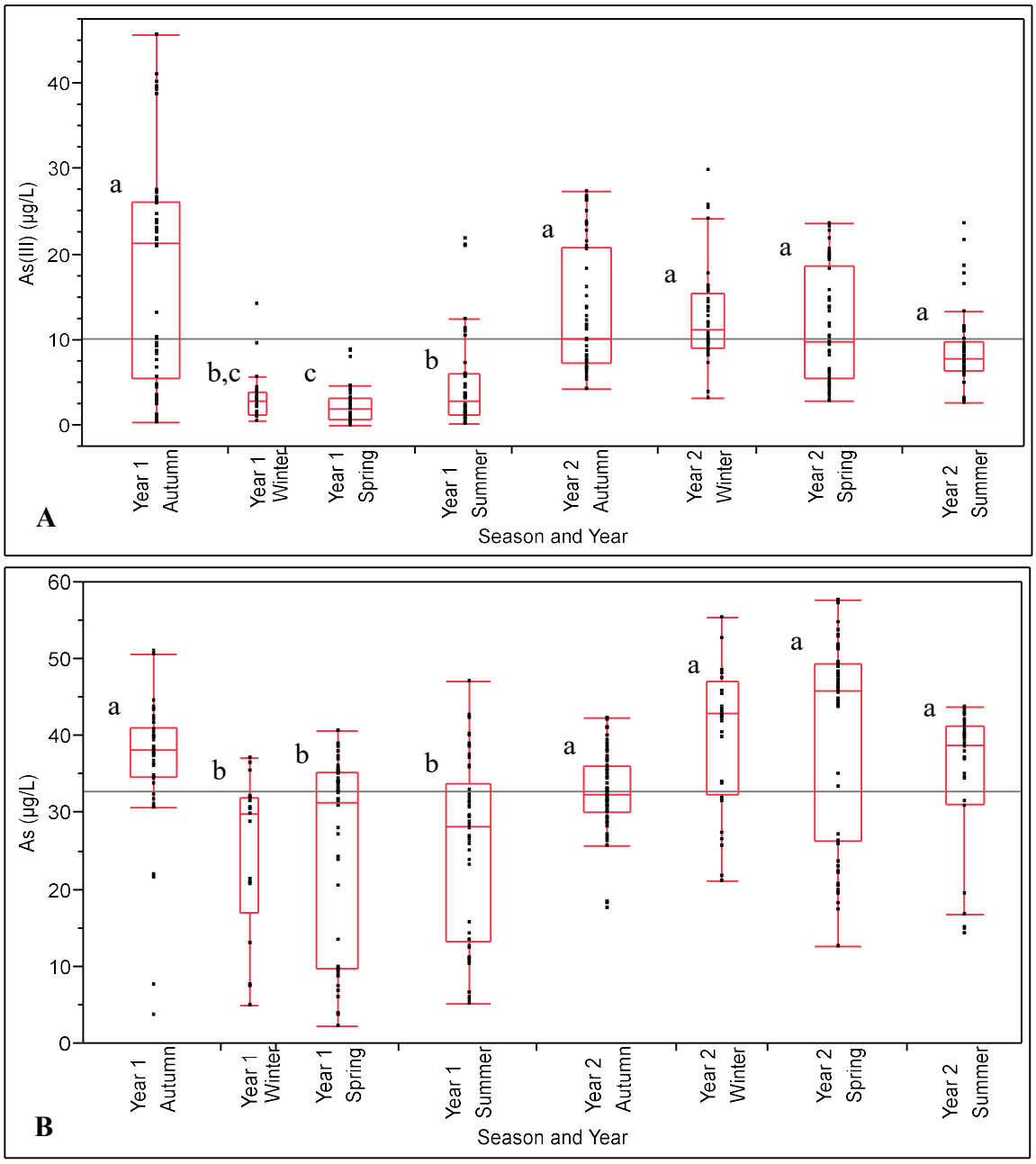

Fig. 9. Quantile box plots for As(III) (A) and total As (B) by season and year. Red line within the box is median value, box indicates 25th and 75th percentile, whiskers indicate 10th and 90th percentile, dots are data spread, and grey line is the global mean. Values compared using one-way ANOVA. Lower case letters indicate statistical significance. Seasons not connected by same letter are significantly different (α=0.05) by Tukey's honestly significant difference test.

Similarly, groundwater at the study site likely traversed through shallow soil profiles during the wet year and during high seasonal runoff. These profiles contained high DO and DOC concentrations (vadose zone) (Meng et al. 2017). In contrast, during the dry year and times of low seasonal runoff, groundwater infiltration was likely from deeper soil profiles (redox-transition zone) (Meng et al. 2017) with lower DO and DOC compared to the shallow profiles. This resulted in effects on As(III) and As concentrations similar to observations made by Schaefer et al. (2016) and Duan et al. (2019) although on the basis of a 2-year cycle in this study compared to an annual cycle in those studies.

PHREEQC modeling also indicated that, at the present study site during times of high runoff in the first year, goethite (FeOOH) was oversaturated and likely to precipitate (Fig. A-6). Potentially, influx of oxygenated water would cause the precipitation of even small concentrations of Fe (hydr)oxides effectively removing As from the surrounding pore water through favored sorption processes similar to findings of Schaefer et al. (2016) and Xiao et al. (2018).

5.2.2 Arsenic and Redox Parameters

Redox parameters (DO, Eh, DOC, Mn, sulfides, Fe and As species) in P-2 were significantly different from the other two wells (Fig. 10, Table 3, Table A-2). DO concentrations and Eh measurements were significantly lower in P-2 while DOC, Mn, sulfides and Fe concentrations were significantly higher (Fig. 10-A, B, C, D, E, F). This indicates that reducing conditions were more favorable in P-2 than in the other wells and is consistent with higher measured As(III) concentrations (Fig. 6). Although reducing

conditions are usually associated with low DOC concentrations, the higher DOC measured in P-2 may indicate that more carbon was available in this well for microbial reduction compared to P-1 and P-3.

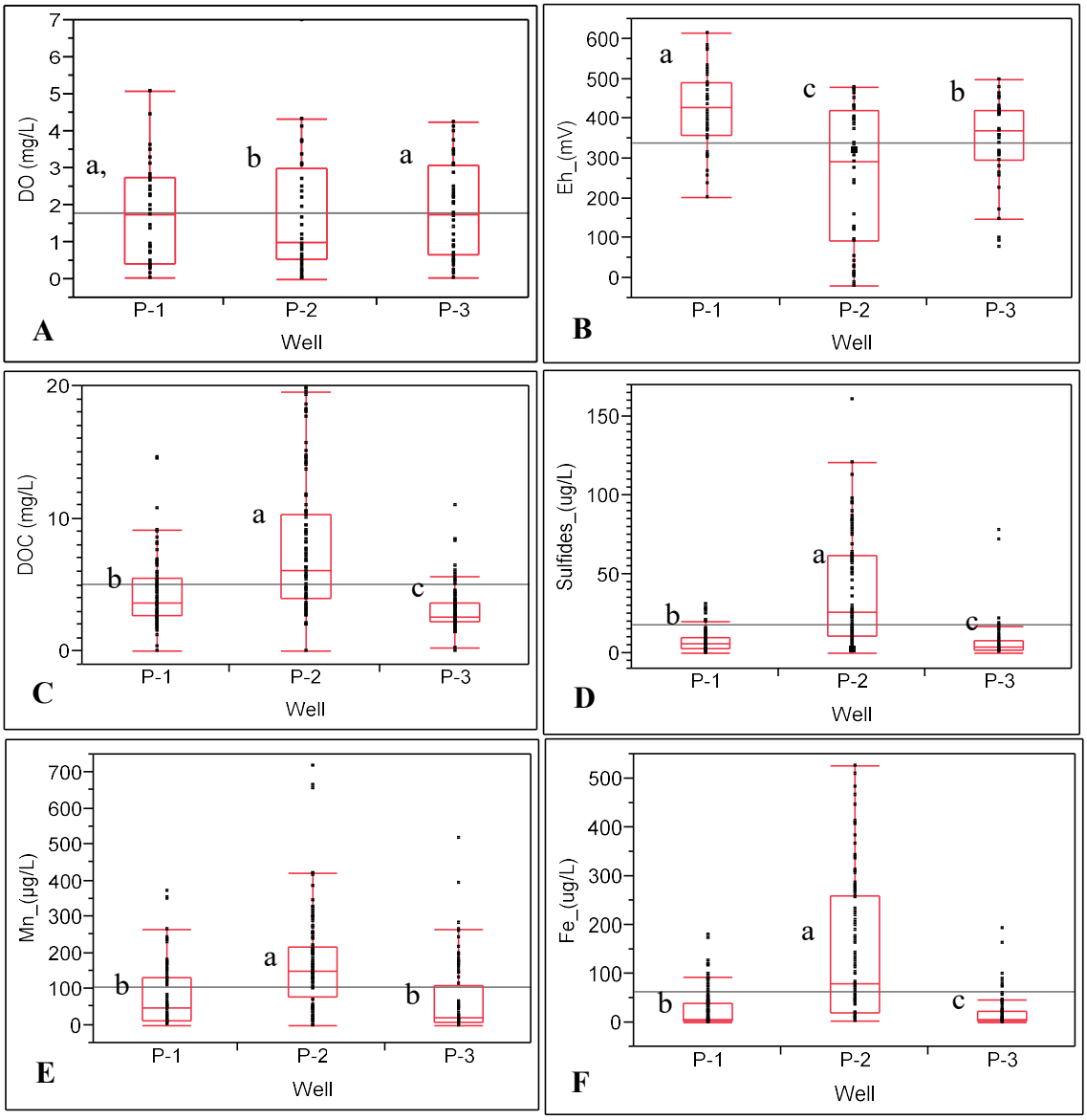

Fig. 10. Quantile box plots for DO (A), Eh (B), DOC (C), Sulfides (D), Mn (E), and Fe (F) by well. Red line in the box is median value, box indicates 25th and 75th percentile, whiskers indicate 10th and 90th percentile, dots are data spread, and grey line is the global mean. Values compared using one-way ANOVA. Lower case letters indicate statistical significance. Seasons not connected by same letter are significantly different (α=0.05) by Tukey's honestly significant difference test.

Redox parameters, when considered by season over the study period, were consistent with the annual variation in water infiltration and consistent with findings of Schaefer et al. (2016). DO concentrations were highest in autumn, winter, and spring of the first year when water infiltration was high and influenced by surface processes. DO then dropped in summer of both years and spring of the second year when water levels were decreasing. Autumn and winter of the second year contained higher concentrations of DO than summer, but were less than the same seasons of the first year (Fig. 11-A). This is consistent with the reduced volume of water influx during the second year (Fig. 7). Average DOC concentrations were higher in winter and spring of both years when water levels were higher and influx from external water sources included high DOC. The rate of carbon replenishment was then less than the rate of consumption during lower water levels, resulting in lower concentrations in summer and autumn (Fig. 11-B) favoring reducing conditions without excess DOC and subsequent low DO concentrations. Favored reducing conditions in summer were also evidenced by low Eh measurements and high sulfides, dissolved Mn, and Fe concentrations (Fig. 11-C, Fig. 12-A,B,C).

Nitrite and nitrate were consistent across all wells and seasons (Table A-3). However, this is due to low measured concentrations of NO_x (< ~0.3 mg/L of each species) and was not useful in determining redox conditions. Iron levels in groundwater were also low (Table A-3). Since only groundwater was collected in the field study with no collection of surrounding soil this may explain the low concentration of Fe in this otherwise chemically/biologically active system. Any Fe(II) or Fe(III) dissolved

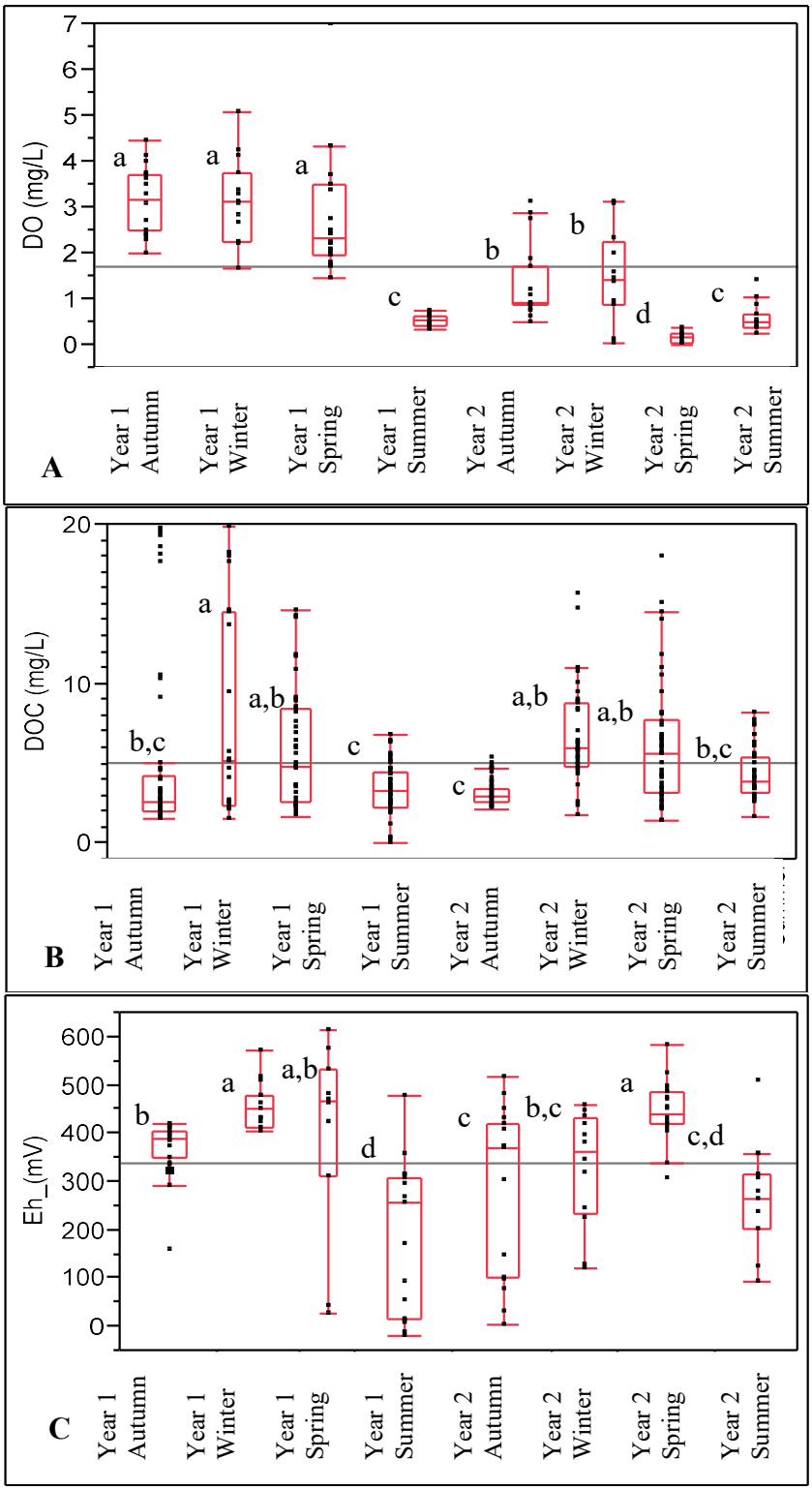

Fig. 11. Quantile box plots for DO (A), DOC (B), and Eh (C) by season. Red line in the box is median value, box indicates 25th and 75th percentile, whiskers indicate 10th and 90th percentile, dots are data spread, and grey line is the global mean. Values compared using one-way ANOVA. Seasons not connected by same letter are significantly different (α=0.05) by Tukey's honestly significant difference test.

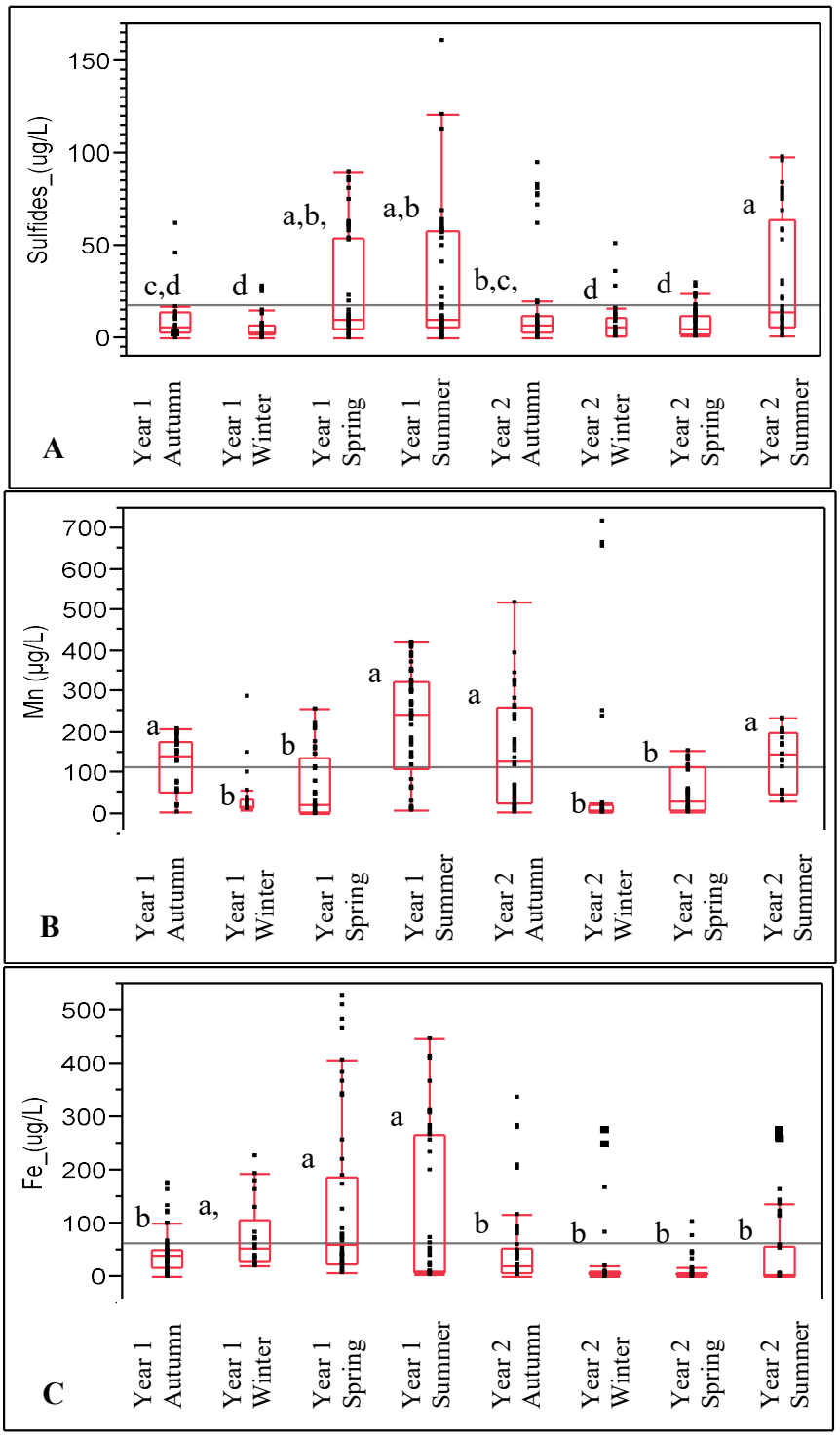

Fig. 12. Quantile box plots for Sulfides (A), Mn (B), and Fe (C) by season. Red line in the box is median value, box indicates 25th and 75th percentile, whiskers indicate 10th and 90th percentile, dots are data spread, and grey line is the global mean. Values compared using one-way ANOVA. Seasons not connected by same letter are significantly different (α=0.05) by Tukey's honestly significant difference test.

into the groundwater would precipitate or sorb to the aquifer solids (Meng et al. 2016, Wang et al. 2018, Xiao et al. 2018). Comparison of Fe speciation may not be a good indicator of redox if only the aqueous phase is measured. During the study period, Fe(II) regularly measured >100% of total Fe. This high concentration of Fe(II) relative to total Fe may be due to Fe sorption combined with sample preparation and analytical technique issues. Fe(II) was analyzed in the field using HACH field kits with lower precision, higher MDL, and unfiltered water. Analysis of total Fe was done on ICPMS with higher precision, lower MDL, and filtered water samples. Measurements conducted in the field using unfiltered water may have included Fe(II) associated with suspended solids (>0.2 μm) while measurements in the lab was only for dissolved Fe species. Therefore, analysis of Fe(II) concentrations and Fe(II)/Fe(III) ratios were not reliable with the data that were collected. Therefore, only total Fe by ICPMS analysis was used in data analysis and modeling input, and Fe(II) data were not used.

Geochemical modeling of As(III) concentrations by PHREEQ indicated that As was rarely in thermodynamic equilibrium, consistent with findings of Cullen and Reimer (1989) and Johnston et al. (2015). In the model, water in wells P-1 and P-3 was usually in an oxidizing state and As(III) was modeled to be below detection limits. At times when the wells were determined to be in a reducing state, the model predicted As(III) to account for 100% of the measured As species. Field measurements indicate that As(III) varied between 2% and 97%, but averaged 20-30% and did not match the model predictions. Measurements from well P-2 followed the model predictions more closely at certain times of the year (Fig. 13). However, many times As(III) was modeled to be

below detection limits similar to P-1 and P-3. This would indicate that As speciation was influenced by additional factors, including kinetic limitations, beyond redox potential. Even in well P-2, where redox appears to have more influence than the other two wells, there are periods where redox potential alone does not account for As(III) concentrations.

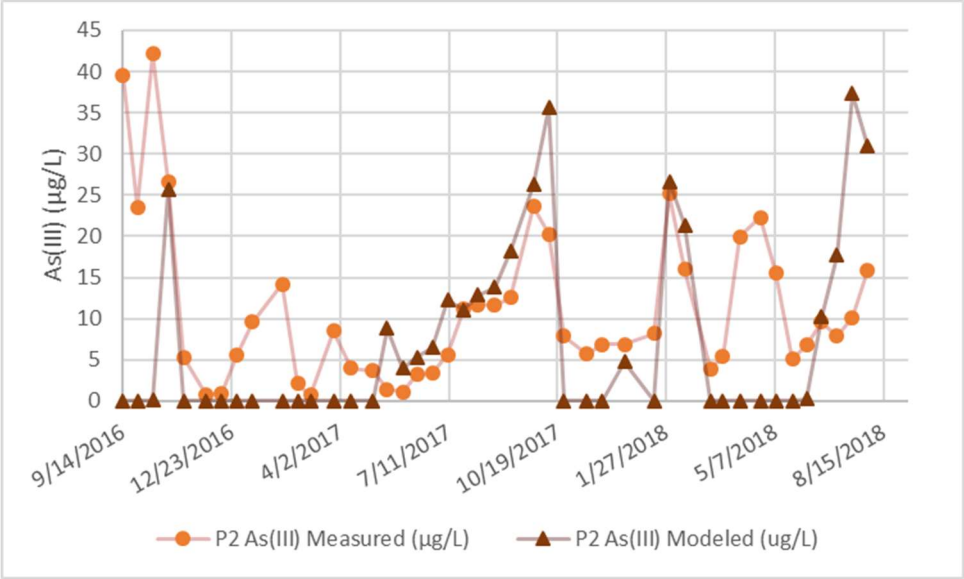

Fig. 13. Comparison of field measurements versus PHREEQC modeled As(III) concentrations in well P-2.

5.2.3 Arsenic and Dissolved Carbonate Parameters

All three wells were statistically different in precipitation/dissolution parameters of alkalinity (as HCO_3), Mg, and PO_4-P, with P-2 being lower in average Mg and HCO_3 concentrations and higher in average PO_4-P concentrations compared to the other wells (Fig. 14-A,B,C, Table A-4). Average Ca concentrations were statistically higher in P-2, but the difference is not large compared to the spread of data (Fig. 14-D).

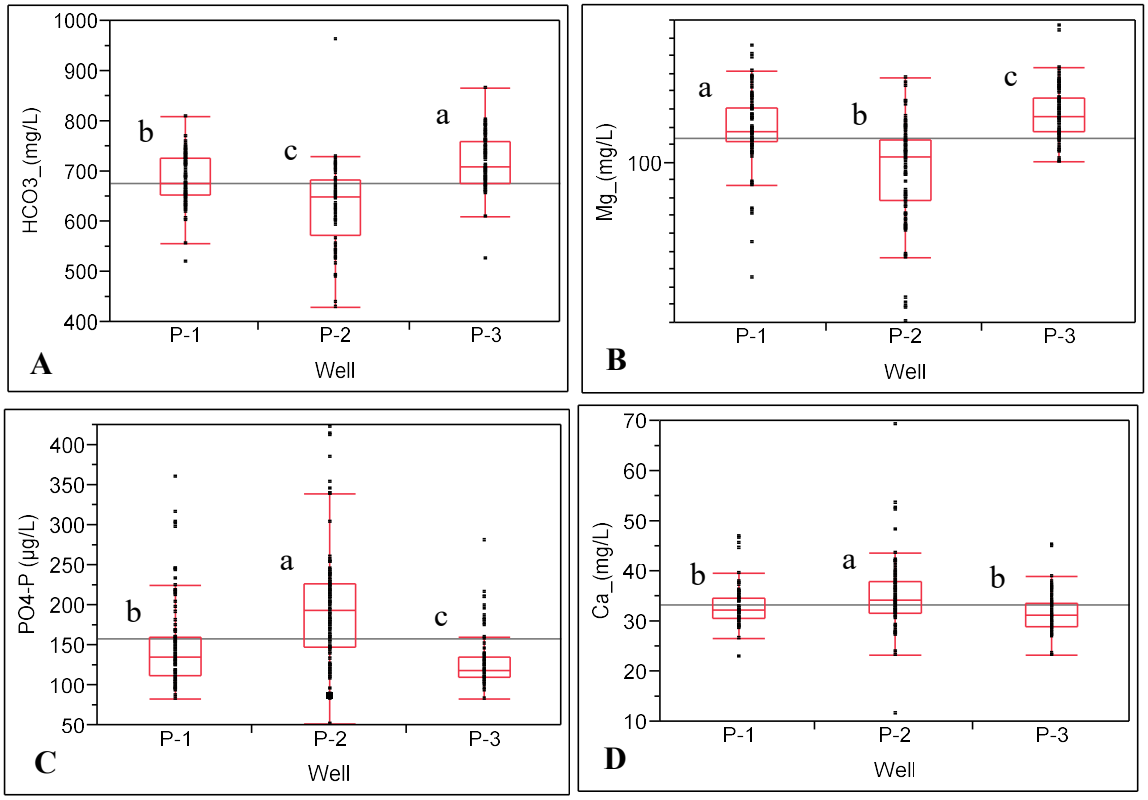

Fig. 14. Quantile box plots for HCO_3 (A), Mg (B), PO_4-P (C), and Ca (D) by well. Red line in the box is median value, box indicates 25th and 75th percentile, whiskers indicate 10th and 90th percentile, dots are data spread, and grey line is the global mean. Values compared using one-way ANOVA. Lower case letters indicate statistical significance. Wells not connected by same letter are significantly different (α=0.05) by Tukey's honestly significant difference test.

Precipitation/dissolution parameters tended to follow cyclical patterns when comparing seasons for the 2 years. Alkalinity (as HCO_3), Mg, and PO_4-P concentrations were more variable in the first year compared to the second year with HCO_3 and Mg concentrations being highest in the summer of the first year (Fig. 15-A,B) while PO_4-P concentrations were higher during the first year and into autumn of the second year (Fig. 16-A). Ca had higher concentrations in the first year compared to the second year, but remained more consistent for both years compared to HCO_3^-, Mg, and PO_4-P (Fig. 16-B).

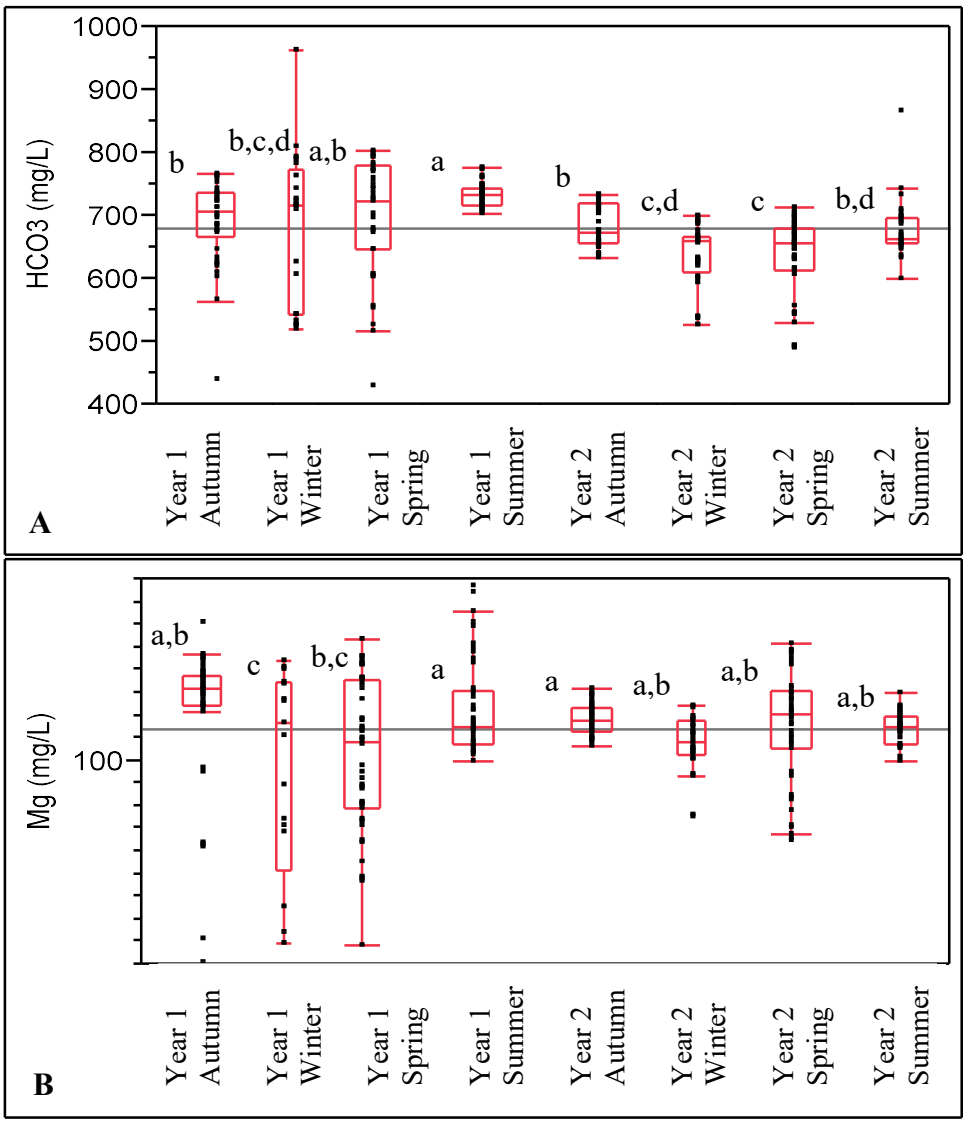

Fig. 15. Quantile box plots for HCO_3 (A), Mg (B) by season. Red line in the box is median value, box indicates 25th and 75th percentile, whiskers indicate 10th and 90th percentile, dots are data spread, and grey line is the global mean. Values compared using one-way ANOVA. Lower case letters indicate statistical significance. Seasons not connected by same letter are significantly different (α=0.05) by Tukey's honestly significant difference test.

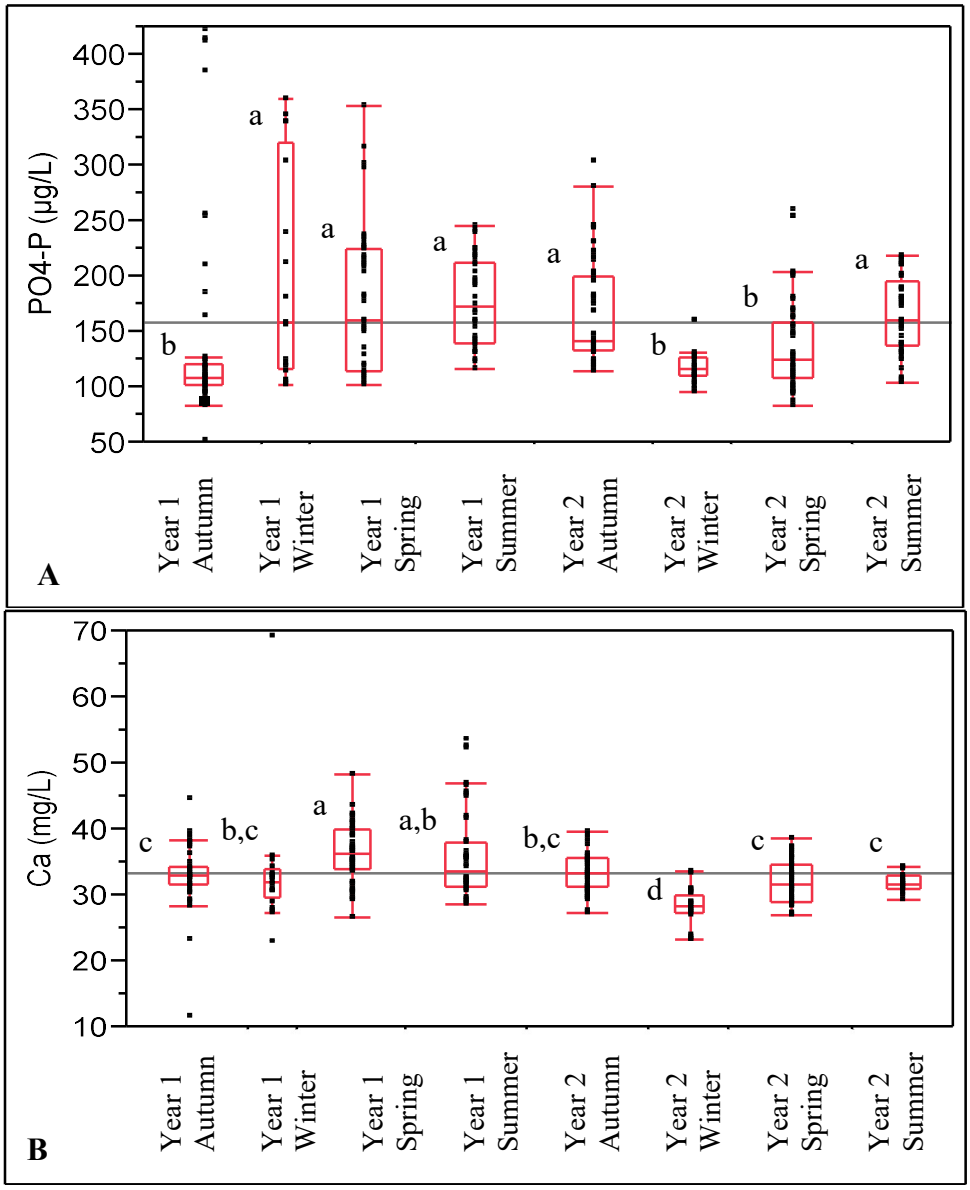

Fig. 16. Quantile box plots for PO_4 (A), and Ca (B) by season. Red line in the box is median value, box indicates 25th and 75th percentile, whiskers indicate 10th and 90th percentile, dots are data spread, and grey line is the global mean. Values compared using one-way ANOVA. Lower case letters indicate statistical significance. Seasons not connected by same letter are significantly different (α=0.05) by Tukey's honestly significant difference test.

Piper diagrams indicate that all three wells were dominated by HCO_3^- (Fig. 17-A). Groundwater is of Ca-Mg-HCO_3 type with Mg dominating over Ca. The groundwater chemistry in well P-3 remained consistent throughout the 2 years of collection. Wells P-1 and P-2 drifted toward Na-HCO_3 and Na-Cl type; however Cl never dominated and Na only dominated for brief periods of time. These shifts occurred during spring, winter, and, to a lesser extent, autumn (Fig. 17-B) when water levels were at their highest (Fig. 7). This further indicates the influence of external groundwater influx into the study site during those time periods, particularly influx that has travelled through the shallow profiles where Na and Cl have higher concentrations (Meng et al. 2017). The Piper diagrams also indicate that weak acids (HCO_3^-) exceed strong acids ($Cl^- + SO_4^{2-}$) in all wells and all seasons.

Molar ratios can be used to determine the dominant source of measured ions in groundwater. A Ca^{2+}/Mg^{2+} ratio of <1 indicates the dissolution of magnesite ($MgCO_3$) and dolomite ($(MgCa)CO_3$) while a ratio of 1-2 indicates the dissolution of $CaCO_3$ (Mayo and Loucks, 1995). Ca^{2+}/Mg^{2+} ratios averaged 0.2 and never exceeded 1.0 through the entirety of the collection period. This indicates that the source of ions in the groundwater was overwhelmingly from dissolution of Mg-based carbonates.

PHREEQC modeling indicates that groundwater did not remain in equilibrium with major carbonate species for long periods of time during the entirety of the 2-year collection period (Fig. 18-A). $CaCO_3$ was generally oversaturated during the first, wet year of collection before transitioning to undersaturation in the second, dryer year. This

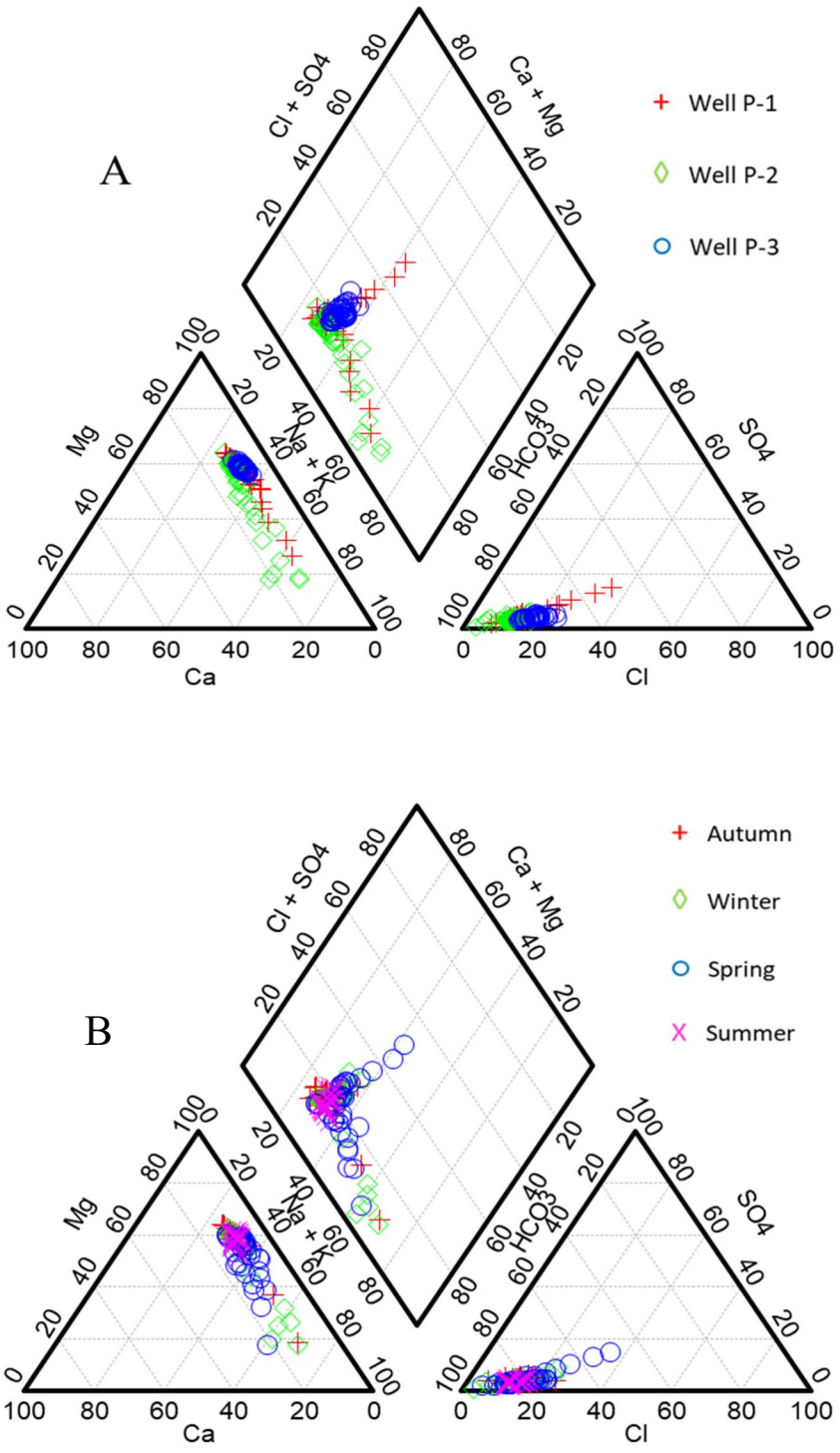

Fig. 17. Piper plots of collected groundwater samples organized by well (A) and season (B).

would indicate that $CaCO_3$ was more likely to precipitate out of groundwater during the first year while it was more likely to dissolve into the groundwater during the second year. This is also evident in that all three wells tended to not remain under or oversaturated for long periods of time and would regularly attempt to move back towards the equilibrium value before cycling back to under/oversaturation.

Although it could be expected that $CaCO_3$ concentrations would be diluted during times of higher water volume and instead create a state of undersaturation, an analysis of the possible sources of groundwater collected at the site provides an explanation for the observed data. As previously stated, during seasonal runoff, groundwater infiltration at the site originates from snowmelt transported from surrounding mountains by the Logan River and other surface waters. These surrounding mountains also contain high levels of carbonate minerals. During the first, wetter year higher runoff volumes in the Logan River and other surface waters along with shallow groundwater infiltration near the site may have transported more of these carbonates to the study site culminating in the highest concentration levels in the summer of the first year. Conversely, lower runoff volumes during the second, dryer year likely resulted in a lower total mass of carbonate minerals being transported to the study site.

Modeling of Mg-based carbonates followed a similar saturation pattern as $CaCO_3$ (Fig. 18-B; Fig. A-4). $MgCO_3$ had generally higher saturation values with the first-year oversaturation peak and the second-year undersaturation point occurring at the same time as $CaCO_3$. However, a brief undersaturation point does occur in P-1 and P-2 during early spring (April-June) in the first year of collection. Dolomite followed the same pattern as

$MgCO_3$ but with higher oversaturation values and lower undersaturation values (Fig. A-4).

Finally, $MnCO_3$ followed a different pattern than Ca or Mg-based carbonates (Fig. A-5). $MnCO_3$ was undersaturated through almost the entire 2 years of collection and had greater variability among the three wells, particularly when comparing P-2 to the other two wells. $MnCO_3$ only reached oversaturation at the same point when all other carbonate species were highly oversaturated and only in P-2.

5.2.4 Relationship Between Arsenic and Groundwater Parameters

PCA indicates potential associations of As with other groundwater parameters (Fig. 19, Table A-5). When all data were considered, the first two principal components explain 50.6% of the variance. By examining the eigenvectors (Table A-5) PC1 includes As, sulfides and sulfates, Fe, DOC, Mn, and Eh factors descriptive of redox conditions, plus phosphate, Cl, K, Mg, and bicarbonate, factors descriptive of dissolution/desorption. PC2 includes pH, DO, Eh, DOC, nitrate, As(III), Na, K, Mn, Mg. The loading plot (Fig. 19) shows the vectors: the longer the vector, the more influential the component. Two vectors that are close together are correlated, 90° no relationship, and at 180° are negatively correlated. PCA data (Fig. 19) indicates that As has positive correlations with Mg and bicarbonates as well as sulfates and Cl, while also indicating a negative correlation with phosphates, sulfides, and Fe. As(III) is also indicated to have a positive correlation with Ca, Mg, and bicarbonates and a negative correlation with DO and water level.

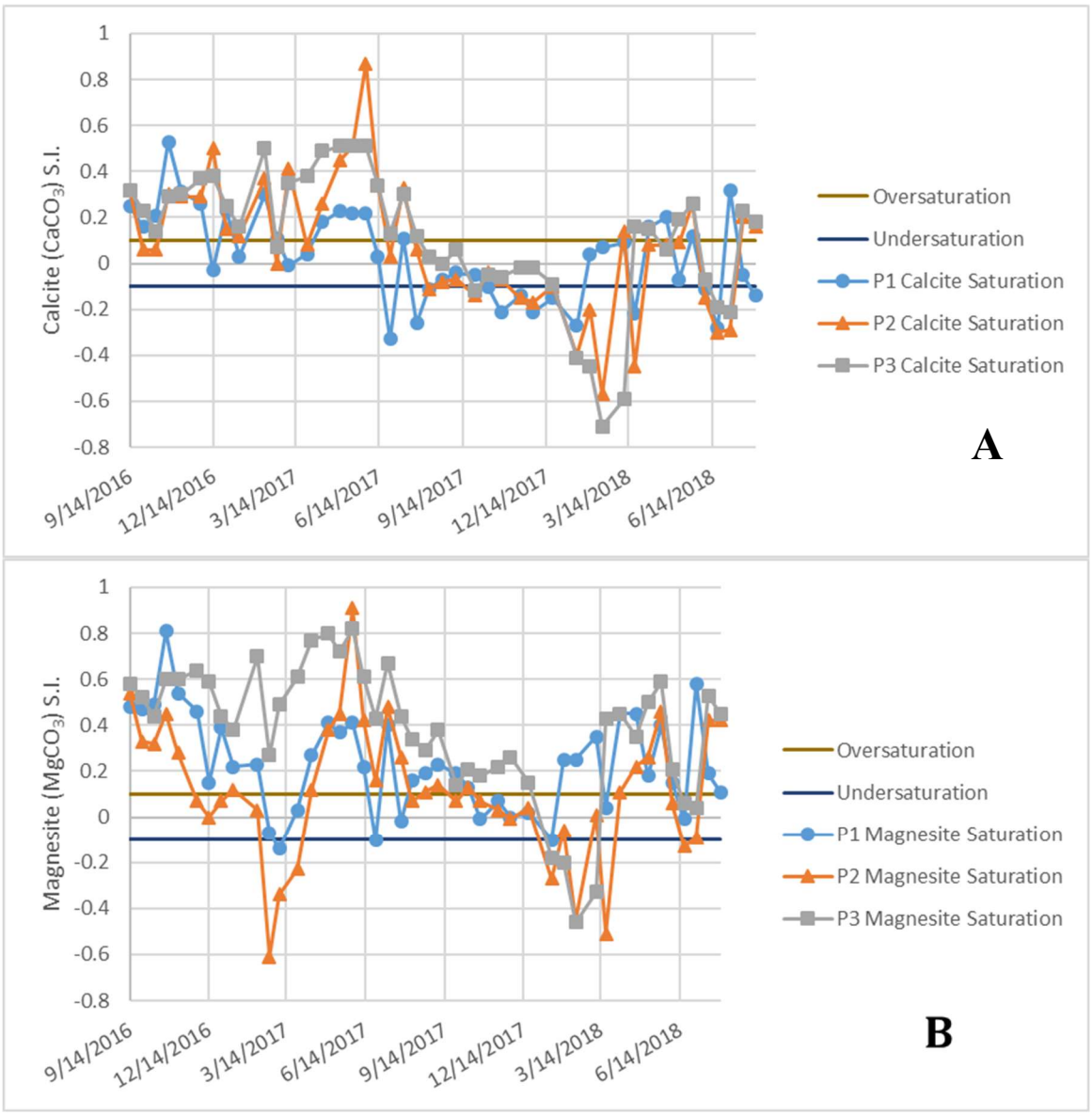

Fig. 18. PHREEQC modeled $CaCO_3$ (A) and $MgCO_3$ (B). Equilibrium was considered to be at a model generated Saturation Index value of 0 with an error of ±0.1 represented by horizontal lines (Langmuir 1971).

Pairwise comparison of these parameters provides additional insight into these correlations (Table 4). Arsenic had a negative correlation with DOC. Schaefer et al. (2016) evaluated seasonal changes in groundwater As concentration as influenced by

groundwater recharge and discharge. During periods of drawdown, Schaefer et al. (2016) speculated that DOC was consumed and As(III) increased due to microbial reduction of As(V) and associated oxides. Wang et al. (2018) observed a positive correlation between As concentrations, reducing conditions, and degradation of organic carbon (using the increased concentration of NH_4^+-N as an indicator of organic matter degradation). This correlation was based on samples taken along flow paths with a redox gradient in aquifers instead of on a temporal scale, but with the same conclusions of microbial consumption of DOC creating reducing conditions and increasing As concentrations in solution.

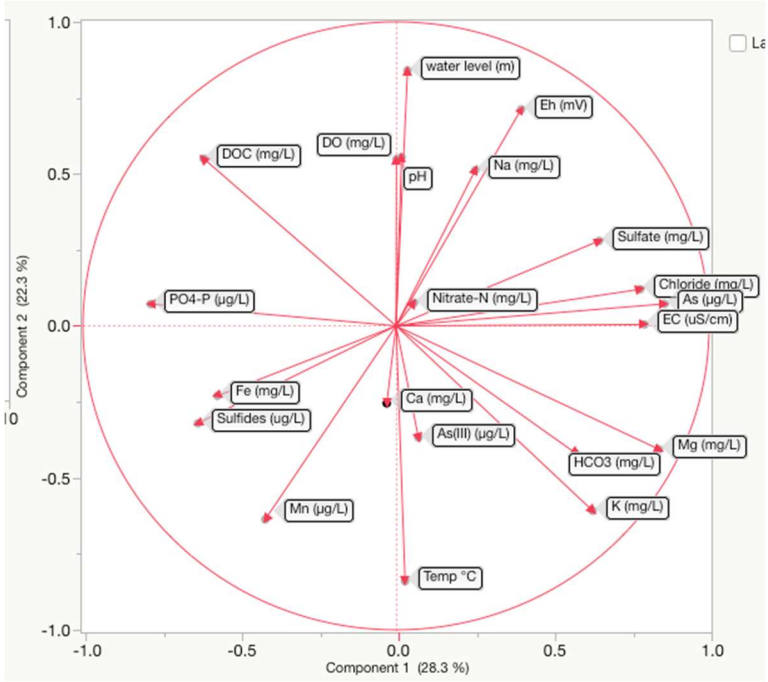

Fig. 19. PCA loading plot for all collected groundwater data.

When iron/sulfur redox chemistries are controlling As solubility, it is expected that correlation of As to Fe and sulfide would be positive. However, in this study, As had

negative correlations with Fe and sulfides (Table 4) indicating that additional or different mechanisms from those observed by Schaefer et al. (2016) were influencing release of As to groundwater. This negative correlation between As and Fe and sulfides in groundwater from NP13 was also observed by Meng (2015) indicating that reductive dissolution of Fe oxides driven by microbial activity might not be the dominant mechanisms of As solubilization in these aquifer solids.

As(III) had a positive correlation with dissolved Mn (Table 4). This is likely a result of Mn being influenced by redox conditions. Analysis of As(III), however, determined fewer significant correlations with other redox parameters. It is likely that As(III) concentrations were additionally influenced by kinetic limitations (Cullen and Reimer 1989, Johnston et al. 2015) or some parameter that was not measured in the study such as activity of As specific-reducing microbes (Malasarn et al. 2004, Mirza et al. 2014, 2017). Other potential mechanisms include direct reduction of As(V) from mineral surfaces not requiring the dissolution of the host mineral (Ahmann et al. 1997) or the continuous release of As(V) from solid surfaces as the released As(V) is reduced to As(III) driving further desorption of As without dissolution of a mineral phase (Langner and Inskeep 2000).

Arsenic had a positive correlation with bicarbonate (HCO_3^-) (Table 4). However, Ca was not positively correlated with As. Instead Mg is positively associated with HCO_3 and As. This further indicates that Mg-based carbonates instead of $CaCO_3$ may be the controlling carbonate species in these wells. Meng et al. (2017) observed correlations between As and carbonate minerals in these same aquifers suggesting that these Mg-

based carbonates hosted a significant amount of As. The same study also observed a negative correlation between As(V) and total Fe, Mn, and DOC indicating that reductive dissolution of Fe/Mn oxides was not the dominant mechanism of As solubilization in this aquifer. Arsenic had a negative correlation with phosphate (Table 4), as also reported by Meng et al. (2017), confirming previously observed competition between the ligands for sorption sites (Dixit and Hering 2003, O'Day 2006, So et al. 2012).

Table 4. Correlations of arsenic species and groundwater parameters determined by JMP multivariate statistical analysis. Values in bold ($p<-0.1, >0.1$; $\alpha=0.05$) as determined by pairwise comparison by JMP are considered significant. Only parameters significant to either As or As(III) are included in table. Redundant parameters were also omitted. Other parameters considered included water level, DO, sulfates, Fe, and NO_x

	pH	*EC*	*Eh*	*Sulfide*	*Fe*	*HCO3*	*PO4*	*DOC*	*Ca*	*Mn*	*Mg*	*As(III)*	*As*
pH	1.00												
EC	0.04	1.00											
Eh	**0.29**	**0.12**	1.00										
Sulfide	**-0.10**	**-0.34**	**-0.64**	1.00									
Fe	0.09	**-0.23**	**-0.61**	**0.67**	1.00								
HCO3	-0.01	**0.58**	**-0.14**	**-0.17**	**-0.27**	1.00							
PO4	0.09	**-0.51**	**-0.26**	**0.49**	**0.40**	**-0.37**	1.00						
DOC	**0.20**	**-0.41**	0.09	**0.23**	**0.30**	**-0.64**	**0.55**	1.00					
Ca	**0.15**	0.09	**-0.27**	**0.23**	**0.43**	**0.32**	0.00	-0.05	1.00				
Mn	**-0.29**	**-0.25**	**-0.68**	**0.41**	**0.43**	0.01	**0.32**	0.02	**0.24**	1.00			
Mg	**-0.12**	**0.64**	0.03	**-0.35**	**-0.27**	**0.68**	**-0.70**	**-0.76**	**0.23**	-0.09	1.00		
As(III)	**-0.28**	0.02	**-0.12**	-0.05	-0.06	-0.01	-0.09	**-0.10**	-0.08	**0.48**	**0.14**	1.00	
As	**-0.10**	**0.55**	**0.47**	**-0.64**	**-0.70**	**0.28**	**-0.71**	**-0.43**	**-0.26**	**-0.42**	**0.64**	**0.16**	1.00

5.3 Conclusion

Groundwater fluctuation at the site influenced As concentrations and speciation similar to findings of Schaefer et al. (2016, 2017). However, while the influence of water

level fluctuations Schaefer et al. (2016) observed were seasonal and influenced directly by local precipitation, water level influence at this study site was observed to be on an annual basis and influenced by changes in seasonal runoff from the surrounding area. During seasons in a year of high runoff (winter and spring of the first year), when groundwater is influenced by surface process and is high in DO, oxidation tended to be favored, and modeling indicated FeOOH was oversaturated and likely to precipitate. At these times, As concentrations in groundwater were lowest, consistent with findings of previous studies (Nordstrom 2002, Schaefer et al. 2016, Duan et al. 2019). This low As state persisted through summer of the first year. During the second year and drier seasons when influx was low, groundwater traversed through deeper soil profiles where oxygen is limited and reducing conditions were favored. During these times, DO and DOC concentrations were low, As was released into groundwater and reduced to As(III).

In many aquifers world-wide the dominant mechanism for this release of As is the microbially driven reductive dissolution of the host Fe oxide mineral. In these cases, As and Fe reactions should be coupled both during the oxidation process retaining As by Fe oxide minerals and during the reductive process with release of As and Fe with mineral dissolution. However, in this study, negative correlations between As and Fe were observed regardless of how the data are organized (by year, season, high water table, etc.) indicating that additional or different mechanisms were influencing the fate of As. Xie et al. (2015) also observed these negative correlations during As release in aquifers in a semi-arid region of China. (2016). Xie et al. (2015) proposed that high sulfide (1-10 mg HS/L) waters directly promoted abiotic reduction of Fe(III) causing mobilization of As,

the mobilized As formed soluble complexes with sulfide, and Fe was removed from solution through precipitation of Fe and sulfur-based minerals. At the present study site, however, sulfide concentrations were low (1-100 μg/L). Meng et al. (2015) also reported a negative correlation between As and Fe at NP13 and theorized that Fe(III) minerals may have been reduced with release of As, but Fe(II) was either sorbed or precipitated as FeS or siderite ($FeCO_3$). However, PHREEQC modeling indicated that these Fe minerals were undersaturated throughout the entirety of the field study and without analysis of the aquifer solids these mechanisms cannot be verified.

Other influences, including kinetic limitation, may have influenced results, particularly when considering the influence of redox on As species. As(III) concentrations were correlated with fewer parameters than As. Microbes that specifically reduce As may have directly influenced As(III) concentrations independent of any measured parameter (Malasarn et al. 2004, Mirza et al. 2014, 2017, Abu-Ramaileh 2015). Guo et al. (2013) also observed changes in As, specifically without changes in Fe, and attributed this to the reductive desorption of As with release of As(III) without dissolution of Fe minerals. There also appears to be a lag in establishment of redox conditions with fluctuating groundwater levels. This is evidenced by redox parameters that statistically favored reducing conditions in summer of the first year, but As(III) concentrations were statistically higher in autumn of the second year. Also, As(III) was rarely in thermodynamic equilibrium, particularly in P-1 and P-3. Finally, when groundwater levels were below the designated carbonate enrichment zone, water samples were still collected. However, these samples were more likely to be from the redox-

transition zone due to well screening installation. Redox states may have been different in this zone and influenced As speciation. Arsenic concentrations were also high in autumn of the first year. This may be the result of water runoff from the previous year before samples were collected or as a result of the disturbance created by construction of the wells.

It is important to note that this study determined high groundwater levels promoted oxidizing conditions and low water levels were associated with reducing conditions. In contrast, previous studies by Guo et al. (2013), Xie et al (2015), and Duan et al. (2015) found that higher groundwater levels were associated with reducing conditions and lower levels with oxidizing conditions. However, these studies were also conducted in areas that were different from the present study site in multiple ways, including geology, influence of local precipitation and irrigation practices on groundwater levels, and transport velocity of aquifer pore water. Therefore, it is the site hydrology and not specific depth of the water table that affects redox conditions.

The potential influence of carbonates on As concentrations is also most apparent on an annual scale. In the first year of data collection, carbonates in groundwater were usually oversaturated and therefore more favored to precipitate. During this year, As levels were lower indicating that as carbonates precipitated, As may have been integrated into the solid phase minerals similar to observations of So et al. (2008) and Bardelli et al. (2011) and removed from the surrounding groundwater. During the second, dryer year, when carbonates were undersaturated in the groundwater these solid minerals would then dissolve. As these carbonates dissolved, associated As like that in the carbonate

enrichment zone identified by Meng et al. (2017) were also released into the surrounding groundwater resulting in higher concentrations observed in the second year.

Mg-based carbonates were more influential in these wells than $CaCO_3$. Modeling results along with analysis of Mg/Ca ratios indicates that Mg dominated over Ca in groundwater samples. Mg is also the only measured cation that is statistically correlated with HCO_3 and all As concentrations. This would indicate that Mg-based carbonates were more prevalent in the soil and may be more kinetically favored to dissolve or precipitate and affect associated As concentrations compared to Ca-based carbonates. Additionally, Catelani et al. (2018) observed that the presence of Mg during calcite precipitation positively affected As uptake. A similar influence on As uptake may be occurring in these wells due to high Mg concentrations.

Monitoring of groundwater for As and potential biogeochemical associated parameters is useful for determining correlations that may indicate when and how As concentrations will fluctuate, but they do not necessarily explain why. To better understand the processes behind these fluctuations, the solids in the aquifer must also be studied. This is the purpose of the laboratory column study.

CHAPTER 6

COLUMN STUDY

6.1 Materials and Methods

A laboratory column study was conducted to study wet-dry and redox cycles under controlled conditions. The study was conducted using columns containing soil and groundwater from the study site.

Twelve soil core samples were collected from an area directly to the west of the installed piezometers at NP13. The soil cores were drilled to a depth of approximately 1.5 m to ensure complete collection of the carbonate enrichment zone. Each core was contained in individual plastic sleeves, capped on both ends, and transported immediately to the UWRL. Upon arrival at the Lab, all cores were placed in an anaerobic glove bag with an N_2 atmosphere in a constant temperature room at 16±1˚C. The cores were then visually inspected to determine layers high in carbonate minerals according to the depth and coloring detailed by Meng et al. (2017). These high carbonate sections were removed from the rest of the core sample, bagged, and stored in the same anaerobic glove bag. Approximate depth of the sections was 0.8 to 1.3 m and were not influenced by surface conditions including concrete slabs that were located on the site.

Groundwater from Piezometer 2 was collected for use in the laboratory study. This piezometer was chosen due to its relatively low concentration of As found during groundwater sampling. This provided water that was chemically representative of the study area while minimizing interference from background As concentrations. The study used this groundwater in three different treatments. The first treatment was the

groundwater without any amendments to observe reactions controlled by natural conditions, including bioavailability of natural organic matter. The second treatment was poisoned with 500 mg mercuric chloride ($HgCl_2$)/kg (Abu-Ramaileh 2015) to eliminate any biological influence in its respective columns. Finally, the third treatment was spiked with 5 mM C as glucose plus 5 mM C as acetate (10 mM total carbon) to encourage microbial growth.

Columns for the study were constructed to allow for wetting and drying of soil samples. Preliminary tests determined a column construct that worked well for these test cycles (Fig. 20). The bottom of the column is a Fisher Scientific two-piece Buchner funnel (Fig. 21). The "cup" portion of the funnel is perforated on the bottom to allow water to pass through it. A paper filter inside the funnel is utilized to separate soil particles from water flow. The funnel half was only used for water collection during drying phases. The column is clear polycarbonate pipe 15 cm long and 6.4 cm diameter. Both ends were capped by vinyl caps to minimize evaporation and unwanted drainage. The top cap was loose to allow for air transfer while minimizing microbial contamination.

Previously mentioned high-carbonate soil samples were dried and crushed using a mortar and pestle. All dried, crushed soil was combined to create a homogenous mixture. A sample of this dried homogenous soil was sent to the Utah State University Analytical Laboratories for analysis of pH, salinity, total organic carbon, cation exchange capacity, particle size distribution using the hydrometer method (Klute 1986), and calcium carbonate equivalent using acid addition with CO_2 evolution (Sparks et al. 1996). The

mixed soil was then measured and packed into each column at a soil density of 1.2 g/cm^3, approximately 100 g per column (Fig. 22). The columns were then evenly and randomly divided among the three groundwater treatments and placed into respective

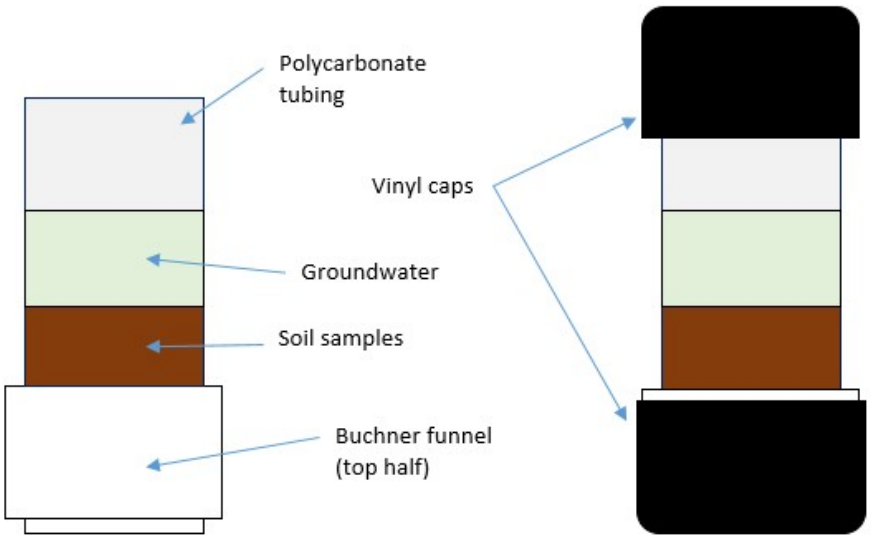

Fig. 20. Study columns, without and with vinyl caps.

Fig. 21. Two-piece Buchner funnel, cup and funnel. Thermo Scientific 42800550.

tubs of water (Fig. 22-step A) allowing for capillary rise of water to saturate each column. These columns were allowed to achieve hydraulic equilibrium over 48 hours. The columns were then capped and placed into dry holding tubs according to treatment and planned wet/dry cycling (Fig. 22-step B). At the same time, one set of columns (five per treatment, 15 total) was sacrificed for a time zero analysis (Fig. 22-step S_0).

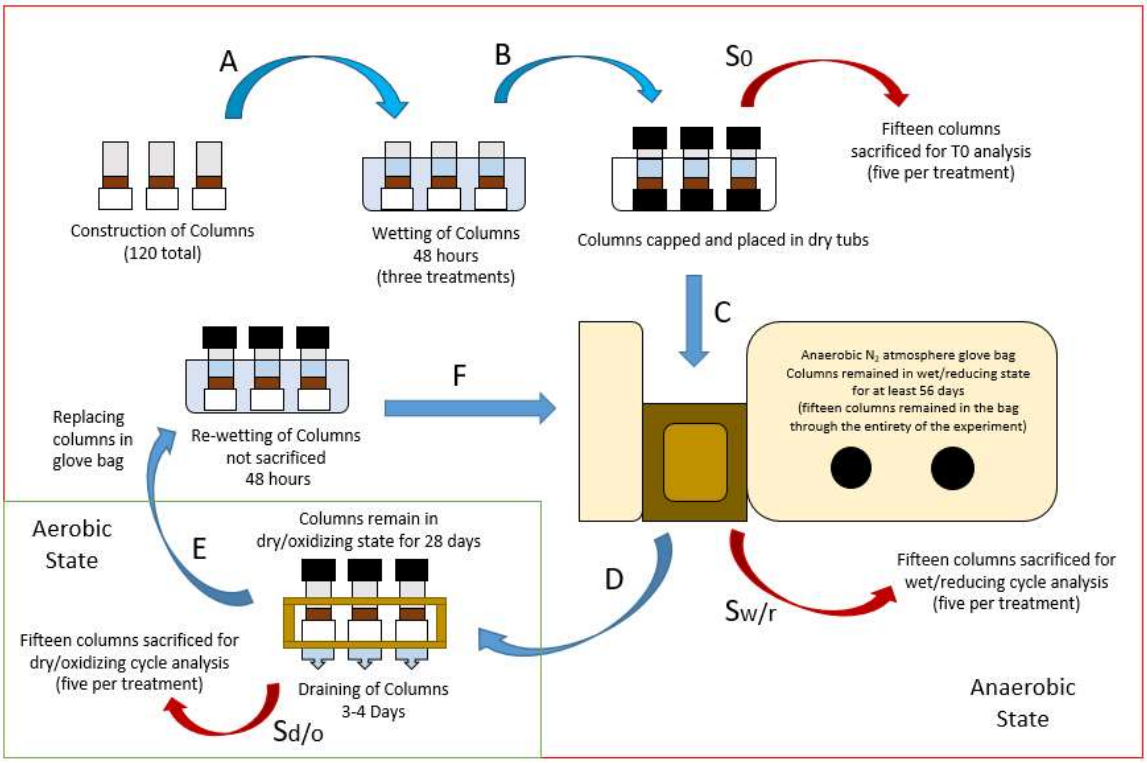

Fig. 22. Graphical representation of column experiment.

The initial setup of the columns occurred in an anaerobic glove bag with an N_2 atmosphere in a constant temperature room at 16±1 ˚C. The columns then remained in the glove bag to achieve full reducing conditions (Fig. 22-step C, Fig. B-2). Abu-Ramaileh (2015) observed that aqueous phase As(III) rose above background levels by Day 17 and

reached steady-state conditions by Day 28. The release of HCl extractable Fe(II) did not stabilize until Day 63. In addition, measurements of groundwater level at the study site indicated that the site remains completely saturated for a period of approximately 4 months. Based on these findings and time restrictions for the study, the columns initially remained in the glove bag for 70 days to ensure complete reducing conditions.

At the end of the wet/reducing cycle one set of columns was set up in the glove bag to drain and collect pore water. Once drained, the columns were sacrificed (Fig. B-3) to analyze pore water and soil conditions resulting from reducing conditions (Fig. 22-step $S_{w/r}$). The remaining columns were removed from the glove bag and set up to allow pore water to drain until soil in the columns achieved field capacity (Fig. 22-step D). Groundwater from the study site, saturated with oxygen, was then passed through the columns to promote oxidizing conditions. Preliminary tests using red dye indicated that water used for flushing columns displaced pore water currently in the column, thus promoting oxidation. Draining and oxidation was achieved within 3-4 days while evaporation continued to drive the soil moisture below field capacity after 1 week. The columns remained in this drained, oxidized condition for 28 days. Another set of columns was then sacrificed (Fig. B-3) and analyzed at this point (Fig. 22-step $S_{d/o}$). The remaining columns were then placed back into the glove bag and rewetted using the previously mentioned procedure (Fig. 22-step E) to begin another wet/dry cycle. At this time, 500 mg/L $HgCl_2$ was added to water used to rewet poisoned columns and 10 mM C was added to water used to rewet carbon-enhanced columns. After the first sacrifice, it was determined that 56 days was sufficient to achieve reducing conditions based on

coloration in non-poisoned columns. This allowed the dry/oxidizing cycle to be increased to 42 days, thus improving the overall drying of soil in the columns. These cycles continued until all columns were sacrificed and analyzed. This provided one set of columns that went through one wet/dry cycle, one set through two wet/dry cycles, and one set through three wet/dry cycles. Additionally, one set of columns remained in the anaerobic glove bag for the entirety of the experiment then was sacrificed and analyzed near the end of the three cycles.

Water and soil collected from the sacrificed columns were analyzed to determine changes in redox or carbonate dissolution/precipitation parameters that occurred during the previous cycle. All water drained through the soil column to begin dry/oxidizing cycles was collected for analysis. Additionally, for time zero and the first wet/reducing cycle, water above the soil column was decanted and collected for analysis. Next, soil pore water extractions for all sacrifices were collected by combining and mixing 15 g of wet soil with 20 mL Double Deionized Water (DDW). Two centrifuge tubes were used for each column for a total of 30 g wet soil and 40 mL DDW per sample. The tubes were shaken for 30 minutes then centrifuged for 20 minutes at 10,000 x g. Water was then decanted and same samples recombined for analysis. All collected water was analyzed using the same procedures outlined for groundwater in Section 4.2 with the exception of As speciation. As(III) and As(V) were determined by LC ICP-MS as described in Meng (2017). Arsenic speciation was preserved with 5% v/v of 0.25 M EDTA. The MRL for As(V) was 0.08 µg/L and As (III) was 0.05 µg/L. Arsenic speciation was preserved with 5% v/v of 0.25 M EDTA. Fig. 23 provides a graphical outline of these collection steps.

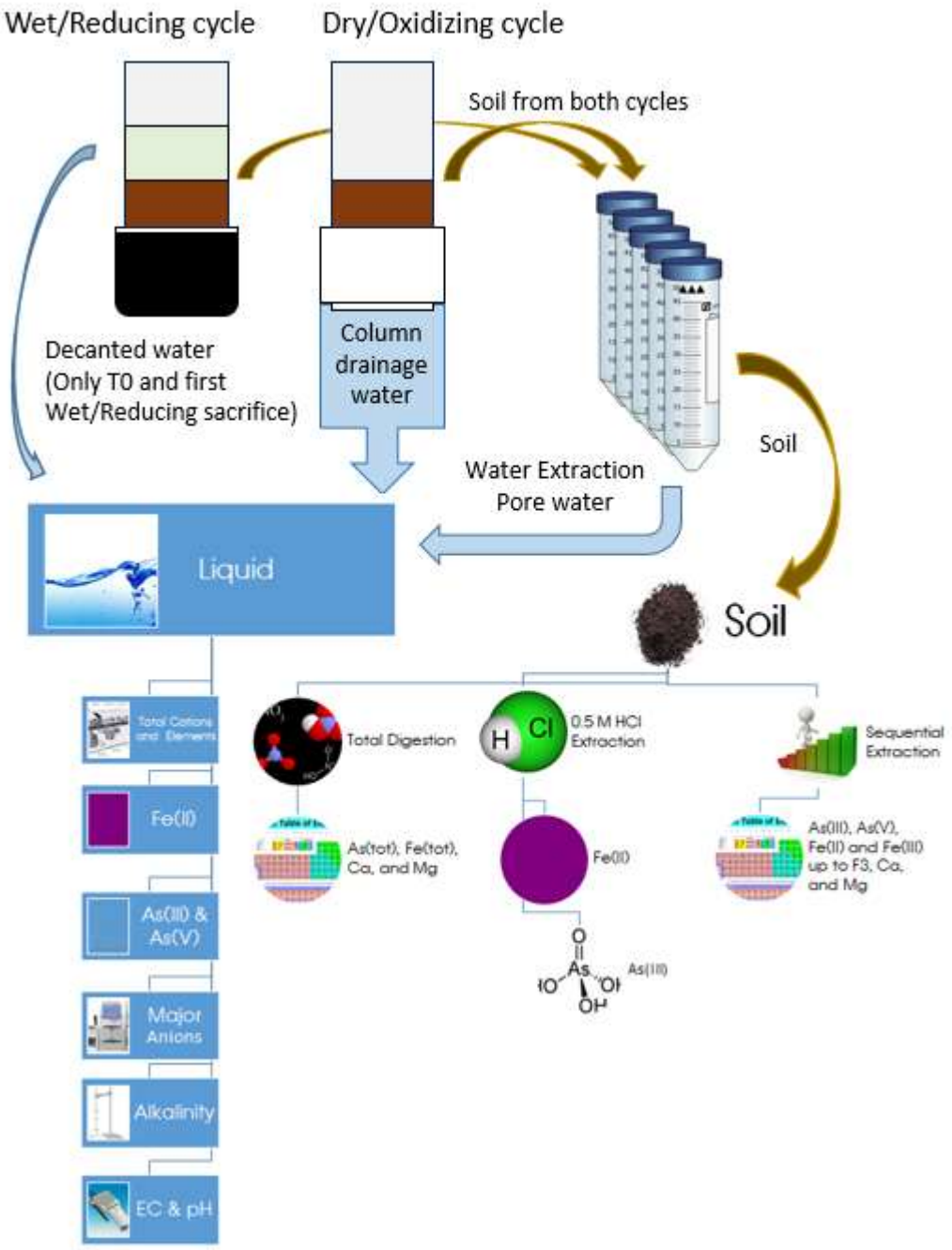

Fig. 23. Column sacrifice flow diagram, adapted from Kelsey Wagner (2017).

Soil sample analyses included an HCl extraction, an eight-step sequential extraction, and a residual digestion. The HCl extraction was performed using 0.5 M HCl

to recover Fe from $FeCO_3$, FeS, and poorly crystalline Fe oxides. This process also recovered As associated with these Fe minerals and other minerals with similar solubilities (Heron et al. 1994, Meng et al. 2017). In this study, 1.5 g wet weight solids and 20 mL of 0.5 M trace metal grade HCl was used. Samples were shaken for 2 hours and centrifuged at 10,000xg for 20 minutes. Supernatant was filtered through 0.2 μm nylon filters before analysis. The eight-step sequential extraction and residual digestion was conducted on a separate soil sample using 0.5 g wet weight solids and steps modified from Amacher (1996) and Huang and Kretzschmar (2010) procedures (Table 5).

The first two steps (F1, F2) are modified Amacher (1996) steps and were used instead of the first Huang and Kretzschmar (2010) step to avoid sodium diethyldithiocarbamate (NaDDC) complexing with Fe(II) and interfering with ferrozine analysis (F1). In addition, Huang and Kretzschmar (2010) do not include a carbonate step (F2). The ligand exchangeable Amacher (1996) step is modified with ammonium phosphate to provide anionic competition with ligand exchangeable arsenic oxyanions. The Amacher (1996) carbonate step is modified to a 24-hour shake time to increase the acido-soluble fraction as recommended by Gleyzes et al. (2002). The remaining steps (F3-F8) follow the Huang and Kretzchmar (2010) procedure as published. All extractions, including soil pore water, HCl extractions, and sequential steps F1-F4 were analyzed for Fe(II) using ferrozine reagent with spectrophotometry. Cations and trace elements were determined by ICP-MS. As(III) and As(V) were determined by LC ICP-MS as described in Meng (2017). Arsenic speciation was preserved with 5% v/v of 0.25 M EDTA for fractions F1 through F5. EDTA was not used for F6 and F7 due to

Table 5. Sequential Extraction (Amacher 1996, Huang and Kretzschmar 2010)

FRACTION	ARSENIC MINERAL ASSOCIATION	METHOD SUMMARY
F1	Ligand exchangeable	5 mM $NH_4H_2PO_4$ + 1 M NH_4Cl, pH=7, 20mL, vortex mix, 2-hr shaking, 20-min centrifuge, 0.2 µm filter
F2	Carbonates	1 M NH_4OAc (ammonium acetate), pH=5, 20mL, vortex mix, 24-hr shaking, 20-min centrifuge, 0.2 µm filter
F3	Organics	0.1 M sodium pyrophosphate + 0.2% NaDDC, 20mL, vortex mix, 1-hr shaking, 20-min centrifuge, 0.2 µm filter
F4	Acid volatile sulfides, Mn oxides, very poorly crystalline Fe oxides	1 M HCl + 10% HOAc (v/v) + 50 mM $HgCl_2$, 10mL per repetition, 1-hr shaking, 2 repetitions, 20-min centrifuge, 0.2 µm filter
F5	Amorphous iron oxides	0.2 NH_4^+-oxalate buffer (pH=3.25) + 10 mM $HgCl_2$, 10mL per repetition, vortex mix, 2-hr shaking in dark, 2 repetitions, 20-min centrifuge, 0.2 µm filter
F6	Sulfides	4 M HNO_3 + 0.5% APDC (w/v), 10mL per repetition, vortex mix, 1-hr shaking at 65°C, 2 repetitions, 20-min centrifuge, 0.2 µm filter
F7	Crystalline iron oxides	4 M HCl + 10% HOAc (v/v), 10mL, 1-hr shaking at 95°C, 20-min centrifuge, 0.2 µm filter
F8	Residual	Nitric Acid, microwave digestion (USEPA 3052)

precipitation of EDTA occurring at low pH. Soil samples from all sacrifices were weighed and corrected for dry weight during analysis. Wet soil was used in extractions to prevent any changes in redox states from drying.

6.1.1 Quality Control

All analyses followed the standard EPA method for project quality assurance and control (USEPA SW-846). This included blanks, calibration curves, and matrix spikes. Various blank samples were used to determine any contamination from instruments, during sample collection, or from reagent materials as appropriate. Calibration curves were used to determine the correct range and response from specific instruments. Continuous calibration verification (CCV) samples were used to verify no drift in the instrumentation. Matrix spikes were used to indicate any interference within a particular method on instrument readings.

6.1.2 Data and Statistical Analysis

All column data sets consisted of five independent columns for each treatment. Data below the minimum detection limit (MDL) were imputed using regression on Rankits method (Berthouex and Brown 2002) using log-normal distribution of quantifiable data and assigning a value randomly based on an extrapolation of that log-normal distribution. The method was only applied if >60% of the data were reportable to define the distribution of known values. With the exception of pH and Eh, data were log transformed to achieve normal distributions.

JMP 8.0 statistical software by SAS was used for all statistical analysis. Data were compared by one-way ANOVA to determine difference with sacrifice time within

treatment as well as differences among treatments within a sacrifice time. Post hoc testing was done with significant ANOVA's by Student's t-test or Tukey's HSD with $\alpha = 0.05$. Dunnett's test with $\alpha = 0.05$ was used to compare each sacrifice time to t0.

6.2 Results and Discussion

6.2.1 Initial Arsenic Concentrations and Soil Parameters in Column Study

Groundwater taken from P-2 for column construction was filtered through 0.45 μm nylon filters, homogenized, and separated according to each treatment, biotic (no treatment), carbon-enhanced (10 mM total C), and poisoned (500 mg/kg $HgCl_2$ when added to pre-column soil, 499.5 mg/L when added to water before inundation for second and third cycle). Samples from each treatment were taken for analysis prior to column construction. This pre-column construction groundwater contained an average As concentration of 22.9 ± 0.4 μg/L (Table 6) which was in the same range as the average As concentration observed during field sample collection (21.6 ± 11.8 μg/L, Table 5). Water not used to inundate the columns remained separated by treatment, stored in the N_2 atmosphere glovebag at 16 ± 1˚C and was supplemented by groundwater collected later from P-2 for inundation of Cycle 2 and 3 columns. This water was not routinely analyzed at each inundation step. Before the last inundation step, samples were again analyzed for As concentrations from this water for each treatment. The average As concentration had increased to 33.8 ± 6.1 μg/L (Table 6) due to seasonal variation of As concentrations as observed in the field study affecting the groundwater that was collected later. This concentration was higher than the average for P-2 but still within the overall range observed during field sampling (3.9-50.8 μg/L, Table 5). However, As(III) concentrations

in groundwater used for biotic and carbon-enhanced columns increased from 0.1 µg/L to 19.2 µg/L and 0.3 µg/L to 12.3 µg/L respectively while As(III) in poisoned columns decreased from 0.8 µg/L to 0.2 µg/L (Table 6). This indicates that microbial reduction of As was still occurring in the groundwater during storage and without suspended solids present; natural dissolved carbon sources in the unamended treatment were sufficient for As reduction, and the poisoned treatment was biologically inactive in reference to reduction of As. The groundwater was alkaline (pH = 8.02 ± 0.05, total alkalinity = 678 ± 87 mg $CaCO_3$/L). Other water quality parameters included: EC = 1.22 ± 0.14 S/m, DOC = 18.0 ± 5.3 mg/L, sulfate = 20.6 ± 0.26 mg/L, Mn = 75.8 ± 2.6 µg/L, Fe < 5.0 µg/L.

Table 6. Arsenic concentrations for water used in column study

Sampling time		Biotic	Carbon-Enhanced	Poisoned
Pre-column construction	As (µg/L)	22.9	22.5	23.3
	As(III) (µg/L)	0.1	0.3	0.8
End of study	As (µg/L)	40.7	27.2	32.9
	As(III) (µg/L)	19.2	12.3	0.2

Soil used in the columns was high in carbonates and fine-textured silty-clay (Table 7). Water extractable As concentrations from the soil was 0.08 ± 0.01 mg/kg (Table 8). The largest concentration of As was associated with carbonate minerals (F2) when comparing all sequential steps (Table 8, Fig. B-1) accounting for 28.1±% of the total As. Very amorphous Fe oxides, Mn oxides and acid volatile sulfides (F4) associated As, accounted for 24.4±% of the total As followed by ligand exchange (F1) at 14.7±%

and all other fractions at 4-11%. This is consistent with the findings of Abu-Ramaileh (2015) and Meng et al. (2016, 2017). This is however in contrast to studies of As contaminated sites where As was found to be primarily associated with Fe oxides (Wenzel et al. 2001, Pantuzzo and Ciminelli 2010, Kim et al. 2014) although Wenzel et al. (2001) and Kim et al. (2014) did not utilize a carbonate extraction step in their sequential extraction process. Most studies reported in the literature have focused on the importance of the relationship between Fe oxides in As biochemistry (Nordstrom 2002, Smedley and Kinniburgh 2002, Islam et al. 2004, Oremland and Stolz 2005, O'Day 2006, Huang 2014, Schaefer et al. 2016) without reporting on any role of carbonates.

Table 7. Analysis of initial soil parameters by USU Analytical Laboratories

pH	Salinity	Organic Carbon	Cation Exchange Capacity	Calcium Carbonate	Texture	Sand	Silt	Clay
	dS/m	%	cmol/kg	%		----------%----------		
8.4	0.67	0.4	5.2	40.2	Silty Clay	0	41	59

Table 8. Distribution of As concentrations for soil used in column study*.

	Water Extraction	F1	F2	F3	F4
As (mg/kg)					
Mean	0.08	1.89	3.71	0.50	3.08
SD (±)	0.01	0.07	0.04	0.06	0.22
Maximum	0.08	1.93	3.76	0.53	3.20
Minimum	0.06	1.80	3.69	0.43	2.82

*Water extraction is As easily desorbed/dissolved by double deionized water. F1-F4 are the first four steps of the sequential extraction operationally defining ligand exchangeable As (F1), associated with carbonate minerals (F2), organic matter (F3), and very amorphous Fe oxides, Mn oxides, and acid volatile sulfides (F4)

6.2.2 Time Zero Distribution of Arsenic

Arsenic concentrations in the water drainage collected at t0 increased significantly from initial groundwater concentrations (Fig. 24). As(III) concentrations also increased in biotic and carbon-enhanced columns, but remained consistent with initial concentrations in poisoned columns (Table 9). Although the biologically active columns released greater concentrations of As into the associated water, As was still released in abiotic columns consistent with findings of Abu-Ramaileh (2015).

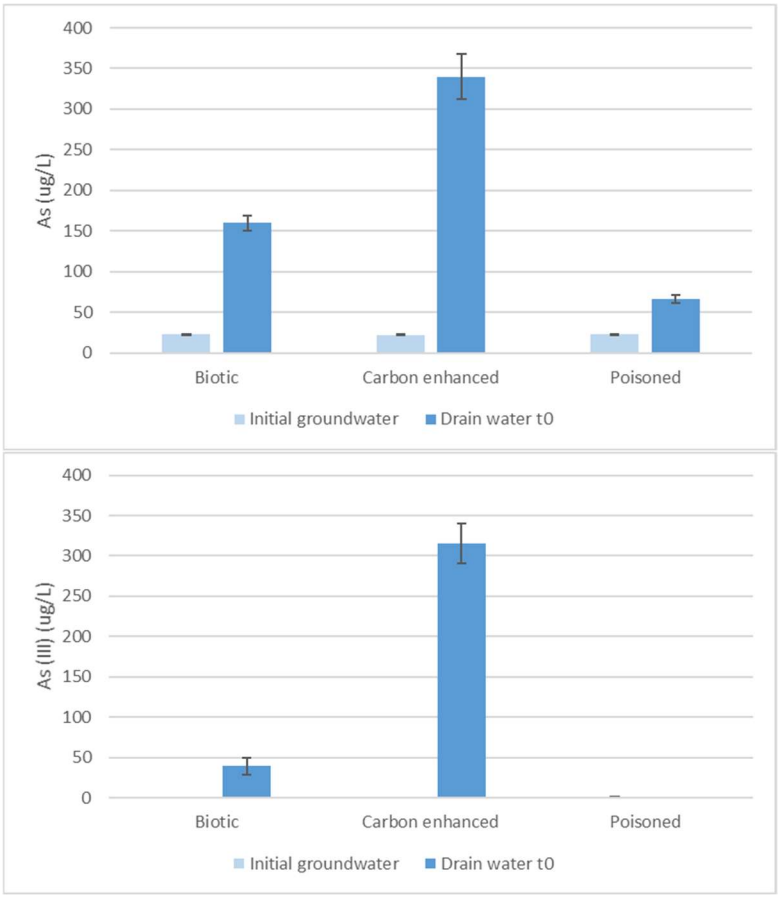

Fig. 24. Comparison of As and As(III) initial concentrations in groundwater and drained water at t0. Values for As(III) initial were 0.1, 0.3, and 0.8 µg/L in the groundwater and 0.2 ± 0.1 µg/L in the drainage water at t0 for the poisoned control.

Table 9. Arsenic concentrations in water drained from columns at time zero

	As (µg/L)	As(III) (µg/L)
Biotic		
Mean	160	39.8
SD (±)	9.0	10.5
Carbon-Enhanced		
Mean	340	315
SD (±)	28.2	24.6
Poisoned		
Mean	66.4	0.2
SD (±)	4.4	0.1

6.2.3 Mass Balance

Mass balance calculations were used to compare As in each sacrifice to As measured in the groundwater and soil under pre-column construction conditions and at t0. Arsenic concentrations were measured in water collected while draining columns. Due to no water being drained from the columns during oxidizing sacrifices, water from oxidizing columns was collected and analyzed at the same time as for the reducing columns. Soil concentrations are the sum of As measured in all sequential extraction steps conducted during respective sacrifices. Concentrations were corrected for total mass in the columns assuming 80 mL of water and using 100 g dry weight of soil. In all treatments and all sacrifices, percent recovery of As was >70% compared to pre-column conditions and only the third reducing sacrifices were <80% (Table 10). Comparisons to t0 concentrations also reflected >70% recovery for all treatments and sampling events. Changes in As concentration observed in source groundwater from the first inundation to the final inundation (Table 6) was less than 1% of aqueous As concentrations measured during each sampling event and was therefore not considered in calculations.

Table 10. Mass balance calculations for column sacrifices compared to pre-column and t0 As concentrations. Percent recovery based on total As concentrations measured in water collected during column drainage and in sequential extractions from column soil after each sampling event

Treatment	Sampling event	As (µg)	% recovery from pre-column	% recovery from t0
Biotic	Pre-column	1322		
	t0	1384	105%	
	Reducing 1	1269	96%	92%
	Oxidizing 1	1240	94%	90%
	Reducing 2	1100	83%	79%
	Oxidizing 2	1125	85%	81%
	Reducing 3	1002	76%	72%
	Oxidizing 3	1100	83%	80%
Carbon-enhanced	Pre-column	1322		
	t0	1297	98%	
	Reducing 1	1065	81%	82%
	Oxidizing 1	1186	90%	91%
	Reducing 2	1181	89%	91%
	Oxidizing 2	1140	86%	88%
	Reducing 3	962	73%	74%
	Oxidizing 3	1253	95%	97%
Poisoned	Pre-column	1247		
	t0	1304	105%	
	Reducing 1	1095	88%	84%
	Oxidizing 1	1242	100%	95%
	Reducing 2	1221	98%	94%
	Oxidizing 2	1200	96%	92%
	Reducing 3	1218	98%	93%
	Oxidizing 3	1349	108%	104%

6.2.4 Redox Conditions in Columns

Data indicate alternating aeration and redox conditions in laboratory columns were able to influence As speciation. For biotic, carbon-enhanced, and poisoned columns, measured DO in water drainage samples collected from columns drained in the N_2 atmosphere glovebag during reducing sacrifices contained DO concentrations <1 mg/L. Drainage water from columns designated for oxidizing sacrifices was also collected at the

same time, but were drained outside the glove bag in the ambient atmosphere. These water samples contained between 6 to 8 mg/L DO (Fig. 25) which was likely entrained in the water during sample collection. This indicates that oxygen was successfully purged from the water phase of the columns during reducing sacrifices. In comparison, field samples ranged from <1 mg/L to 5 mg/L DO.

To confirm altering redox conditions were occurring with treatment and cycling and that the poisoned columns were biologically inactive, the redox state of Fe extracted using the sequential extractant for dissolution of very amorphous Fe oxides (F4) was evaluated. Concentrations and speciation followed redox cycling in biologically active columns. In biotic columns, Fe(II) concentrations alternated according to reducing or oxidizing conditions while total Fe remained stable or decreased slightly compared to overall concentrations (Fig. 26-A). Carbon-enhanced columns followed the same alternating pattern as biotic columns for Fe(II), but total Fe was not as consistent (Fig. 26-B). In poisoned columns, Fe(II) concentrations did not alternate and instead gradually decreased while total Fe remained consistent (Fig. 26-C). For these poisoned columns, the oxidation state of Fe was not affected by alternating redox conditions indicating no biological activity.

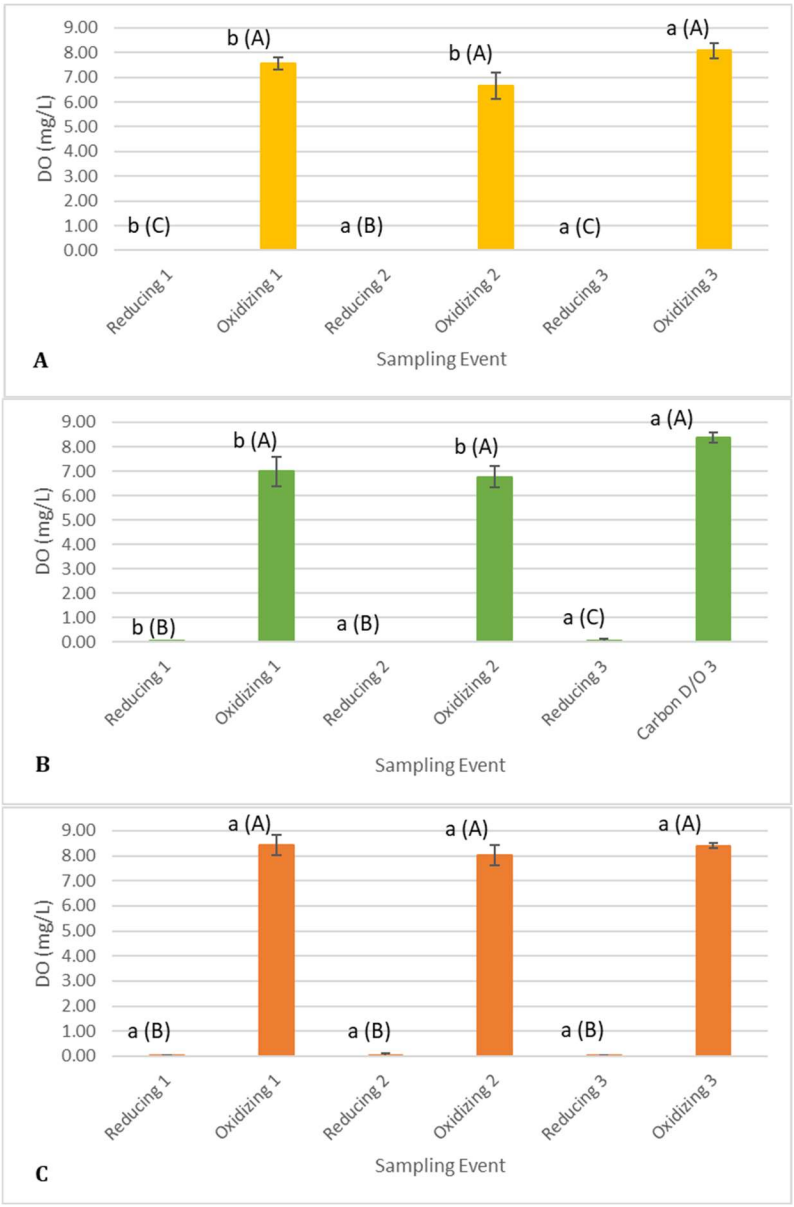

Fig. 25. Dissolved oxygen concentrations associated with drainage water for biotic (A), carbon-enhanced column treatments (B), and poisoned (C). Error bars represent standard deviation. Values compared using one-way ANOVA by the main effects individual treatments across sampling time and individual sampling time across treatments. Values in each treatment not connected by same letter are significantly different (α=0.05) by Tukey's honestly significant difference. Small letters reflect the comparison among treatments within a sampling event (within reducing 1 for example). Capital letters reflect the comparison across sampling events within a treatment (sampling events within the biotic treatment for example).

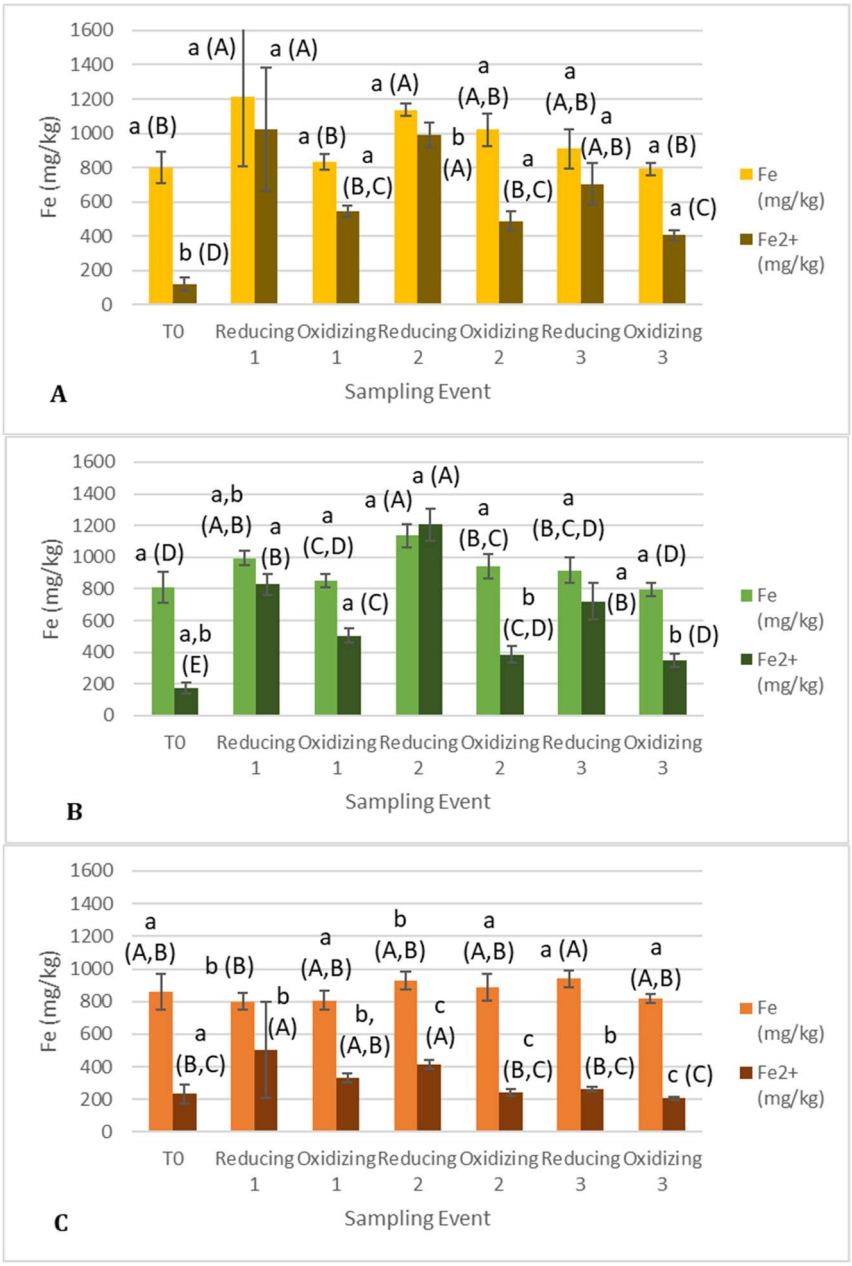

Fig. 26. Very amorphous total Fe and Fe(II) concentrations associated with soil as operationally defined in sequential step F4 for biotic (A), carbon-enhanced (B), and poisoned (C) column treatments. Error bars represent standard deviation. Values compared using one-way ANOVA by the main effects of sampling event within a treatment and treatment within each sampling event. Values in each treatment and for each Fe species not connected by same letter are significantly different (α=0.05) by Tukey's honestly significant difference. Small letters reflect the comparison among treatments within a sampling event. Capital letters reflect the comparison across events within a treatment.

To further determine biological inactivity in poisoned columns, redox indicators in the column water were analyzed by redox condition and by column treatment (Table 11). Mn and Fe concentrations, which are sensitive to redox conditions, were significantly higher during reducing conditions in biotic and carbon-enhanced columns compared to oxidizing conditions while their concentrations in the poisoned columns remained consistent. This same pattern of significant differences in biotic and carbon-enhanced columns and consistency in poisoned columns was observed for sulfide and sulfate concentrations as well as Eh (Table 11). This supports the assumption of non-biological activity in the poisoned columns. Additionally, this indicates that the biotic columns were providing a bioavailable source of C sufficient for microbial reduction chemistry. Meng (2015) also observed this similar bioavailability of C at the study site.

Table 11. Redox indicator parameters in column pore water. Values compared by two-way ANOVA. Values not connected by same letter are significantly different (α=0.05) by Tukey's honestly significant difference

	Oxidizing conditions		Reducing conditions	
Mn (µg/L)	Biotic	3.7^{C}	Biotic	14.9^{B}
	Carbon-enhanced	2.9^{C}	Carbon-enhanced	19.5^{A}
	Poisoned	2.3^{C}	Poisoned	3.3^{C}
Fe (µg/L)	Biotic	9.0^{B}	Biotic	15.6^{AB}
	Carbon-enhanced	9.7^{B}	Carbon-enhanced	43.7^{A}
	Poisoned	7.8^{B}	Poisoned	9.5^{B}
Sulfide (mg/L)	Biotic	11.6^{C}	Biotic	26.4^{A}
	Carbon-enhanced	12.7^{BC}	Carbon-enhanced	22.6^{AB}
	Poisoned	12.3^{BC}	Poisoned	17.2^{ABC}
Sulfate (mg/L)	Biotic	17.6^{B}	Biotic	1.3^{D}
	Carbon-enhanced	25.8^{A}	Carbon-enhanced	0.1^{D}
	Poisoned	7.0^{C}	Poisoned	8.2^{C}
Eh (mV)	Biotic	364^{A}	Biotic	170^{B}
	Carbon-enhanced	384^{A}	Carbon-enhanced	243^{B}
	Poisoned	360^{A}	Poisoned	16.5^{A}

Finally, visual observation of the columns also provided evidence of biological activity in biotic and carbon enhanced columns and non-reactivity in the poisoned columns. Soil in both biotic and carbon enhanced columns changed color from light tan to gray (biotic) or dark green (carbon-enhanced) during the first reducing cycle and remained in this state regardless of redox condition throughout the experiment. Additionally, carbon enhanced columns contained large amounts of dark green (biological) matter floating in the water above the column during wet cycles. Poisoned columns remained light tan in color for the entirety of the experiment (Fig. B-4).

6.2.5 Redox Activity of As in Columns

The total mass of As(V) and As(III) the sum of mass in the aqueous phase (drainage water) and solid phase As(V) and As(III) cycled according to redox conditions in biologically active columns (Fig. 27). In biotic and carbon-enhanced columns, As(III) increased under reducing conditions with a corresponding decrease in As(V). As(III) then decreased under oxidizing conditions while As(V) increased (Fig. 27-A, B). This further indicates that naturally occuring carbon in the columns was sufficient to promote microbial reduction of As without any supplemental source of carbon as was also observed by Meng (2015). Poisoned columns did not cycle As speciation according to redox condition and instead As(III) generally decreased over time (Fig. 27-C). Further analysis will focus on the native biotic and abiotic controls.

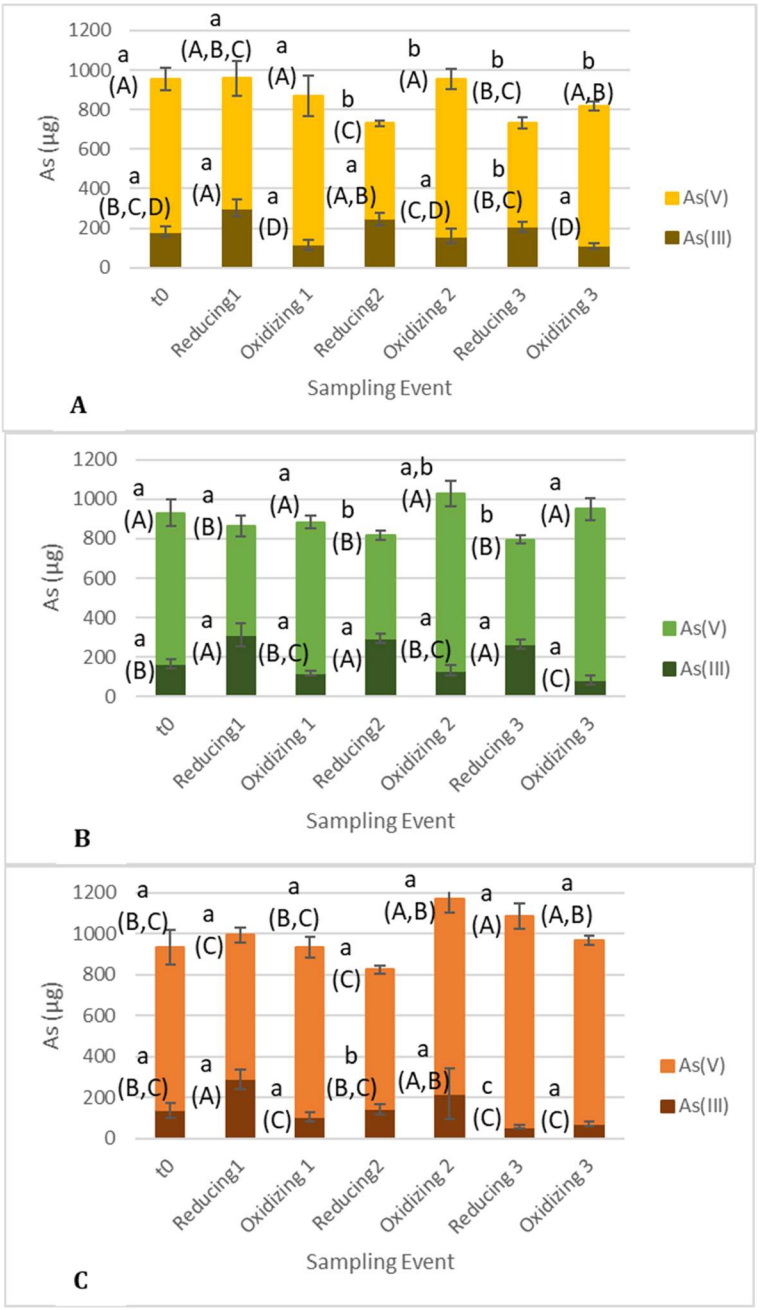

Fig. 27. Arsenic speciation measured in columns for biotic (A), carbon-enhanced (B), and poisoned (C) columns. Mass measured includes As in drainage water and soil. Arsenic concentrations in water were corrected assuming 80 mL of water per column. Arsenic concentrations in soil were corrected with measured 100 g of dry soil per column. Error bars represent standard deviation. Values compared using one-way ANOVA by the main effects of sampling event within a treatment. Values in each sacrifice not connected by same letter are significantly different (α=0.05) by Tukey's honestly significant difference. Small letters reflect the comparison among treatments within a sampling event. Capital letters reflect the comparison across events within a treatment.

6.2.6 Fate of Arsenic Associated with Column Water

Arsenic was released to the drainage water from biotic and abiotic treatments in every sacrifice cycle (Fig. 28). Arsenic concentrations in water collected when columns were drained were statistically higher in all redox cycles compared to t0 with the exception of the third oxidizing cycle in the biotic columns. This indicates both biologically driven and abiotic releases of As to the column water. All concentrations measured after t0 were also consistently greater than the MCL for As of 10 μg/L by at least one magnitude regardless of redox conditions in both biotic and abiotic columns (Fig. 28). This is consistent with the findings of Abu-Ramaileh (2015) which indicated As was released to water regardless of the biological or redox state of the sample. However, As leached from biotic columns was statistically greater compared to abiotic columns in all sacrifices (Fig. 28).

Water drained from the columns was not useful in determining redox cycling of As due to water drainage from both reducing and oxidizing columns being collected at the same time after each reducing cycle. Since drained water for reducing cycle columns was collected in the glove bag under nitrogen and drained water for oxidizing columns was collected at the same time in the ambient atmosphere, the oxidation state of As would only be dependent on speciation changes occurring during collection. Additionally, since oxidizing columns were kept dry for 4 weeks after the end of reducing cycles no drainage water was available for collection after oxidizing cycles. Therefore, water extractions of the sediments were performed to determine the oxidation state of As. Water extractions were intended to collect As associated with water still held

by soil in the columns as well as easily exchangeable As on soil surfaces (hereafter collectively referred to as pore water).

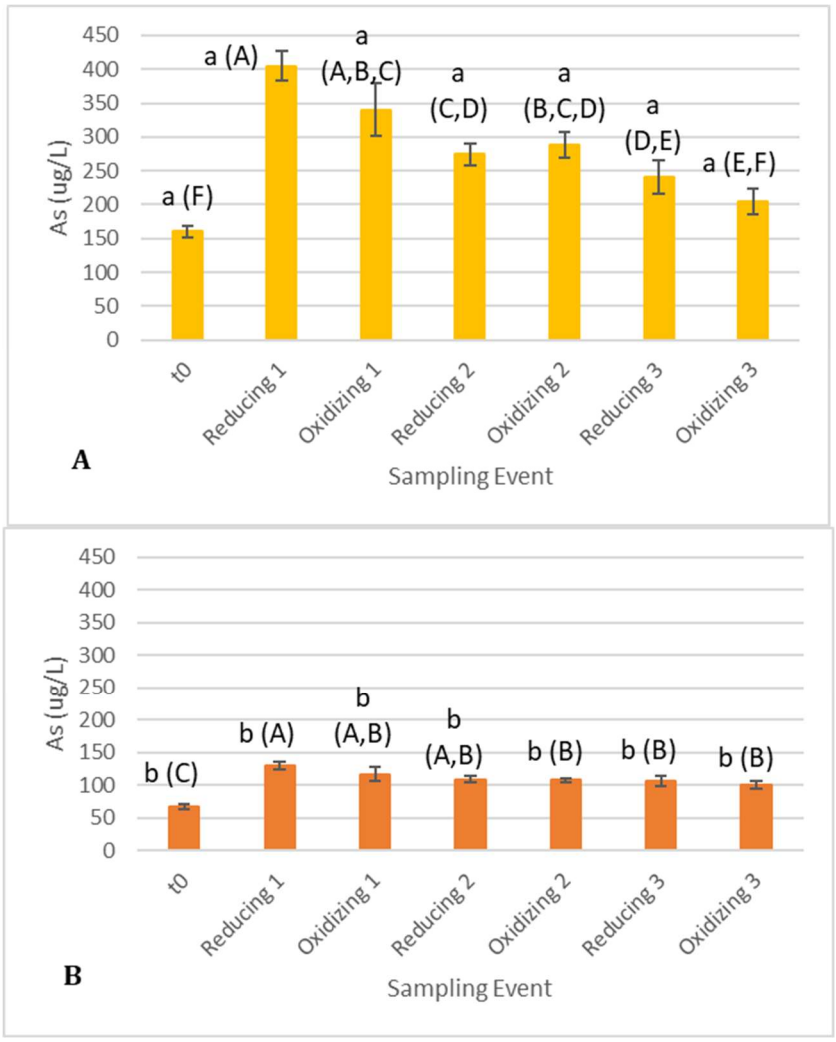

Fig. 28. Arsenic concentrations in drainage water collected before reducing sacrifices for biotic (A) and abiotic (B) treatments. Error bars represent standard deviation. Values compared using one-way ANOVA. Values not connected by same letter are significantly different (α=0.05) by Tukey's honestly significant difference. Small letters reflect the comparison between treatments within a sampling event. Capital letters reflect the comparison across events within a treatment.

Microbe-controlled redox cycling influenced As speciation in column pore water. For biotic columns, As(III) accounted for >40% of total As concentrations in all reducing sacrifices. As(III) concentrations in all oxidizing sacrifices was significantly lower (Fig. 29-A). In comparison, As speciation did not cycle in abiotic columns and As(III) remained consistently below 5% of total As in all sacrifices (Fig. 29-B). This difference in As cycling among the column treatments is consistent with Abu-Ramaileh's (2015) findings that the presence of As(III) in solution was dependent on microbial activity.

Total As concentrations in pore water also increased significantly after t0, but then remained consistent for all remaining sacrifices regardless of redox condition or biological activity (Fig. 30). Biotic columns did have a trend of decreasing As concentrations, but only oxidizing sacrifice 3 and reducing sacrifice 1 are statistically different (Fig. 30-A). Values observed ranged from 0.05 mg/kg As to 0.25 mg/kg As. These values are equivalent to 38.5 to 192 μg/L As in the pore water, exceeding the MCL for As. Others (Nordstrom 2002, Smedley and Kinniburgh 2002, Islam et al. 2004, O'Day 2006, Schaefer et al. 2016, 2017, Duan et al. 2019) reported increase release of As under anerobic conditions due to the reductive dissolution of Fe(III) oxides. This study did not observe any statistically significant differences in total As in the pore water as a function of redox condition after t0.

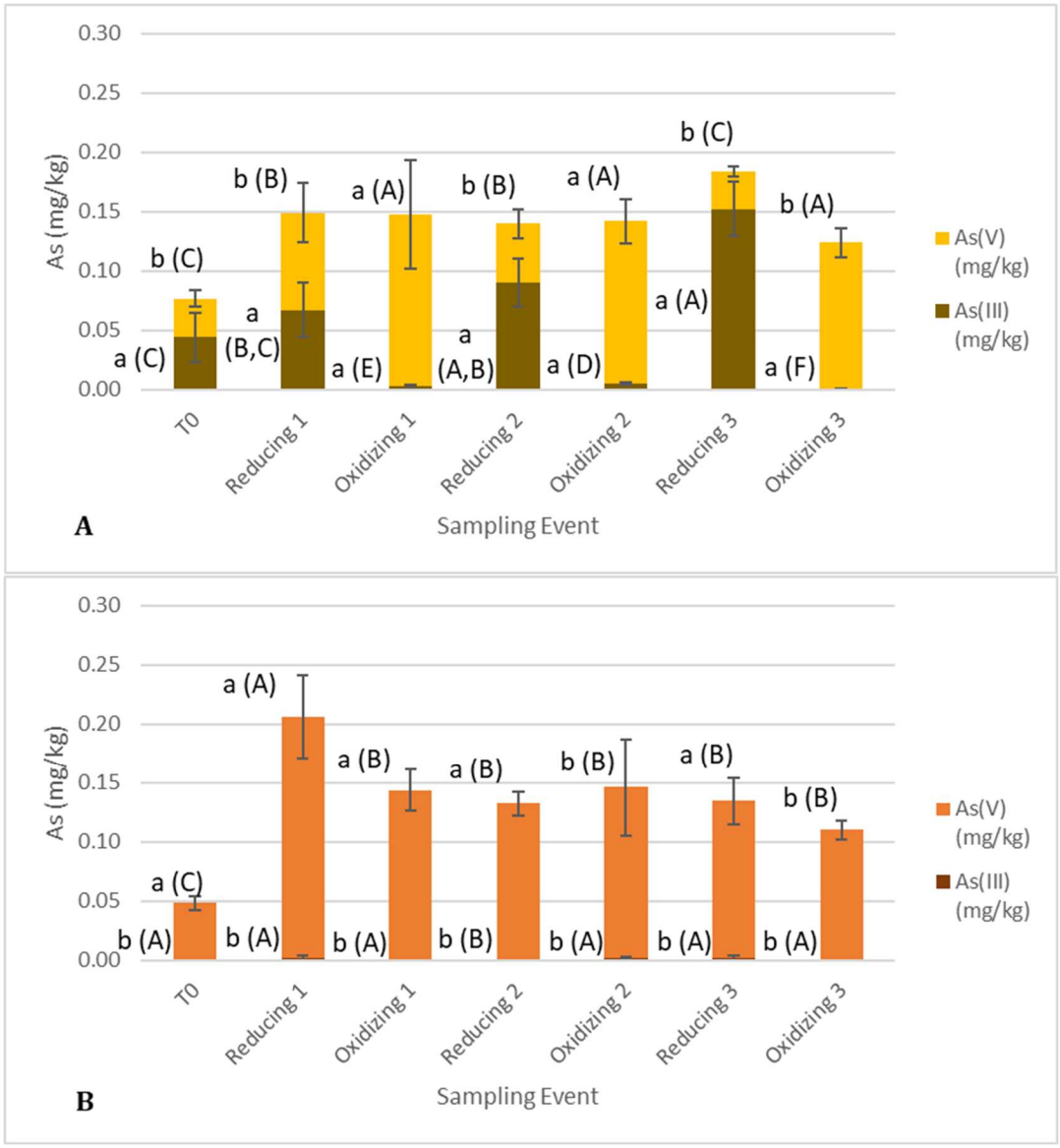

Fig. 29. Arsenic speciation associated with pore water in biotic (A) and abiotic (B) column treatments. Error bars represent standard deviation. Values compared using one-way ANOVA. Values for each speciation not connected by same letter are significantly different (α=0.05) by Tukey's honestly significant difference. Small letters reflect the comparison between treatments within a sampling event. Capital letters reflect the comparison across events within a treatment.

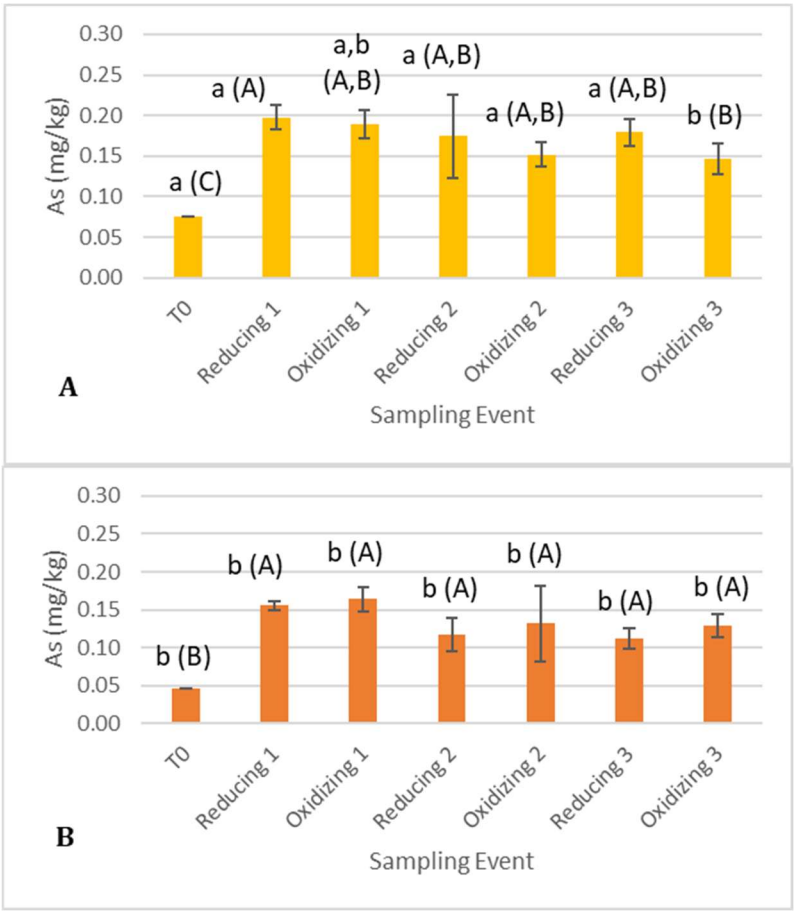

Fig. 30. Pore water arsenic concentrations for biotic (A), and abiotic (B) column treatments. Samples collected by addition of double-deionized water to column soils followed by centrifuge separation of liquids and solids. Liquid concentrations were then corrected using dry soil weight. Error bars represent standard deviation. Values compared using one-way ANOVA. Values not connected by same letter are significantly different (α=0.05) by Tukey's honestly significant difference. Small letters reflect the comparison among treatments within a sampling event. Capital letters reflect the comparison across events within a treatment.

Concentrations of As measured in drainage water were consistently higher (160-404 µg/L) in all sacrifices (Fig. 28) compared to the averages measured in the groundwater used for column inundation (23-34 µg/L) (Table 6). The continued release of As to drainage water, despite regular flushing of As from the columns, indicates that

As was being supplied from various solid phases in the columns. The observation that total As concentrations in the pore water were consistent within treatments over time and relatively consistent across treatments (Fig. 30) indicates that the pore water-solids return to the same equilibrium conditions, but redox species changed in biologically active systems (Fig. 29). Therefore, what is controlling As solubility is independent of time/redox cycling and although abiotic processes cause the release of less As than biotic processes, abiotic processes still result in consistent As release. Arsenic is then reduced in solution after it is solubilized as opposed to As being reduced directly from the solids.

6.2.7 Fate of Arsenic Associated with Column Soil

Arsenic was leached out of the columns (Fig. 28, 29). Therefore, As was being released from the column soil. Analysis of As-associated mineral phases as defined by sequential extractions indicates the primary sources of this release (Fig. 31, 32, Table 12, 13). Easily exchangeable ligands (F1) released a significant amount of As after the first reduction/oxidation cycle with the second and third reducing cycles being significantly lower than initial conditions (Fig. 31, Table 12). Arsenic then accumulated under oxidizing conditions. This indicates that surfaces are acting as both a source and sink for As with more As associated with F1 under oxidized conditions when columns are drained compared to reducing/wet conditions. These surfaces then release As under reducing conditions when inundated. Organic matter (F3) initially serve as a sink for As in the first reducing step, but As is then lost from organic matter with time with slightly more retention under reducing conditions. Another source of As was from Mn oxides and very amorphous Fe oxides (F4) in both reducing and oxidizing sacrifices (Fig. 31-A,B).

Statistically, only the values measured in F4 in the final reducing or oxidizing sacrifice are significantly different from the respective first reducing or oxidizing sacrifice. However, both redox conditions show a consistent trend of decreasing values through progressive cycles. Amorphous iron oxides (F5) released a significant amount of As after t0 then also remained consistent through the remainder of the cycles (Table 12). In general, F1, F3, F4, and F5 behaved in a similar manner with an overall loss of As associated with each of their respective mineral phases, the only difference being the timing and rate of release. Arsenic concentrations associated with carbonate minerals (F2), however, remained consistent for all redox conditions and sequential steps including t0 (Fig. 31, Table 12).

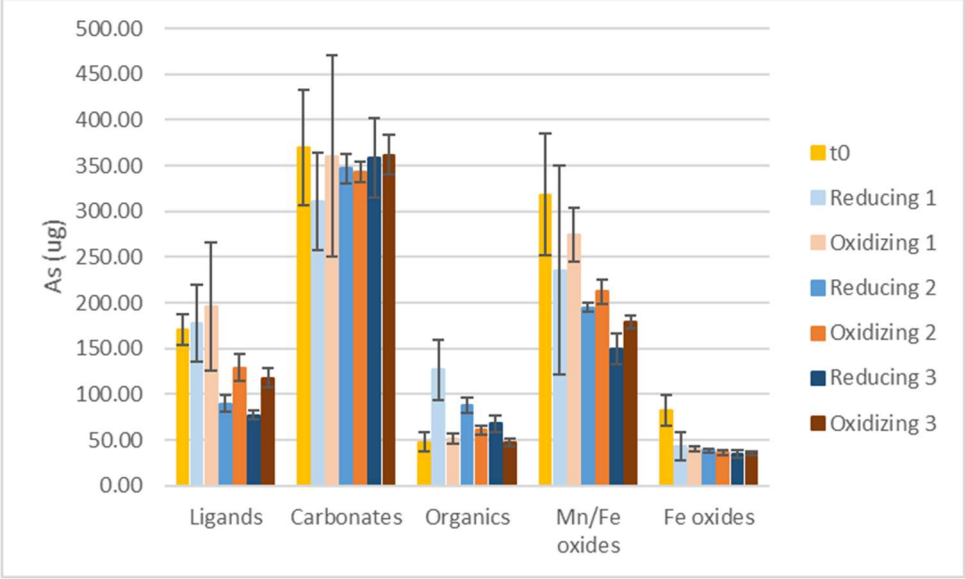

Fig. 31. Mass of As associated with sequential extraction steps performed on column soil for each sampling event in biotic columns. Error bars represent standard deviation.

Table 12. Mass of As associated with sequential extraction steps performed on column soil for each reducing and oxidizing sacrifice in biotic columns with statistical analysis. Values were compared using one-way ANOVA. Values not connected by same letter for each sequential step are significantly different by Tukey's HSD.

Sequential Step	t0 (μg)	Reducing 1	Oxidizing 1	Reducing 2	Oxidizing 2	Reducing 3	Oxidizing 3
F1	171 A,B	178 A,B	195 A	90 D,E	129 B,C	77 E	118 C,D
F2	369 A	311 A	360 A	347 A	343 A	358 A	362 A
F3	48 D	127 A	51 C,D	88 B	61 C,D	68 B,C	47 D
F4	318 A	235 A,B,C	275 A,B	195 B,C	212 A,B,C	150 C	179 C
F5	82 A	43 B	40 B	38 B	36 B	34 B	35 B
F6	145 A	155 A	132 A	119 A,B	138 A	99 B	119 A,B
F7	173 A	123 A	107 A	111 A	110 A	92 A	114 A
F8	65 A	64 A	52 A	57 A	45 A	50 A	60 A

The trend of As release from the organic (F3), Mn oxide and very amorphous Fe oxide (F4) and amorphous Fe oxide (F5) phases is not observed in the abiotic columns (Fig. 32, Table 13); total As associated with these organics and minerals does not change with time or redox condition. The ligand exchange (F1) step is the only sequential step to experience a sustained loss of As with significant decreases in mass after reducing/oxidizing cycle 1. The mass of As then remains consistent through the remaining cycles (Fig. 32, Table 13) unlike the biotic columns that showed cycling of the source/sink for As associated with the F1 step. All other sequential steps either remain consistent from t0 to sacrifice 3 or experience an increase in associated As mass. This is also reflected with a lower cumulative mass of As associated with drainage water in abiotic columns (27.6 ± 0.9 μg) compared to biotic (73.5 ± 1.3 μg).

Arsenic associated with carbonates (F2) in abiotic columns was lower for reducing step 1 compared to t0, but had an increasing trend in each following step (Fig. 32, Table 13). Additionally, data from sequential step F2 shows that As concentrations

were the same for biotic and abiotic samples across time (Fig. 33). This consistency indicates that carbonate minerals may serve as a reliable sink for As contamination in groundwater consistent with the findings of Costagliola et al. (2013) regardless of redox conditions or biotic/abiotic processes. The association of As with carbonate minerals was observed in the field study where As was positively correlated with Mg and carbonates.

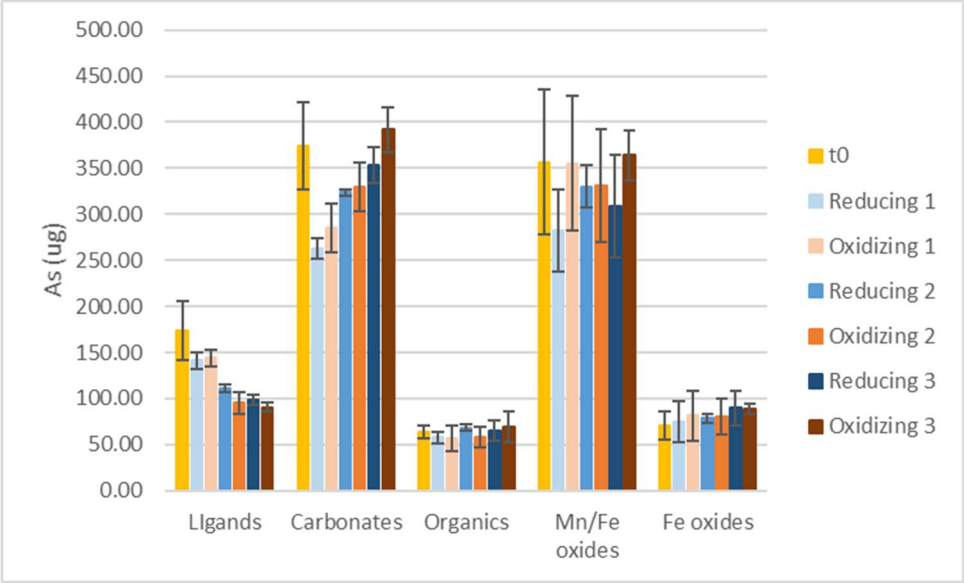

Fig. 32. Mass of As associated with sequential extraction steps performed on column soil for each sampling event in abiotic columns. Error bars represent standard deviation.

Table 13. Mass of As associated with sequential extraction steps performed on column soil for each reducing and oxidizing sacrifice in abiotic columns with statistical analysis. Values were compared using one-way ANOVA. Values not connected by same letter for each sequential step are significantly different by Tukey's HSD.

Sequential Step	t0 (µg)	Reducing 1	Oxidizing 1	Reducing 2	Oxidizing 2	Reducing 3	Oxidizing 3
F1	173 A	141 A	144 A	110 B	95 B	99 B	90 B
F2	374 A,B	262 D	285 C,D	324 B,C	329 B,C	353 A,B	392 A
F3	64 A	58 A	57 A	68 A	58 A	65 A	69 A
F4	357 A	282 A	355 A	330 A	331 A	309 A	364 A
F5	71 A	75 A	81 A	78 A	80 A	89 A	89 A
F6	133 A,B	130 A,B	148 A	120 B	149 A	121 B	136 A,B
F7	69 C	88 A,B	110 A,B	113 A,B	101 A,B	102 A,B	122 A
F8	58 A	49 A,B	52 A,B	57 A	39 B	53 A	62 A

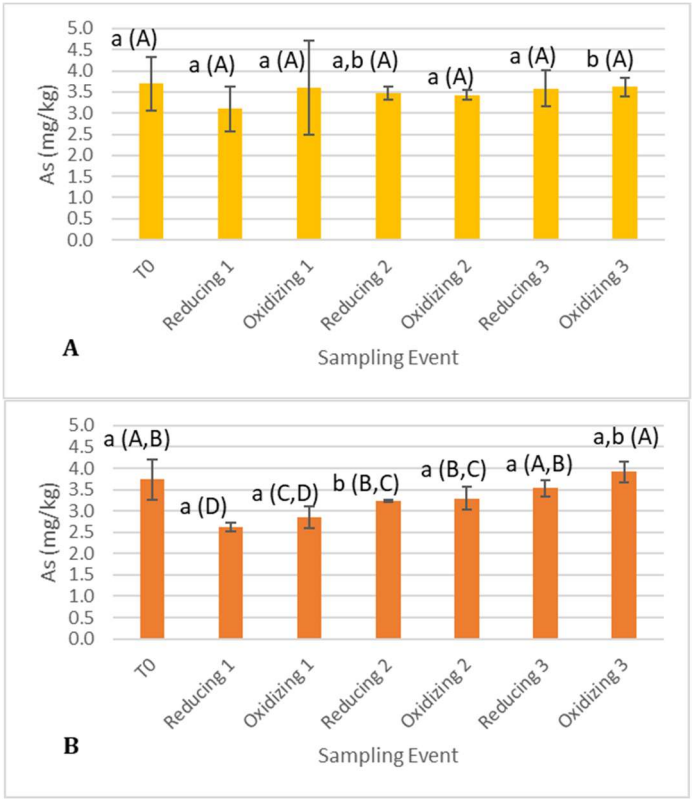

Fig. 33. Total As concentrations associated with carbonate minerals for biotic (A) and abiotic (B) column treatments. Error bars represent standard deviation. Values compared using one-way ANOVA. Values in each treatment not connected by same letter are significantly different (α=0.05) by Tukey's honestly significant difference. Small letters reflect the comparison among treatments within a sampling event. Capital letters reflect the comparison across events within a treatment.

6.2.8 Redox Cycling of As Associated with Column Soil

Analysis of changes in As speciation in column soil provides insight into the processes causing release of As from specific mineral phases. In biotic columns, As(III) associated with Mn and very amorphous Fe oxides (F4) increased in the first reducing sacrifice compared to t0 while As(V) decreased (Fig. 31, Table 14). For the remaining sacrifices, As(III) gradually declined (with the exception of the second oxidizing sacrifice) while As(V) remained in a depleted state. This indicates that most As(V) was reduced to As(III) before the first reducing sacrifice. This reduction of As(III) was in conjunction with reduction of Fe associated with F4 (Fig. 26-A) likely causing release of As associated with these oxides. As(III) associated with these oxides was never oxidized back to As(V) in any remaining sacrifices and instead was gradually removed from these minerals while Fe continued to cycle according to redox conditions (Fig 26-A). This shows that As associated with Mn oxides/Fe oxides was not directly affected by redox cycling or by the cycling of Fe. Data also did not display a positive correlation between As and Fe to indicate release of As with reductive dissolution of Fe(III) oxides nor reincorporation of As with precipitation of the oxides under oxidizing conditions. Instead As(V) was permanently removed from the Fe oxide structure by the first reducing step and not coprecipitated with the oxide minerals.

Resorption of As(V) under oxidizing conditions was observed in surface interactions (F1). This is similar to findings of Schaefer et al. (2016, 2017) and Duan et al. (2019) who observed diminishing Fe(II) and As concentrations during oxidizing periods and concluded that Fe oxides sorbed As through the formation of surface

complexes, removing As from the groundwater. Details of As sorption to various Fe oxide surfaces are given in Waychunas et al. (1993), Fendorf et al. (1997), and Dixit and Hering (2003). A key difference between this thesis work and these previous studies is that microcosm studies reported by Schaefer et al. (2016,2017) and Duan et al. (2019), that were associated with field observations, were stagnant, allowing for more resorption of As to occur. The removal of As during drainage in this study after each reducing step minimized how much As could be resorbed.

For As associated with carbonate minerals (F2), As(III) concentrations increased in reducing sacrifices and decreased in oxidizing sacrifices while As(V) concentrations cycled inversely to As(III) (Fig. 31, Table 14). Organic associated (F3) minerals show an increase in As(III) concentrations during reducing conditions. However, As(V) did not cycle indicating that speciation was not based on cycling of As associated with F3 and was based on the redistribution of As(III) in the columns.

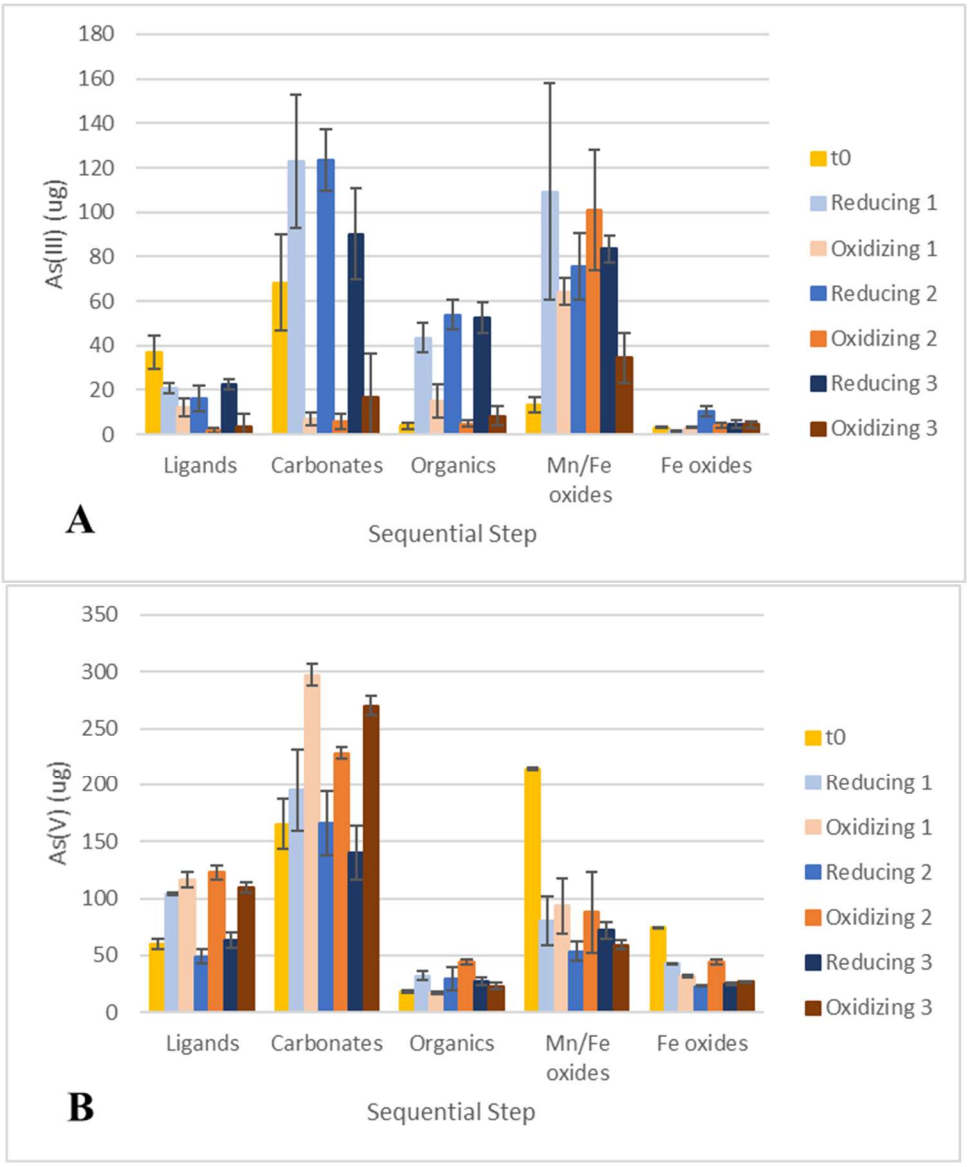

Fig. 34. Mass of As(III) (A) and As(V) (B) associated with sequential extraction steps performed on column soil for each sacrifice in biotic columns. Error bars represent standard deviation.

Table 14. Mass of As(III) and As(V) associated with sequential extraction steps performed on column soil for each sacrifice in biotic columns with statistical analysis. Values were compared using one-way ANOVA. Values not connected by same letter for each sequential step are significantly different by Tukey's HSD.

As(III)							
Sequential Step	t0 (µg)	Reducing 1	Oxidizing 1	Reducing 2	Oxidizing 2	Reducing 3	Oxidizing 3
F1	46 A	14 C,D	16 B,C,D	32 A,B	9 D	26 A,B,C	11 D
F2	99 A	121 A	12 C	92 A	18 B,C	81 A	28 B
F3	3 C	19 A	4 B,C	34 A	4 C	25 A	7 B
F4	10 E	134 A	69 B,C	62 B,C	102 A,B	53 C,D	35 D
F5	4 A,B	2 C	3 B,C	5 A	5 A,B	4 A,B	3 A,B,C
F6	13 A	4 A,B	4 B,C	4 C	11 A,B	7 A,B,C	14 A
F7	6 A	2 B,C	1 C	0.5 D	3 A,B	2 B,C	3 A,B
As(V)							
Sequential Step	t0 (µg)	Reducing 1	Oxidizing 1	Reducing 2	Oxidizing 2	Reducing 3	Oxidizing 3
F1	60 B	104 A	116 A	49 B	123 A	64 B	110 A
F2	165 C,D	195 B,C	297 A	166 C,D	228 A,B	140 D	270 A
F3	18 C	32 A,B	17 C	29 A,B	44 A	23 B,C	23 B,C
F4	214 A	80 B	94 B	54 B	88 B	72 B	72 B
F5	74 A	43 B	32 B,C	23 C	45 B	25 C	27 C
F6	145 A	109 B,C	122 A,B,C	97 C	151 A	118 A,B,C	129 A,B
F7	85 A,B	82 B,C	61 D	65 C,D	107 A	78 B,C,D	80 B,C

In abiotic columns, for As associated with Mn oxides and very amorphous Fe oxides (F4), As(V) was reduced to As(III) before the first reducing sacrifice similar to biotic columns (Fig. 35, Table 15). This is again in conjunction with an increase in Fe(II) from t0 to reducing sacrifice 1 despite a lack of redox cycling in the remaining steps in the abiotic columns (Fig. 26-C). This indicates that, as the columns were in reducing conditions for the first 70 days, either cessation of biological activity in the abiotic columns was not immediate or abiotic redistribution of Fe(II) and As(III) occurred during the initial inundation of the columns. As(III) then shows a similar trend of removal of mass from these oxide minerals over time as observed for the biotic columns. As(V) remains consistent, again similar to biotic columns but at significantly higher

concentrations than observed for the biotic treatment. These observations along with no observed cycling of Fe in abiotic columns (Fig. 26-C) indicate that loss of As(III) from these minerals was from abiotic processes and not related to Fe reduction. For As associated with easily exchangeable ligands (F1), As(III) decreases significantly after the first reducing sacrifice while As(V) remains consistent and no redox cycling was observed (Fig. 35, Table 15).

Cycling of As speciation associated with carbonate minerals was also observed in abiotic columns (Fig. 35, Table 15) and no cycling of Fe in F4 (Fig 26-C). As(V) increased with oxidation and As(III) increased with reducing conditions. This cycling was unexpected due to As(V) reduction to As(III) requiring microbial activity (Mirza et al. 2014, Abu-Ramaileh 2015, Meng et al. 2016, Chang et al. 2018). After the first oxidizing step, As(III) concentrations should have remained low and not increased in any later step. As(III) was present in the groundwater used to inundate the columns at the start of each reducing step (Table 6). However, the greatest concentration of As(III) measured in this groundwater was 19.2 μg/L. Each column held approximately 80 mL of groundwater and 100 mg of soil. Therefore, the maximum concentration of As(III) that was added during each inundation would equal $1.5x10^{-3}$ mg/kg, or 0.3% of the lowest As(III) concentration measured in the abiotic columns during a reducing sacrifice. Reagent and sample blanks analyzed throughout the project did not show As contamination of the acetate buffer (pH=5.0) used to extract As from carbonate minerals. EDTA was added to the supernatant after extraction to preserve the oxidation state of the

As. Therefore there is no evidence of a systematic error in this extraction step to account for the redox cycling under abiotic conditions.

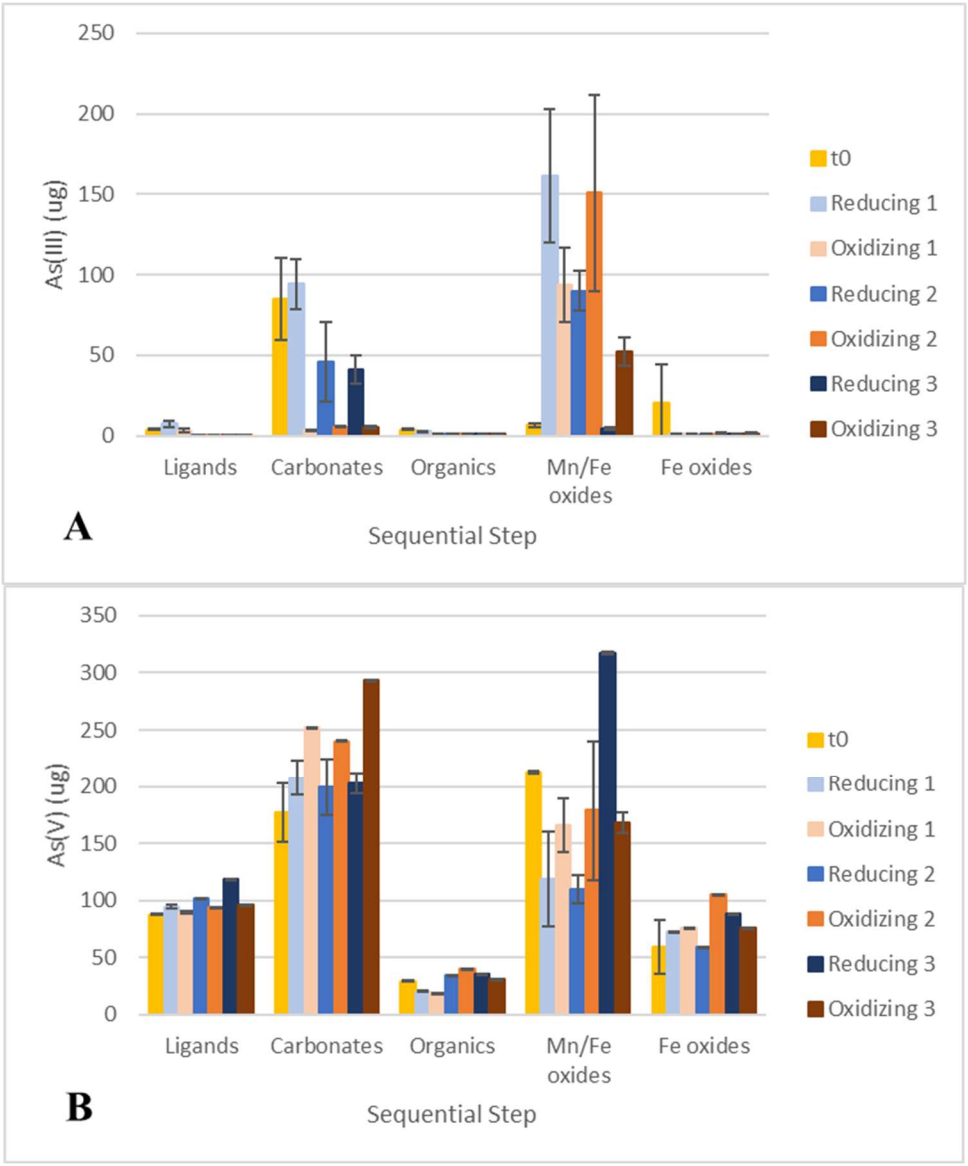

Fig. 35. Mass of As(III) (A) and As(V) (B) associated with sequential extraction steps performed on column soil for each sacrifice in abiotic columns. Error bars represent standard deviation.

Table 15. Mass of As(III) and As(V) associated with sequential extraction steps performed on column soil for each sacrifice in abiotic columns with statistical analysis. Values were compared using one-way ANOVA. Values not connected by same letter for each sequential step are significantly different by Tukey's HSD.

As(III)							
Sequential Step	t0 (µg)	Reducing 1	Oxidizing 1	Reducing 2	Oxidizing 2	Reducing 3	Oxidizing 3
F1	4 A	7 A	3 B	<0.1 C	<0.1 C	0.3 B	0.2 B
F2	85 A,B	94 A	4 C	46 B	6 C	41 A,B	5 C
F3	4 A	3 B	1 C	1 C	1 C	1 C	1 C
F4	7 D	162 A	94 B	90 B	151 A,B	5 D	52 C
F5	21 A	1 B	1 B	1 B	1 B	1 B	2 B
F6	12 A	6 A	3 A	4 A	9 A	6 A	9 A
F7	5 A	15 A	1 B	0.4 B	49 A	2 A,B	2 A,B
As(V)							
Sequential Step	t0 (µg)	Reducing 1	Oxidizing 1	Reducing 2	Oxidizing 2	Reducing 3	Oxidizing 3
F1	88 B	94 B	89 B	101 A,B	94 B	119 A	96 B
F2	177 E	208 C,D	252 A,B	199 D,E	240 B,C	203 D,E	293 A
F3	30 B	20 C	18 C	35 A,B	40 A	35 A,B	31 B
F4	213 A,B	119 C,D	166 B,C,D	110 D	179 B,C	317 A	168 B,C,D
F5	59 B	73 A,B	76 A,B	60 B	105 A	88 A,B	76 A,B
F6	139 C	115 D	150 B,C	103 D	201 A	168 B	149 B,C
F7	84 A	69 A	67 A	67 A	87 A	91 A	74 A

However, while the sequential extraction reagents were used to target specific mineral phases, each reagent is not exclusive to that mineral (Meng 2015). Dissolution of non-targeted minerals, resorption of As to other solids, and other interactions not considered in this study may have influenced the results. Collection of soil from columns sacrificed during oxidizing steps did expose the soil to higher oxygen concentrations in the atmosphere compared to columns that were sacrificed during reducing steps. However, the exposure time was limited to less than 10 minutes and oxidation of As(III) due to atmospheric oxygen has been found to be slow (Frank and Clifford 1986, Kim and Nriagu 2000). Finally, in the abiotic columns, no redox cycling was observed in As associated with pore water (Fig. 29-B), or easily exchangeable ligands (F1) (Fig. 35,

Table 15). In addition, there was variability, but no observed redox cycling of Fe associated with carbonate minerals (F2) in abiotic columns (Fig. 36), but cycling was observed in biotic columns (Fig. 36). The abiotic columns being biologically inactive as shown in Section 6.4.4 and the lack of any evidence of redistribution from other minerals indicates that the cycling of As speciation associated with carbonate minerals was an abiotic process. Biologically active columns still contained concentrations of As(III) twice the concentrations in abiotic columns for reducing steps 2 and 3 (Table 14, 15) indicating that microbial activity was still significant in As speciation cycling.

Abiotic transformation of As has been coupled with Fe and S redox chemistry, but has been found to be significantly slower than microbial processes. Palmer and von Wandruszka (2010) demonstrated humic acid as a reducing agent in the reduction of As(V) to As(III). Huang (2014) reviewed the process by which both Fe oxide and Mn oxide surfaces have been shown to oxidize As(III) to As(V), with Mn oxides being more reactive than Fe oxides (Manning et al. 2002). Perez et al. (2019) also observed enhanced reduction of As due to the surface associated Fe(II)-goethite redox couple. For reactivity of As associated with carbonate, Renared et al. (2015) speculate that calcite surfaces may catalyze the oxidation of As(III) with the incorporation of As(V) into the calcite minerals. Yokoyama et al (2012) verified the oxidation of As(III) in the presence of calcite and attributed the reaction to complex formation between Ca-arsenate that drives this oxidation with the presumed oxidant being dissolved oxygen, altering the redox boundary of As(III)/As(V). These studies were with calcite and specific reactivity of other

carbonate minerals is not known, but should be similar in the fundamental interactions of As with carbonate surfaces.

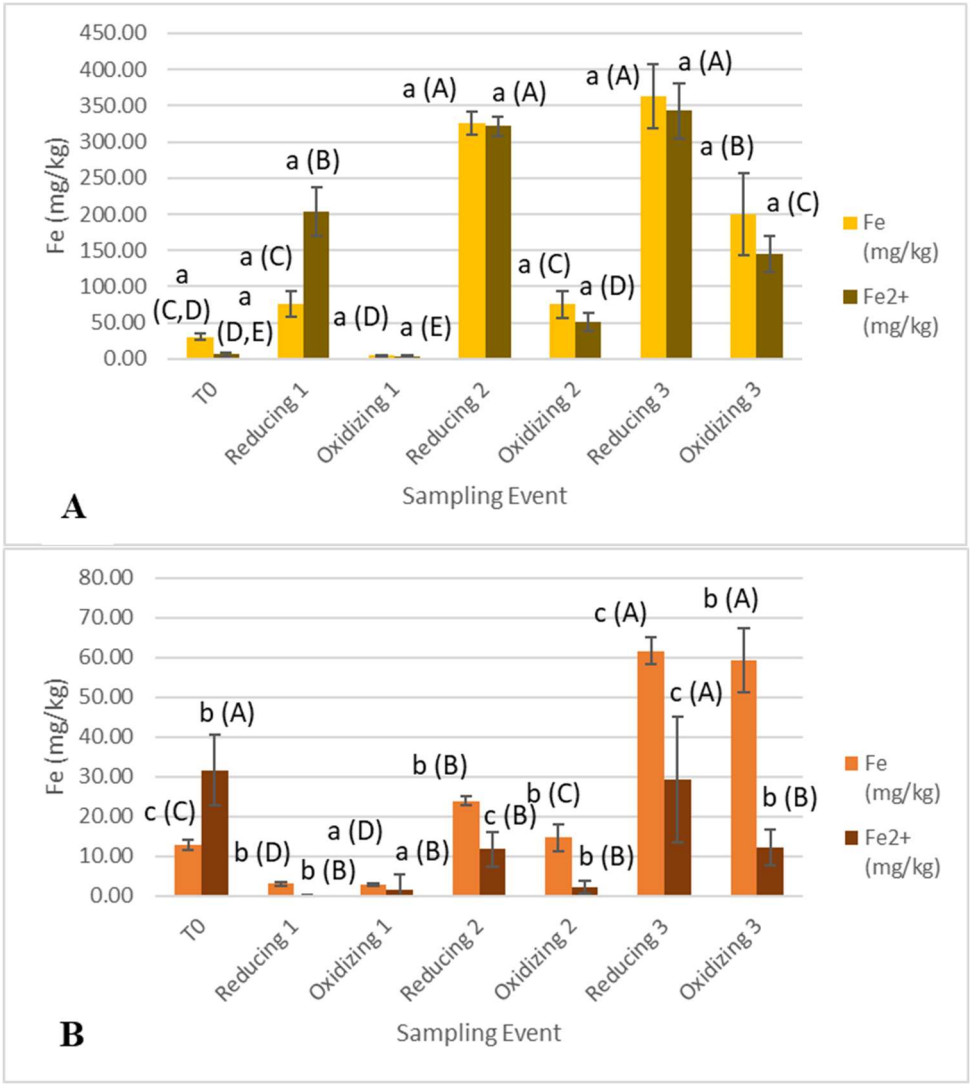

Fig. 36. Fe concentrations associated with carbonate minerals (F2) in column soil for biotic (A) and abiotic (B) treatments. Error bars represent standard deviation. Values compared using one-way ANOVA. Values in each treatment not connected by same letter are significantly different (α=0.05) by Tukey's honestly significant difference. Small letters reflect the comparison among treatments within a sampling event. Capital letters reflect the comparison across events within a treatment.

6.2.9 Fate of As associated with Mg and Ca Carbonates

Abu-Ramaileh (2015) concluded that dissolution from calcite was a factor in As release to surrounding groundwater. However, data from this column study indicate that total As concentrations associated with carbonate minerals did not decrease with time or treatment (Fig. 33). One explanation for this discrepancy is the source of the groundwater used in Abu-Ramaileh's (2015) microcosm study. To avoid background As concentrations, Abu-Ramaileh (2015) collected groundwater from an area near NP13 that was not contaminated with As, but was also lower in concentration of Ca, Mg, and alkalinity. Geochemical differences in this groundwater may have facilitated dissolution of carbonate minerals and release of associated As. Groundwater in these column studies was taken from the study site and was closer to geochemical equilibrium with the column soil.

Analysis of Mg and Ca concentrations in pore water and associated with carbonates in the biotic columns provides additional information (Fig. 37). Significantly larger concentrations of Mg and Ca are released to the pore water at t0 compared to all other sacrifices (Fig. 37-A,C). Additionally, Mg associated with carbonates briefly decreased during the first sacrifices before returning to t0 levels (Fig. 37-B). Abu-Ramaileh (2015) used microcosms without water cycling that may have only reflected these initial steps. Arsenic released in these initial steps may have been associated with non-structured Mg or Ca carbonates as opposed to highly structured carbonate minerals that are less kinetically favored to dissolve (Berner and Morse 1974). Abiotic columns

followed similar patterns with Mg and Ca concentrations associated with pore water and carbonates (Fig. B-5).

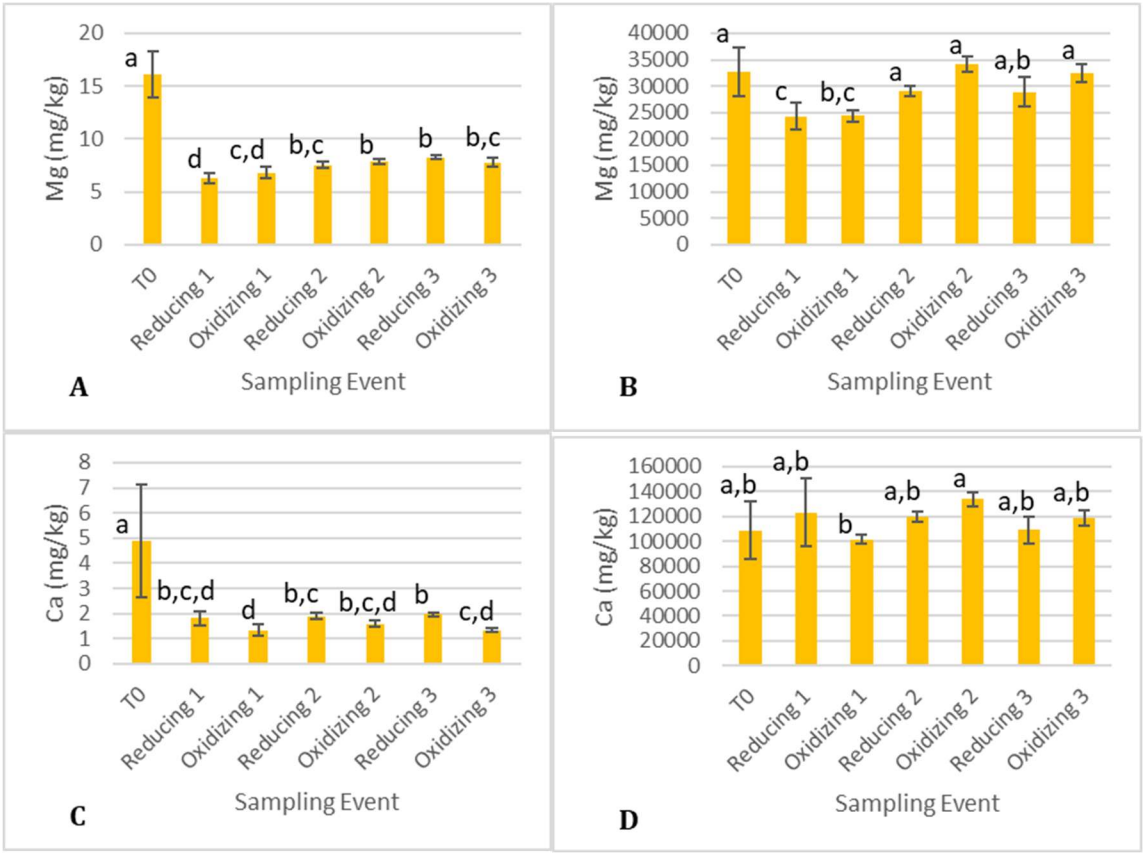

Fig. 37. Concentrations of pore water Mg (A), Mg associated with carbonates (B), pore water Ca (C), and Ca associated with carbonates (D) for biotic columns. Error bars represent standard deviation. Values compared using one-way ANOVA. Values in each graph not connected by same letter are significantly different (α=0.05) by Tukey's honestly significant difference.

Although there is disagreement in the literature, more recent articles using advanced imaging methods illustrate that As(V) associates with calcite through co-precipitation and not surface interactions (Winkel et al. 2013). As(III) is not incorporated

to the same extent as As(V). In this study, As speciation (37% As(III), 63% As(V)) during reducing conditions was the same as reported by Renard et al. (2015) for arsenic incorporated into calcite. Although calcite in this study may not be the main carbonate involved, studies reported in the literature focus only on calcite; whether the interaction of As with other carbonates behaves the same as calcite has not been reported. Sequential extractions in this study were not selective to amorphous versus crystalline carbonate minerals nor selective to calcite ($CaCO_3$) versus magnesite ($MgCO_3$), but As(III) was found to associate with carbonates similar to findings of previous studies (Yokoyama et al. 2009, Bardelli et al. 2011, Costagliola 2013).

6.3 Conclusion

Previous studies (Abu-Ramaileh 2015, Meng et al. 2016, Schaefer et al. 2016, 2017, Duan et al. 2019) used batch microcosm studies to supplement field data collected during the same study or previous related studies. However, these microcosms consisted of small quantities of soil relative to incubation water, used deionized water or groundwater not from the study site, and (with the exception of Duan et al. 2019) were sacrificed without any cycling of redox conditions. Microcosms for this study were specifically constructed to simulate soil/water ratios, groundwater fluctuations, redox cycling, and used water from the study site. Additionally, this study used a quasi-flow system where As was removed from the system during collection of drainage water as opposed to batch systems used by the previously mentioned studies.

Columns were successful in creating alternating redox conditions. In biologically active columns, redox sensitive species, including As in pore water, cycled accordingly

while poisoned columns experienced no cycling. Indigenous organic carbon was also sufficient in quantity and quality to drive microbial reactions within biologically active columns over the course of the study. Arsenic cycling between reducing and oxidizing conditions was observed for As associated with ligand exchangeable (F1), carbonates (F2) and organically associated (F3) solids.

Arsenic speciation associated with carbonate minerals was also influenced by redox conditions regardless of biotic or abiotic conditions within the columns (Fig. 31, Fig. 32). This cycling of As speciation appears to be abiotic due to no evidence of biological activity occurring in the poisoned columns, as well as no evidence of external contamination occurring during sacrifices. Although cycling of As speciation occurred for all treatments, biologically active columns were additionally influenced by microbial reduction of As associated with carbonate minerals.

Concentrations of total As associated with carbonate minerals remained consistent with time regardless of redox condition. Abu-Ramaileh (2015) and Meng et al. (2016) observed release of As from high-carbonate soil profiles with Abu-Ramaileh (2015) observing that release of As was not limited to microbially-driven reducing conditions. This release of As into column water was also observed during the t0 sacrifice regardless of treatment. However, this release of As appears to be associated with loosely bound Mg(Ca)-carbonates naturally occurring in the soil or as a result of disturbance during column construction. Subsequent sacrifices indicated that structured carbonates and associated As concentrations remained stable but As species cycled according to redox condition regardless of treatment. Similarly, Costagliola et al. (2013) found that naturally

occurring calcite can serve as a long-term trap for As since dissolution usually takes place only under acidic conditions and is unaffected by ligand exchange and redox reactions. Winkel et al. (2013) also observed that calcite could trap a large fraction of As when Fe-oxides were not sufficiently abundant to act as a major scavenger of As. Other carbonates may have similar interactions with As, but are not reported in the literature.

The dissolution of As was continuous in both redox conditions and all treatments. Initial release of As, particularly in biologically active columns, was from reductive dissolution of Mn and Fe oxides. Successive releases of arsenic were then associated with surface interactions, as indicated by sequential extraction fraction F1, during reducing conditions as well as continued, gradual releases of As (III) from Mn and Fe oxides. Schaefer et al. (2017) observed a similar, redox-controlled release of As from Fe oxides during seasonal groundwater cycling. Similarly, in this study, data indicate that once As was released from Fe oxide structures in the columns it was removed permanently from that mineral structure and reabsorbed onto mineral surfaces during oxidizing conditions.

The general view from previous studies is that As is released with reductive dissolution of Fe oxides under anaerobic conditions then is resorbed by newly formed Fe oxides under oxic conditions (Nordstrom 2002, Smedley and Kinniburgh 2002, Dixit and Hering 2003, Islam et al. 2004, O'Day 2006, Schaefer et al. 2016, 2017, Duan et al. 2019). Therefore, it is expected to observe connections between Fe and As cycling. In this study, however, the pore water concentrations do not change after initial conditions. The release of As to the drainage water is from As associated with various mineral surfaces not discernable by techniques used in this study. Arsenic was initially released

from Fe/Mn oxides, redistributed onto surfaces during oxidizing conditions, then released by surface interactions under reducing conditions. Guo et al. (2013) observed changes in As, specifically without changes in Fe, and attributed this to the reductive desorption of As with release of As(III) without dissolution of Fe minerals. This reductive desorption of As without dissolution of Fe minerals was also observed in this field study where As(III) was not correlated with other field parameters.

CHAPTER 7

SUMMARY AND CONCLUSIONS

Arsenic concentrations in groundwater at the study site were influenced by annual fluctuations in groundwater recharge. During the first year, when recharge was high with high concentrations of DO and DOC, As concentrations were low. The high concentration of DO promoted conditions conducive to oxidizing conditions favoring precipitation of FeOOH, as predicted by geochemical modeling, with sorption or incorporation of As to these minerals. Mg- and Ca-based carbonates in the groundwater were also oversaturated, promoting precipitation of these minerals that may have contributed to the removal of As from the groundwater through sorption and co-precipitation processes. During the second year and in drier seasons, with lower recharge volumes, As concentrations in groundwater were higher, DO and DOC were lower, reducing conditions were favored, and As was released into groundwater and reduced to As(III). However, negative correlations of As and Fe and sulfides indicates that retention of As in Year 1 and release of As into the groundwater in Year 2 were not exclusively based on association with Fe and sulfur minerals. A lack of correlation between As(III) and Fe or S indicates that release and reduction of As into the groundwater may have been a result of direct microbial reductive desorption of As as opposed to a release of As(III) from dissolution of Fe minerals or other associated minerals. During this second year, carbonate mineral concentrations within the pore water, in particular Mg carbonate, were also undersaturated creating a potential for dissolution of these minerals and the release of associated As.

Arsenic was released in the biotic column study from Mn and Fe oxides; these oxides were subject to reductive dissolution by the first reducing step and released As(V) was reduced to As(III). Once As(V) was released from the Mn and Fe oxides it did not co-precipitate with these same oxides in subsequent redox cycles indicating that co-cycling of As and Fe was not occurring in the columns, supporting the field-study observation of the lack of correlation between Fe and As. As(III) associated with these oxides continuously decreased over time and was also independent of Fe cycling associated with alternating redox conditions. Ligand exchange sites were the source and sink of As over the course of the study, with release of As to the drainage water under reducing conditions and subsequent sorption of As to these surfaces under oxidizing conditions.

Arsenic speciation associated with carbonates was influenced by redox conditions in all treatments. Despite alternating As speciation, total As concentrations associated with carbonate minerals remained constant for all sacrifices after t0. This indicates that carbonates, which are not influenced by fluctuations in redox conditions, serve as a stable reservoir for As, particularly in higher pH environments.

CHAPTER 8

ENGINEERING SIGNIFICANCE

Understanding the influence of water cycles and groundwater recharge on As concentrations in groundwater is important in protecting public safety. Measurements of As concentrations during times of high water levels with high DO concentrations may result in a false negative or a severe underestimation of potential As concentrations in groundwater. Multiple measurements, conducted at different groundwater levels, during different seasons, and even different years will provide a more comprehensive assessment of potential As contamination in shallow groundwater aquifers. Understanding the influence of groundwater level on As concentrations may also provide insight into times when an otherwise As-contaminated well may contain concentrations below the MCL of 10 μg/L, thus decreasing the potential for As poisoning from the ingestion of this water. This knowledge will allow for development of water management strategies to minimize dissolution of As.

Carbonate minerals, although generally not containing as high of concentrations of As compared to Fe oxides or sulfur minerals, may provide a stable and secure sink for As. Carbonate minerals do not react to changes in redox conditions, and structured carbonates tend to dissolve only under acidic conditions. This provides the opportunity for prevention or remediation of As contaminated groundwaters using carbonate minerals. Potential uses may include addition of carbonate minerals or amendments to aquifers that could sorb soluble As, removing it from the aqueous phase, particularly in areas that are subject to frequent redox cycling. Additionally, understanding the stability

of carbonate minerals with respect to As can result in more informed decisions when locating and determining depth of shallow groundwater wells and even stormwater structures.

REFERENCES

Abu-Ramaileh, A. (2015). "The Influence of a Fluctuating Water Table on Arsenic Mobility in a Western U.S. Aquifer." thesis, presented to Utah State University at Logan, UT, in partial fulfillment of the requirements for the Degree of Master of Science in Civil and Environmental Engineering, https://digitalcommons.usu.edu/etd/4582/.

Ahmad, K. (2001). "Report highlights widespread arsenic contamination in Bangladesh." *The Lancet*, 358(9276), 133.

Ahmann, D., Krumholz, L.R., Hemond, H.F., Lovley, D.R., Morel, F.M.M. (1997). "Microbial mobilization of arsenic from sediments of the Aberjona Watershed." *Environmental Science & Technology.* 31, 2923-2930.

Alexandratos, V. G., Elzinga, E. J., and Reeder, R. J. (2007). "Arsenate uptake by calcite: Macroscopic and spectroscopic characterization of adsorption and incorporation mechanisms." *Geochimica et Cosmochimica Acta*, 71(17), 4172–4187.

Ali, W., Mushtaq, N., Javed, T., Zhang, H. Ali, K., Rasool, A., Farooqi, A. (2019). "Vertical mixing with return irrigation water the cause of arsenic enrichment in groundwater of district Larkana Sindh, Pakistan." *Environmental Pollution,* 245, 77-88.

Amacher, M.C. (1996). Nickel, cadmium, and lead. In: Sparks, D., Page, A., Helmke, P., Loeppert, R., Soltanpour, P., Tabatabai, M., Johnston, C., Sumner, M. Methods of Soil Analysis, Part 3-Chemical Methods. *Soil Science Society of America*. Madison, WI, pp. 739-768.

Anning, D. W., Paul, A. P., Mckinney, T. S., Huntington, J. M., Bexfield, L. M., and Thiros, S. A. (2012). "Predicted Nitrate and Arsenic Concentrations in Basin- Fill Aquifers of the Southwestern United States." *USGS Scientific Investigations Report*, 5065.

Appelo, C. A. J., Van Der Weiden, M. J. J., Tournassat, C., and Charlet, L. (2002). "Surface complexation of ferrous iron and carbonate on ferrihydrite and the mobilization of arsenic." *Environmental Science and Technology*, 36(14), 3096–3103.

Bardelli, F., Benvenuti, M., Costagliola, P., Di Benedetto, F., Lattanzi, P., Meneghini, C., Romanelli, M., Valenzano, L. (2011). "Arsenic uptake by natural calcite: An XAS study" *Geochimica et Cosmochimica Acta*, 75, 3011-3023.

Benner, S. G., Polizzotto, M. L., Kocar, B. D., Ganguly, S., Phan, K., Ouch, K., Sampson, M., and Fendorf, S. (2008). "Groundwater flow in an arsenic-contaminated aquifer, Mekong Delta, Cambodia." *Applied Geochemistry*, 23(11), 3072–3087.

Berg, M., Tran, H.C., Nguyen, T.C., Pham, H.V., Schertenleib, R., Giger, W. (2001). "Arsenic contamination of groundwater and drinking water in Vietnam: A human health threat." *Environmental Science & Technology,* 35 (13), 2621–2626.

Berthouex, P. M., and Brown, L. C. (2002). *Statistics for Environmental Engineers,* 2nd Ed., Boca Raton, Florida.

Boggs, S. J. (2009). *Petrology of Sedimentary Rocks*. Cambridge University Press.

Boggs, S. J. (2012). *Principles of Sedimentology and Stratigraphy*. (A. Dunaway and C. Dudonis, eds.), Pearson Education, Inc., Upper Saddle River.

Cao, X., Ma, L. (2004). "Effects of compost and phosphate on plant arsenic accumulation from soils near pressure-treated wood." *Environmental Pollution,* 132(2004), 435-442.

Catelani, T., Perito, B., Bellucci, F., Lee, S. S., Fenter, P., Newville, M., Rimondi, V., Pratesi, G., Costagliola, P. (2018). "Arsenic uptake in bacterial calcite." *Science Direct,* 222, 642-654.

Chang, J. S., Yoon, I. H., Kim, K. W. (2018). "Arsenic biotransformation potential of microbial arsH responses in the biogeochemical cycling of arsenic-contaminated groundwater." *Chemosphere,* 191, 729-737.

Chen, C.J., Chuang, Y.C., Lin, T.M., Wu, H.Y. (1985). "Malignant neoplasms among residents of a blackfoot disease endemic area in Taiwan: high-arsenic artesian well water and cancers." *Cancer Research,* 45(11 Pt 2), 5895–5899.

CHWA. Cache Highline Water Association. (2014). "Logan & Northern Canal Piping & Pressurization Project." < https://www.cachehighline.com/projects/logan-northern-canal-project.html> (November 7, 2018).

Costagliola, P., Bardelli, F., Benvenuti, M., Di Benedetto, F., Lattanzi, P., Romanelli, M., Paolieri, M., Rimondi, V., and Vaggelli, G. (2013). "Arsenic-bearing calcite in natural travertines: Evidence from sequential extraction, μxAS, and μxRF." *Environmental Science and Technology*, 47(12), 6231–6238.

Cullen, W. R., and Reimer, K. J. (1989). "Arsenic speciation in the environment." *Chemical Reviews*, American Chemical Society, 89(4), 713–764.

Dietrich, S., Bea, S. A., Weinzettel, P., Torres, E., and Ayora, C. (2016). "Occurrence and distribution of arsenic in the sediments of a carbonate-rich unsaturated zone." *Environ Earth Sci,* 75:90.

Dixit, S., and Hering, J. G. (2003). "Comparison of arsenic(V) and arsenic(III) sorption onto iron oxide minerals: Implications for arsenic mobility." *Environmental Science and Technology*, 37(18), 4182–4189.

Duan, Y., Gan, Y., Wang, Y., Deng, Y., Guo, X., Dong, C. (2015). "Temporal variation of groundwater level and arsenic concentration at Jianghan Plain, central China." *Journal of Geochemical Exploration,* 149, 106-119.

Duan, Y., Schaefer, M. V., Wang, Y., Gan, Y., Yu, K., Deng, Y., Fendorf, S. (2019). "Experimental constraints on redox-induced arsenic release and retention from aquifer sediments in the central Yangtze River Basin." *Science of the Total Environment,* 649, 629-639.

Evans, J. P., Oaks, R. Q. (1996). "Three-dimensional variations in extensional fault shape and basin form: The Cache Valley basin, eastern Basin and Range province, United States." *GSA Bulletin*, 12(108), 1580-1593.

Fendorf, S., Michael, H. A., Geen, A. Van, Fendorf, S., Michael, H. A., and Geen, A. Van. (2010). "Spatial and Temporal Variations of Groundwater Arsenic in South and Southeast Asia." *Science*, 328(5982), 1123–1127.

Frank, P., Clifford, D. (1986). "Arsenic(III) oxidation and removal from drinking water." *U.S. Environmental Protection Agency Report.* EPA-600-52-86/021.

Goldberg, S. (2002). "Competitive Adsorption of Arsenate and Arsenite on Oxides and Clay Minerals." *Soil Science Society of America Journal*, 66(2), 413.

González, V., García, I., Del Moral, F., and Simón, M. (2012). "Effectiveness of amendments on the spread and phytotoxicity of contaminants in metal–arsenic polluted soil." *Journal of Hazardous Materials*, 205, 72–80.

Guo, X.J., Fujino, Y., Kaneko, S., Wu, K.G., Xia, Y.J., Yoshimura, T. (2001). "Arsenic contamination of groundwater and prevalence of arsenical dermatosis in the Hetao plain area, Inner Mongolia, China." *Molecular and Cellular Biochemistry,* 222(1-2), 137–140.

Guo, H., Wang, Y., Shpeizer, G. M., and Yan, S. (2003). "Natural Occurrence of Arsenic in Shallow Groundwater, Shanyin, Datong Basin, China." *Journal of Environmental Science and Health,* A38(11), 2565-2580.

Guo, H., Zhang, Y., Jia, Y., Zhao, K., Li, Y., Tang, X. (2013). "Dynamic behaviors of water levels and arsenic concentration in shallow groundwater from the Hetao Basin, Inner Mongolia." *Journal of Geochemical Exploration*, 135, 130-140.

Hafeznezami, S., Zimmer-Faust, A. G., Jun, D., Rugh, M. B., Haro, H. L., Park, A., Suh, J., Najm, T., Reynolds, M. D., Davis, J. A., Parhizkar, T., and Jay, J. A. (2017). "Remediation of groundwater contaminated with arsenic through enhanced natural attenuation: Batch and column studies." *Water Research.* 122, 545-556.

Heron, G., Crouzet, C., Bourg, A. C. M., and Christensent, T. H. (1994). "Speciation of Fe (II) and Fe (III) in Contaminated Aquifer Sediments Using Chemical Extraction Techniques." *Environmental Science & Technology*, 28(9), 1698–1705.

Huang, J.H., Kretzschmar, R. (2010). "Sequential extraction method for speciation of arsenate and arsenite in mineral soils." *Annual Chemistry*, 82, 5534-5540.

Huang, J. H. (2014). "Impact of microorganisms on arsenic biogeochemistry: A review." *Water, Air, and Soil Pollution*, 225(2).

Inkenbrandt, P. C. (2010). "Estimates of the Hydraulic Parameters of Aquifers in Cache Valley, Utah and Idaho." thesis, presented to Utah State University at Logan, UT, in partial fulfillment of the requirements for the Degree of Master of Science in Geology, 760.

Islam, F. S., Gault, A. G., Boothman, C., Polya, D. A., Charnock, J. M., Chatterjee, D., and Lloyd, J. R. (2004). "Role of metal-reducing bacteria in arsenic release from Bengal delta sediments." *Nature*, 430(6995), 68–71.

Jain, A., Raven, K. P., and Loeppert, R. H. (1999). "Arsenite and arsenate adsorption on ferrihydrite: Surface charge reduction and net OH- release stoichiometry." *Environmental Science and Technology*, 33(8), 1179–1184.

Johnston, S. G., Diwakar, J., and Burton, E. D. (2015). "Arsenic solid-phase speciation in an alluvial aquifer system adjacent to the Himalayan forehills, Nepal." *Chemical Geology*, 419, 55–66.

Keon, N.E., Swartz, C.H., Brabander, D.J., Harvey, C., Hemond, H.F. (2001). "Validation of an arsenic sequential extraction method for evaluating mobility in sediments." *Environmental Science & Technology*, 35, 3396-3396.

Kim, E. J., Yoo, J. C., Baek, K. (2014). "Arsenic speciation and bioaccessibility in arsenic-contaminated soils: Sequential extraction and mineralogical investigation." *Environmental Pollution,* 186, 29-35.

Kim, M. J., Nriagu, J. (2000). "Oxidation of arsenite in groundwater using ozone and oxygen." *Science of The Total Environment,* 247(1), 71-79.

Kim, M. J., Nriagu, J., and Haack, S. (2000). "Carbonate ions and arsenic dissolution by groundwater." *Environmental Science & Technology*, 34(15), 3094–3100.

Klute, A. (1986). Methods of Soil Analysis. Part 1. Physical and Mineralogical Methods. American Society of Agronomy, Inc., Madison, WI.

Kocar, B. D., Polizzotto, M. L., Benner, S. G., Ying, S. C., Ung, M., Ouch, K., Samreth, S., Suy, B., Phan, K., Sampson, M., and Fendorf, S. (2008). "Integrated biogeochemical and hydrologic processes driving arsenic release from shallow sediments to groundwaters of the Mekong delta." *Applied Geochemistry*, 23(11), 3059–3071.

Kottek, M., Grieser, J., Beck, C., Rudolf, B., and Rubel, F. (2006). "World map of the Köppen-Geiger climate classification updated." *Meteorologische Zeitschrift*, 15(3), 259–263.

Koutros, S., Lenz, P., Hewitt, S. M., Kida, M., Jones, M., Schned, A. R., Baris, D., Pfeiffer, R., Schwenn, M., Johnson, A., Karagas, M. R., Garcia-Closas, M., Rothman, N., Moore, L. E., Silverman, D. T. (2018). "RE: Eleveated Bladder Cancer in Northern New England: The Role of Drinking Water and Arsenic." *Journal National Cancer Institute,* 110(11), 45.

Langmuir, D. (1971). "The geochemistry of some carbonate ground waters in central Pennsylvania." *Geochimica et Cosmochimica Acta,* 35, 1023-1045.

Larsen, F., Pham, N. Q., Dang, N. D., Postma, D., Jessen, S., Pham, V. H., Nguyen, T. B., Trieu, H. D., Tran, L. T., Nguyen, H., Chambon, J., Nguyen, H. Van, Ha, D. H., Hue, N. T., Duc, M. T., and Refsgaard, J. C. (2008). "Controlling geological and hydrogeological processes in an arsenic contaminated aquifer on the Red River flood plain, Vietnam." *Applied Geochemistry*, 23(11), 3099–3115.

Lievremont, D., Bertin, P., Lett, M. C. (2009). "Arsenic in contaminated waters: Biogeochemical cycle, microbial metabolism and biotreatment processes". *Biochimie*, 91(2009), 1229-1237.

Lowe, M., Wallace, J., Bishop, C., Hurlow, H., 2003. Ground-water Quality Classification and Recommended Septic Tank Soil-absorption-system Density Maps. Utah Geology Survey, Salt Lake City, UT.

Mackay, A. A., Gan, P., Yu, R., and Smets, B. F. (2014). "Seasonal arsenic accumulation in stream sediments at a groundwater discharge zone." *Environmental Science and Technology*, 48(2), 920–929.

Malasarn, D., Saltikov C. W., Campbell K. M., Santini J. M., Hering J. G., and Newman D. K. (2004). "arrA is a reliable marker for As(V) respiration." *Science* 306:455.

Mandal, B., and Suzuki, K. (2002). "Arsenic round the world: a review." *Talanta*, 58(1), 201–235.

Manning, B. A., and Goldberg, S. (1996). "Modeling arsenate competitive adsorption on kaolinite, montmorillonite and illite." *Clays and Clay Minerals*, 44(5), 609–623.

Manning, B. A., and Goldberg, S. (1997). "Adsorption and Stability of Arsenic (III) at the Clay Mineral - Water Interface." 31(7), 2005–2011.

Manning, B. A., Fendorf, S. E., Bostick, B., Suarez, D. L. (2002). "Arsenic(III) oxidation and arsenic(V) adsorption reactions on synthetic birnessite." *Environmental Science and Technology,* 36, 5, 976-981.

Mayo, A.L., Loucks, M.D. (1995). "Solute and isotopic geochemistry and ground water flow in the central Wasatch Range, Utah." *Journal of Hydrology* 172, 31-59.

Meng, X. (2015). "Redox-controlled biogeochemical processes affecting arsenic solubility in sediments from a basin-fill aquifer in Northern Utah." https://digitalcommons.usu.edu/etd/4582/.

Meng, X., Dupont, R. R., Sorensen, D. L., Jacobson, A. R., and McLean, J. E. (2016). "Arsenic solubilization and redistribution under anoxic conditions in three aquifer sediments from a basin- fill aquifer in Northern Utah : The role of natural organic carbon and carbonate minerals." *Applied Geochemistry*, Elsevier Ltd, 66, 250–263.

Meng, X., Dupont, R. R., Sorensen, D. L., Jacobson, A. R., and McLean, J. E. (2017). "Mineralogy and geochemistry affecting arsenic solubility in sediment profiles from the shallow basin-fill aquifer of Cache Valley Basin, Utah." *Applied Geochemistry*, Elsevier Ltd, 1–16.

Mirza, B. S., Muruganandam, S., Meng, X., Sorensen, D. L., Dupont, R. R., and McLean, J. E. (2014). "Arsenic(V) reduction in relation to Iron(III) transformation and molecular characterization of the structural and functional microbial community in sediments of a basin-fill aquifer in Northern Utah." *Applied and Environmental Microbiology*, 80(10), 3198–208.

Mirza, B. S., Sorensen, D. L., Dupont, R. R., McLean, J. E. (2017). "New arsenate reductase gene (arrA) PCR primers for diversity assessment and quantification in environmental samples." *Applied and Environmental Microbiology*, 83(4), e02725-16.

Morse, J. W., and Arvidson, R. S. (2002). "The dissolution kinetics of major sedimentary carbonate minerals." *Earth-Science Reviews*, 58(1-2), 51–84.

Ng, J., Wang, J., Shraim A. (2003). "Review: A global health problem caused by arsenic from natural sources." *Chemosphere,* 53(2003), 1353-1359.

Nordstrom, D. K. (2002). "Worldwide Occurrences of Arsenic in Ground Water." *Science, New Series*, 296(5576), 2143–2145.

O'Day, P. A. (2006). "Chemistry and mineralogy of arsenic." *Elements*, 2(2), 77–83.

Ohtsuka, T., Yamaguchi, N., Makino, T., Sakurai, K., Kimura, K., Kudo, K., Homma, E., Dong, D.T., Amachi, S. (2013). "Arsenic dissolution from Japanese paddy soil by a dissimilatory arsenate-reducing bacterium Geobacter sp. OR-1." *Environmental Science & Technology.* 47, 6263-6271

Oremland, R. S., and Stolz, J. F. (2003). "The Ecology of Arsenic." *Science*, 300(5621), 939–944.

Oremland, R. S., and Stolz, J. F. (2005). "Arsenic, microbes and contaminated aquifers." *Trends in microbiology*, 13(2), 45–9.

Palmer, N. E., and von Wandruszka, R. (2010). "Humic acids as reducing agents: the involvement of quinoid moieties in arsenate reduction." *Environmental Science and Pollution Research,* 17, 1362-1370.

Pantuzzo, F. L., Ciminelli, V. S. T. (2010). "Arsenic association and stability in long-term disposed arsenic residues." *Water Research,* 44(19), 5631-5640.

Perez, J. P. H., Freeman, H. M., Schuessler, J. A., Benning, L. G. (2019). "The interfacial reactivity of arsenic species with green rust sulfate (GR_{SO4})." *Science of the Total Environment,* 648, 1161-1170.

Polizzotto, M.L., Harvey, C.F., Sutton, S.R., Fendorf, S. (2005). "Processes conducive to the release and transport of arsenic into aquifers of Bangladesh." *Proc. Natl. Acad. Sci.* 102(52), 18819-23.

Polizzotto, M.L., Harvey, C.F., Li, G.C., Badruzzman, B., Ali, A., Newville, M., Sutton, S., Fendorf, S. (2006). "Solid-phases and desorption processes of arsenic within Bangladesh sediments." *Chemical Geology*, 228, 97-111.

R Foundation for Statistical Computing (RFSC). (2014). *R-Studio*. www.rstudio.com

Renard, F., Putnis, C. V., Montes-Hernandez, G., Ruiz-Agudo, E., Hovelmann, J., Sarret, G. (2015). "Interactions of arsenic with calcite surfaces revealed by in situ nanoscale imaging." *Geochimica et Cosmochimica Acta,* 159, 61-79.

Roman-Ross, G., Cuello, G. J., Turrillas, X., Fernández-Martínez, A., and Charlet, L. (2006). "Arsenite sorption and co-precipitation with calcite." *Chemical Geology*, 233(3-4), 328–336.

Rowland, H.A.L., Gault, A.G., Lythgoe, P., Polya, D.A. (2008). "Geochemistry of aquifer sediments and arsenic-rich groundwaters from Kandal Province, Cambodia." *Applied Geochemistry*, 23, 3029-3046.

SAS Institute Inc. (2008). JMP® 8.0. <www.jmp.com.>

Schaefer, M.V., Ying, S.C., Benner, S.G., Duan, Y., Wang, Y., and Fendorf, S. (2016). "Aquifer Arsenic Cycling Induced by Seasonal Hydrologic Changes within the Yangtze River Basin." *Environmental Science and Technology*, 50(7), 3521–3529.

Schaefer, M.V., Guo, X., Gan, Y., Benner, S.G., Griffin, A.M., Gorski, C.A., Wang, Y., Fendorf, S. (2017). "Redox controls on arsenic enrichment and release from aquifer sediments in central Yangtze River Basin." *Science Direct,* 204, 104-119.

Seddique, A.A., Masuda, H., Mitamura, M., Shinoda, K., Yamanaka, T., Nakaya, S., Ahmed, K.M. (2011). "Mineralogy and geochemistry of shallow sediments of Sonargaon, Bangladesh and implications for arsenic dynamics: focusing on the role of organic matter." *Applied Geochemistry*, 26, 587-599.

Sharma, V., Sohn, M. (2009). "Aquatic arsenic: Toxicity, speciation, transformations, and remediation." *Environment International,* 35(2009), 743-759.

Simon, M., Gonzalez, V., de Haro, S., and Garcia, I. (2014). "Are soil amendments able to restore arsenic-contaminated alkaline soils?" *Journal of Soils and Sediments*, 117–125.

Smedley, P., and Kinniburgh, D. (2002). "A review of the source, behaviour and distribution of arsenic in natural waters." *Applied Geochemistry*, 17(5), 517–568.

Smith, A., Lopipero P., Bates M., Steinmaus C. (2002). "Arsenic Epidemiology and Drinking Water Standards." *Science*, 296(5576), 2145-2146.

Smith, K. A. (1997). "Stratigraphy, Geochronology, and Tectonics of the Salt Lake Formation (Tertiary) of Southern Cache Valley, Utah." thesis, presented to Utah State University at Logan, UT, in partial fulfillment of the requirements for the Degree of Master of Science in Geology, 6546.

Smith, S. (2015). "Arsenic release from dechlorination remediation processes of biostimulation and bioaugmentation." thesis, presented to Utah State University at Logan, UT, in partial fulfillment of the requirements for the Degree of Master of Science in Civil and Environmental Engineering, 4438.

So, H. U., Postma, D., Jakobsen, R., and Larsen, F. (2008). "Sorption and desorption of arsenate and arsenite on calcite." *Geochimica et Cosmochimica Acta*, 72(24), 5871–5884.

So, H. U., Postma, D., Jakobsen, R., and Larsen, F. (2012). "Competitive adsorption of arsenate and phosphate onto calcite; experimental results and modeling with CCM and CD-MUSIC." *Geochimica et Cosmochimica Acta*, 93, 1–13.

Sparks, D.L., Soil Science Society of America, American Society of Agronomy (1996). Methods of Soil Analysis. Part 3, Chemical Methods. Soil Science Society of America. American Society of Agronomy, Madison, WI.

Thakur, J. K., Thakur, R. K., Ramanathan, A. L., Kumar, M., and Singh, S. K. (2011). "Arsenic Contamination of Groundwater in Nepal—An Overview." *Water*, 3(2073), 1-20.

Tufano, K.J., Reyes, C., Saltikov, C.W., Fendorf, S. (2008). "Reductive processes controlling arsenic retention: revealing the relative importance of iron and arsenic reduction." *Environmental Science & Technology.* 42, 8283-8289.

UPR. (2013). "Cache canal projects near completion." < http://www.upr.org/post/cache-canal-projects-near-completion>. (November 7, 2018).

USCD. (2019). U.S. Climate Data. Climate Logan-Utah. <https://www.usclimatedata.com/climate/logan/utah/united-states/usut0147>. (January 7, 2019)

USEPA. (2017). "Drinking Water Requirements for States and Public Water Systems: Drinking Water Arsenic Rule History." <https://www.epa.gov/dwreginfo/drinking-water-arsenic-rule-history>. (February 22, 2018).

USGS. (2018). PHREEQC Welcome Page. <https://wwwbrr.cr.usgs.gov/projects/GWC_coupled/phreeqc/> (December 5, 2018).

Wang, G.Q., Huang, Y.Z., Gang, J.M., Wang, S.Z., Xiao, B.Y., Yao, H., Hu, Y., Gu, Y.L., Zhang, C., Liu, K.T. (2000). "Endemic arsenism, fluorosis and arsenic-fluoride poisoning caused by drinking water in Kuitun, Xinjiang." *Chinese Medical Journal,* 113(6), 524–524.

Wang, Z., Guo, H., Xiu, W., Wang, J., Shen, M. (2018). "High arsenic groundwater in the Guide basin, northwestern China: Distribution and genesis mechanisms." *Science of the Total Environment,* 640-641(2018), 194-206.

Wenzel, W. W., Kirchbaumer, N., Prohaska, T., Stingeder, G., Lombi, E., Adriano, D. (2001). "Arsenic fractionation in soils using an improved sequential extraction procedure." *Analytica Chimica Acta,* 436(2), 309-323.

Wilkie, J. A., and Hering, J. G. (1998). "Rapid Oxidation of Geothermal Arsenic (III) in Streamwaters of the Eastern Sierra Nevada." *Environmental Science and Technology*, 32(5), 657–662.

Winkel, L. H. E., Casentini, B., Bardelli, F., Voegelin, A., Nikolaidis, N. P., Charlet, L. (2013). "Speciation of arsenic in Greek travertines: Co-precipitation of arsenate with calcite." *SciVerse Science Direct,* 106, 99-110.

WU. (2019). Weather Underground. Logan-Cache, UT Station. <https://www.wunderground.com/history/daily/KLGU/date/2016-8-18?dayend=18&monthend=11&yearend=2016&req_city=&req_state=&req_statename=&reqdb.zip=&reqdb.magic=&reqdb.wmo=>. (January 7, 2019)

Waychunas, G. A., Rea, B. A., Fuller, C. C., Davis, J. A., (1993). "Surface chemistry o ferrihydrite: Part 1. EXAFS studies of the geometry of coprecipitated and adsorbed arsenate. *Geochimica et Cosmochimica Acta,* 57, 2251-2269.

Xiao, Z., Xie, X., Pi, K., Yan, Y., Li, J., Chi, Z., Qian, K., Wang, Y. (2018). "Effects of irrigation-induced water table fluctuation on arsenic mobilization in the unsaturated zone of the Datong Basin, northern China." *Journal of Hydrology,* 564(2018) 256-265.

Xie, X., Wang, Y., Li, J., Yu, Q., Wu, Y., Su, C., Duan, M. (2015). "Effect of irrigation on Fe(III)-SO_4^{2-} redox cycling and arsenic mobilization in shallow groundwater from the Datong basin, China: Evidence from hydrochemical monitoring and modeling." *Journal of Hydrology,* 523(2015), 128-138

Yokoyama, Y., Mitsunobu, S., Tanaka, K., Itai, T., Takahashi, Y. (2009). "A study on the coprecipitation of arenite and arsenate into calcite coupled with the determination of oxidation states of arsenic both in calcite and water." *Chemistry Letters,* 38(9) 910-911.

Yokoyama, Y., Iwatsuki, T., Terada, Y., Takahashi, Y. (2012). "Speciation of As in calcite by micro-XAFS: Implications for remediation of As contamination in groundwater." *Journal of Physics: Conference Series,* 430, 012099

Zhang, Y., Xu, B., Guo Z., Han, J., Li, H., Jin, L. Chen, F., Xiong, Y. (2019). "Human health risk assessment of groundwater arsenic contamination in Jinghui irrigation district, China." *Journal of Environmental Management,* 237(2019), 163-169.

Zhou, Y., Guo, H., Zhang, Z., Lu, H., Jia, Y., Cao, Y. (2018). "Characteristics and implications of stable carbon isotope in high arsenic groundwater systems in the northwest Hetao Basin, Inner Mongolia, China." *Journal of Asian Earth Sciences,* 163(2018), 70-79.

APPENDICES

APPENDIX A: FIELD DATA

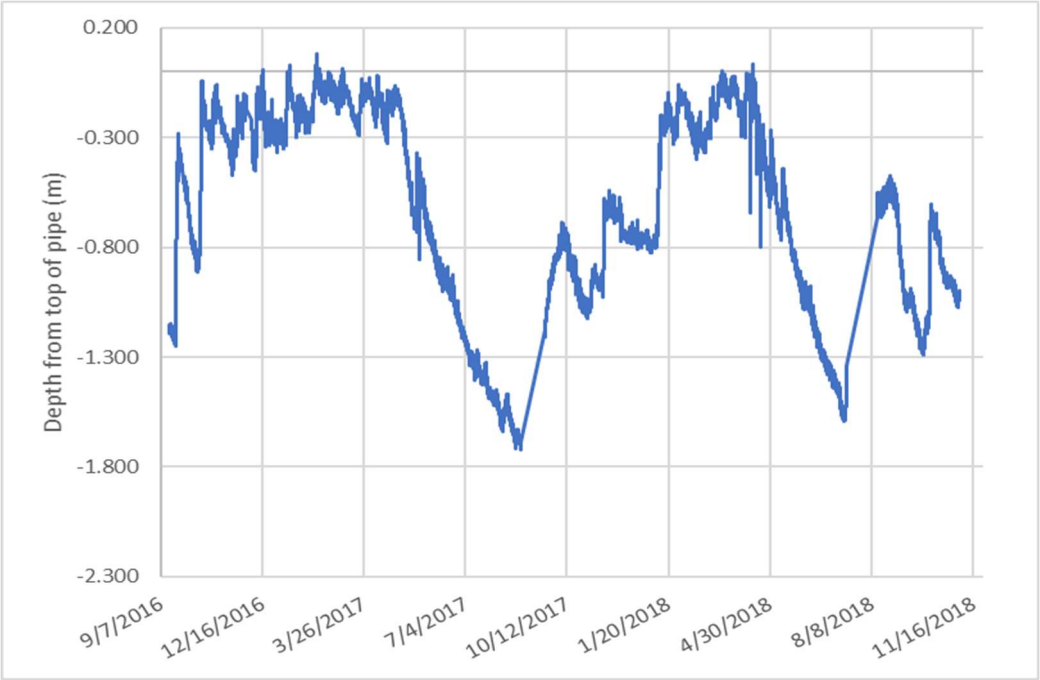

Fig. A-1. HOBO U20 Water Level Logger data in P-2. Logger data were corrected using average daily atmospheric pressure and any data recorded when the logger was outside of the well have been removed.

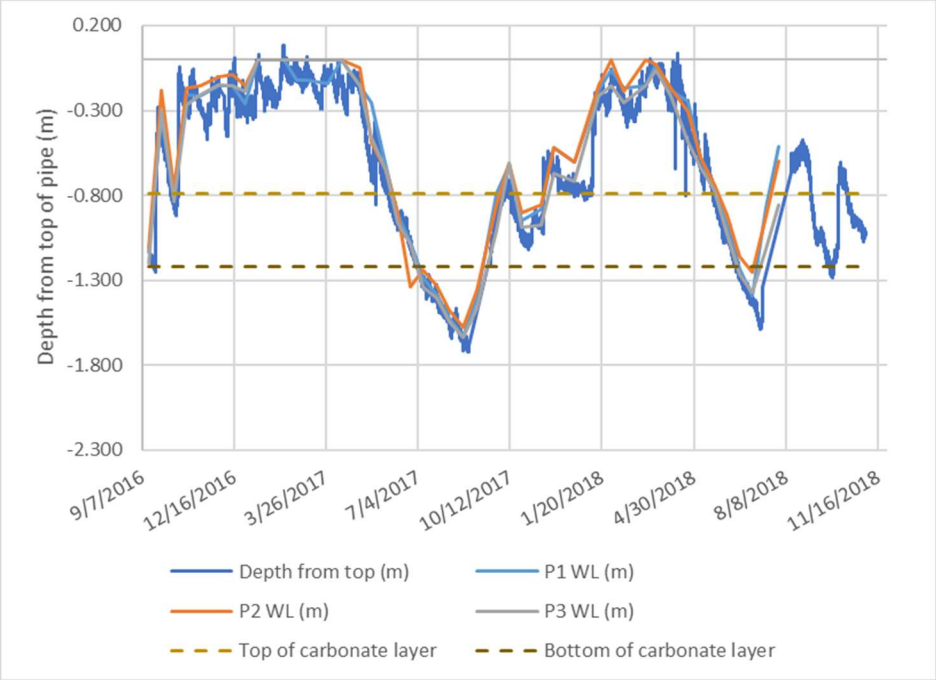

Fig. A-2. HOBO U20 Water Level Logger data in P-2 compared to field-collected water level data in all three wells. Logger data was corrected using average daily atmospheric pressure and any data recorded when the logger was outside of the well has been removed.

Table A-1. Summary of mean concentration and one-way ANOVA by year and by season and year for As(III) and As. Levels not connected by same letter in years are significantly different by student's t-test (α=0.05). Levels not connected by same letter in seasons are significantly different by Tukey's Honestly Significant Difference (α=0.05)

	As(III) (µg/L)	As (µg/L)
Year 1 (Wet)	8.4 b	28.5 b
Year 2 (Dry)	11.5 a	36.7 a
Year 1, Autumn	17.8 a	36.4 a
Year 1, Winter	3.5 b,c	25.0 b
Year 1, Spring	2.3 c	24.7 b
Year 1, Summer	5.1 b	25.3 b
Year 2, Autumn	13.2 a	32.6 a
Year 2, Winter	12.8 a	39.9 a
Year 2, Spring	11.4 a	40.5 a
Year 2, Summer	8.7 a	34.4 a

Table A-2. Summary of mean concentration and one-way ANOVA by Well/Season for redox parameters. Levels not connected by same letter are significantly different by Tukey's Honestly Significant Difference (α=0.05)

	DO (mg/L)	Eh (mV)	DOC (mg/L)	Sulfides (µg/L)	Mn (µg/L)	Fe(II) (mg/L)
P-1	1.84 a,b	208.7 a	4.5 b	7.4 b	73.7 b	0.05 b
P-2	1.67 b	43.5 c	7.9 a	38.8 a	175.8 a	0.21 a
P-3	1.84 a	133.3 b	3.2 c	6.4 c	63.6 c	0.03 c
Year 1, Autumn	3.2 a	147.7 b	4.8 b,c	12.2 c,d	117.3 a	0.04 d
Year 1, Winter	3.2 a	235.9 a	8.1 a	6.9 d	42.6 b	0.04 c,d
Year 1, Spring	2.8 a	175.1 a,b	6.0 a,b	24.9 a,b,c	69.7 b	0.11 b,c
Year 1, Summer	0.5 c	-25.6 d	3.3 c	28.9 a,b	220.5 a	0.17 a
Year 2, Autumn	1.3 b	76.3 c	3.1 c	18.3 b,c,d	152.8 a	0.09 a,b
Year 2, Winter	1.5 b	107.6 b,c	6.7 a,b	8.5 d	84.9 b	0.13 b,c
Year 2, Spring	0.1 d	225.9 a	6.1 a,b	8.0 d	52.5 b	0.08 b,c
Year 2, Summer	0.6 c	43.4 c,d	4.4 b,c	31.9 a	130.6 a	0.13 a,b

Table A-3. Summary of mean concentration and one-way ANOVA by Well/Season for redox parameters. Levels for each parameter not connected by same letter are significantly different by Tukey's Honestly Significant Difference (α=0.05)

	Fe(II) (mg/L)	Sulfate (mg/L)	Nitrite (mg/L)	Nitrate (mg/L)
P-1	0.03 b	42.9 a	0.22 a	0.13 a
P-2	0.14 a	23.1 b	0.23 a	0.13 a
P-3	0.02 b	36.1 a	0.18 a	0.28 a
Year 1, Autumn	0.05 b	39.4 b	ND	0.27 a
Year 1, Winter	0.08 a,b	32.4 b,c	0.26 a	0.33 a
Year 1, Spring	0.13 a	30.8 b,c	0.14 a	0.18 a
Year 1, Summer	0.05 a	27.9 b,c	0.14 a	0.31 a
Year 2, Autumn	0.04 b	26.2 c	0.06 a	0.01 a
Year 2, Winter	0.04 b	33.0 b,c	0.03 a	0.09 a
Year 2, Spring	0.01 b	54.3 a	0.00 a	0.05 a
Year 2, Summer	0.04 b	27.3 b,c	0.18 a	0.16 a

Table A-4. Summary of mean concentrations and one-way ANOVA by Well/Season for dissolution parameters. Levels not connected by same letter are significantly different by Tukey's Honestly Significant Difference (α=0.05)

	HCO_3 (mg/L)	Mg (mg/L)	PO_4^{3-} (µg/L)	Ca (mg/L)
P-1	683.1 b	118.3 a	148.2 b	32.5 b
P-2	628.6 c	93.3 b	194.6 a	34.8 a
P-3	716.9 a	127.5 a	128.0 c	31.5 b
Year 1, Autumn	683.4 b	121.3 a,b	140.6 b	32.8 c
Year 1, Winter	685.0 b,c,d	94.3 c	198.3 a	33.2 b,c
Year 1, Spring	699.1 a,b	102.4 b,c	179.9 a	36.4 a
Year 1, Summer	733.3 a	123.2 a	175.9 a	35.8 a,b
Year 2, Autumn	684.5 b	118.2 a	167.3 a	33.3 b,c
Year 2, Winter	634.8 c,d	107.2 a,b	119.3 b	28.4 d
Year 2, Spring	636.8 c	115.7 a,b	136.4 b	32.1 c
Year 2, Summer	675.7 b,d	114.3 a,b	165.8 a	32.0 c

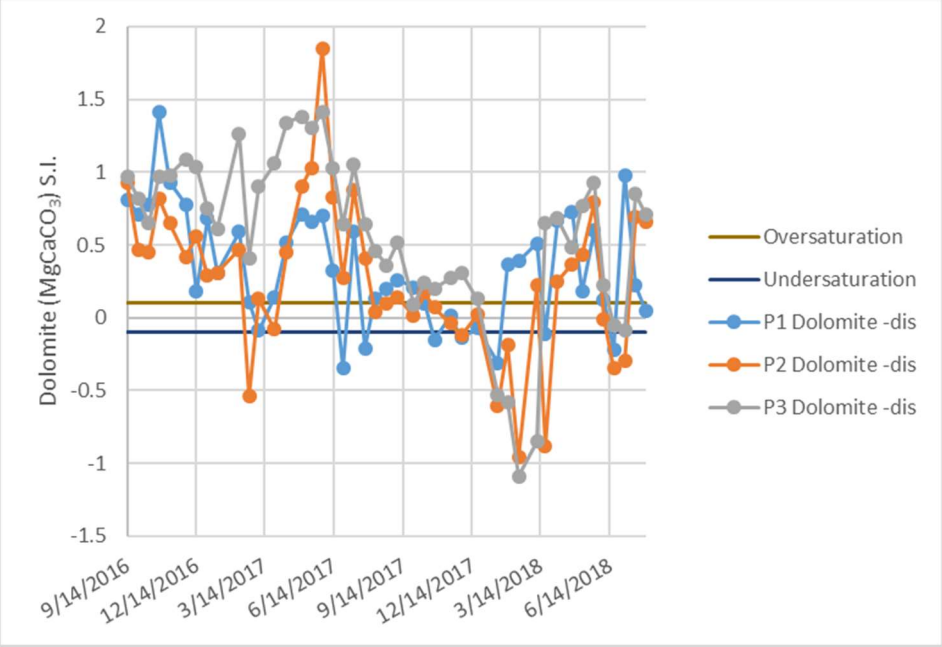

Fig. A-3. PHREEQC modeled $MgCaCO_3$ (dolomite). Equilibrium was considered to be at a model generated Saturation Index value of 0 with an error of ±0.1 represented by horizontal lines (Langmuir 1971).

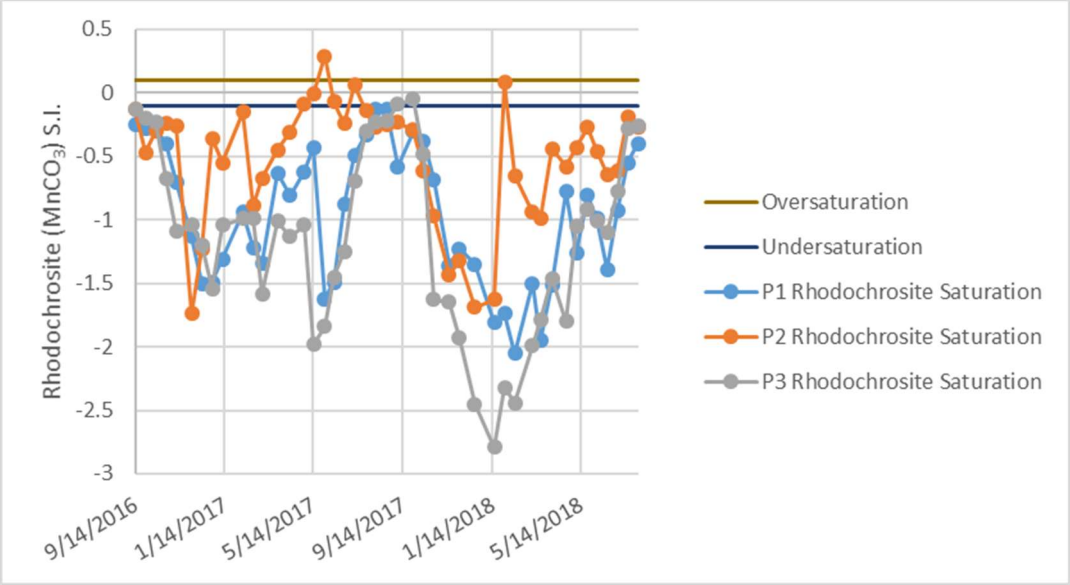

Fig. A-4. PHREEQC modeled $MnCO_3$ (Rhodochrosite). Equilibrium for carbonate and As species was considered to be at a model generated Saturation Index value of 0 with an error of ±0.1 represented by horizontal lines (Langmuir 1971).

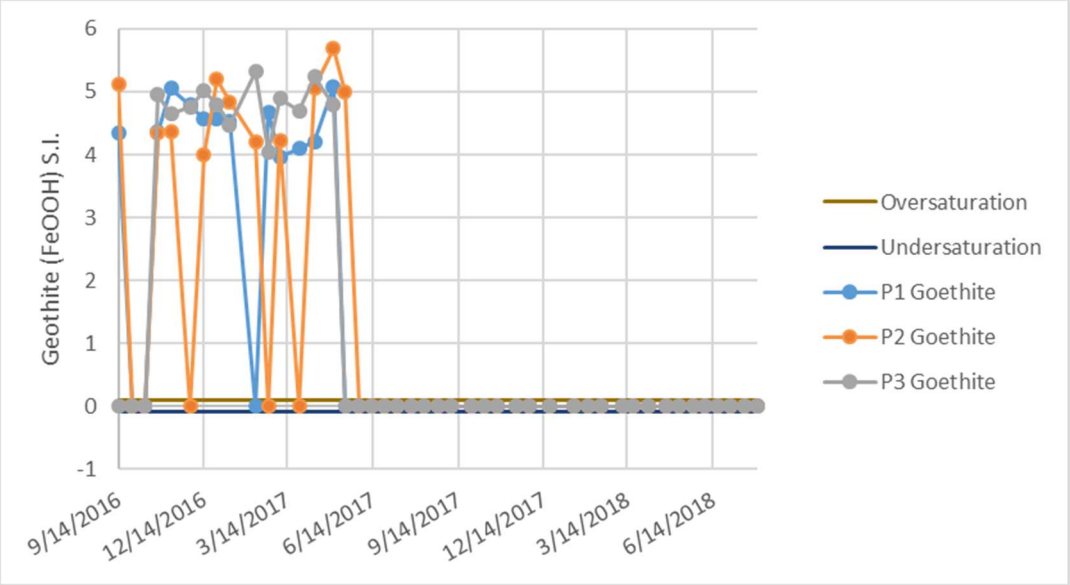

Fig. A-5. PHREEQC modeled FeOOH (Geothite). Equilibrium for carbonate and As species was considered to be at a model generated Saturation Index value of 0 with an error of ±0.1 represented by horizontal lines (Langmuir 1971). Model predicted S.I. value of 0 after June of 2017.

Table A-5. PCA eigenvalues, percentages, and eigenvectors for all field data collected

Principal Components: on Correlations

Number	Eigenvalue	Percent	Percent	Cum Percent
1	5.9509	28.338		28.338
2	4.6731	22.253		50.591
3	2.5078	11.942		62.533
4	1.4604	6.954		69.487
5	1.1773	5.606		75.094
6	0.9958	4.742		79.835
7	0.7957	3.789		83.624
8	0.6793	3.235		86.859
9	0.5333	2.539		89.398
10	0.3848	1.832		91.231
11	0.3054	1.454		92.685
12	0.2959	1.409		94.094
13	0.2887	1.375		95.469
14	0.2139	1.019		96.488
15	0.1975	0.940		97.428
16	0.1592	0.758		98.186
17	0.1197	0.570		98.756
18	0.0997	0.475		99.231
19	0.0752	0.358		99.589
20	0.0582	0.277		99.866
21	0.0281	0.134		100.000

Eigenvectors

	Prin. 1	Prin. 2	Prin. 3	Prin. 4	Prin. 5
WL (ft)	0.01504	0.38872	0.05129	0.00681	0.21414
pH	0.00054	0.25351	0.26851	-0.30087	0.13177
EC (uS/cm)	0.32517	0.00205	0.22038	0.18846	-0.04241
DO (mg/L)	0.00718	0.25670	0.19581	-0.30415	0.44074
Temp C	0.01184	-0.38850	0.06505	0.02577	-0.22931
Eh (mV)	0.16378	0.32945	-0.20277	-0.09974	-0.02733
Sulfides (ug/L)	-0.25940	-0.14826	0.24506	0.14594	-0.13638
Fe (ug/L)	-0.23380	-0.10652	0.37922	-0.00566	0.09418
HCO3 (mg/L)	0.23534	-0.19394	0.24865	-0.24784	-0.05251
Phosphate (µg/L)	-0.32113	0.03312	0.09917	0.09793	-0.10595
DOC (mg/L)	-0.25191	0.25463	0.04598	0.27398	0.01149
Chloride (mg/L)	0.31990	0.05571	0.22071	0.31477	-0.11648
Sulfate (mg/L)	0.26594	0.12942	0.19750	0.44819	0.00262
Nitrate (mg/L)	0.02369	0.03538	0.04129	-0.19761	-0.15882
As(III) (µg/L)	0.02928	-0.16990	-0.14947	0.32881	0.64334
As (µg/L)	0.35157	0.03345	-0.21211	0.06090	0.00956
Na (mg/L)	0.10385	0.23696	0.40223	0.18150	-0.09640
K (mg/L)	0.25740	-0.28142	-0.00205	-0.17510	0.20443
Ca (mg/L)	-0.01221	-0.11783	0.42804	-0.20041	0.09684
Mn (µg/L)	-0.17126	-0.29453	0.08219	0.19270	0.35916
Mg (mg/L)	0.34424	-0.18796	0.08278	-0.10792	0.05984

APPENDIX B: COLUMN STUDY DATA

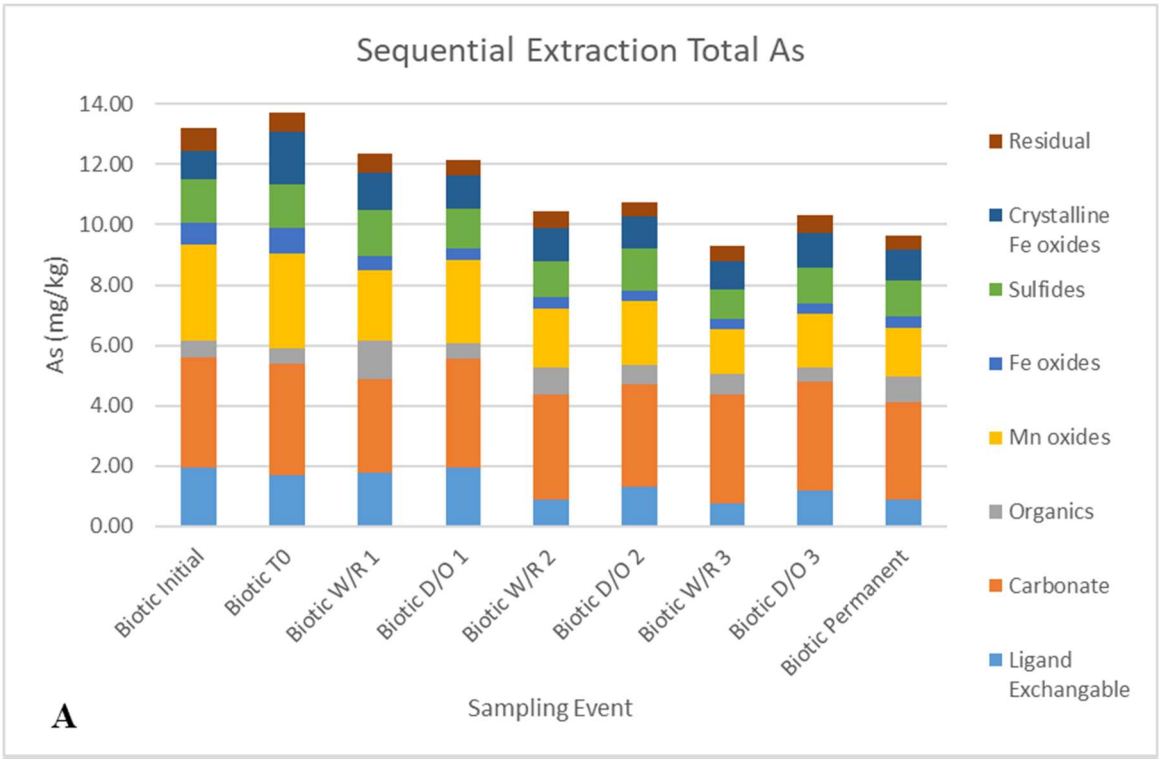
Sequential Extraction Total As
14.00
12.00
10.00
8.00
6.00
4.00
2.00
0.00
As (mg/kg)
Biotic Initial
Biotic T0
Biotic W/R 1
Biotic D/O 1
Biotic W/R 2
Biotic D/O 2
Biotic W/R 3
Biotic D/O 3
Biotic Permanent
Sampling Event
Residual
Crystalline Fe oxides
Sulfides
Fe oxides
Mn oxides
Organics
Carbonate
Ligand Exchangable
A

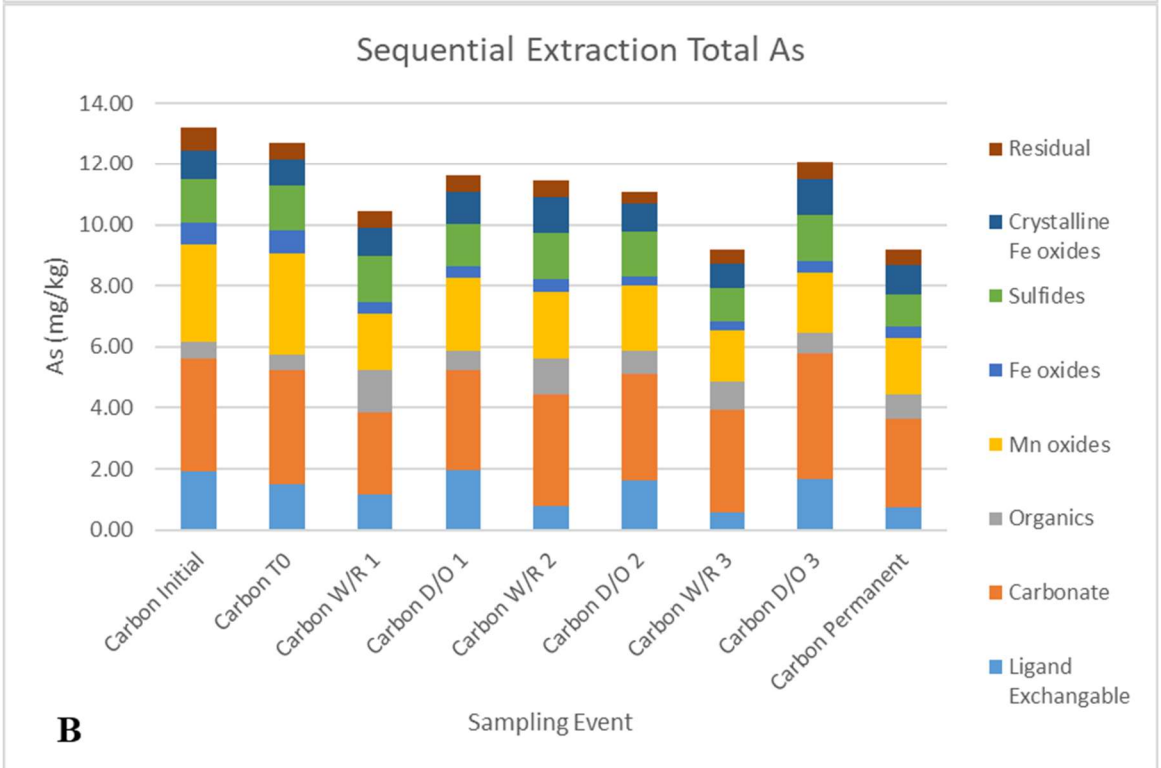
Sequential Extraction Total As
14.00
12.00
10.00
8.00
6.00
4.00
2.00
0.00
As (mg/kg)
Carbon Initial
Carbon T0
Carbon W/R 1
Carbon D/O 1
Carbon W/R 2
Carbon D/O 2
Carbon W/R 3
Carbon D/O 3
Carbon Permanent
Sampling Event
Residual
Crystalline Fe oxides
Sulfides
Fe oxides
Mn oxides
Organics
Carbonate
Ligand Exchangable
B

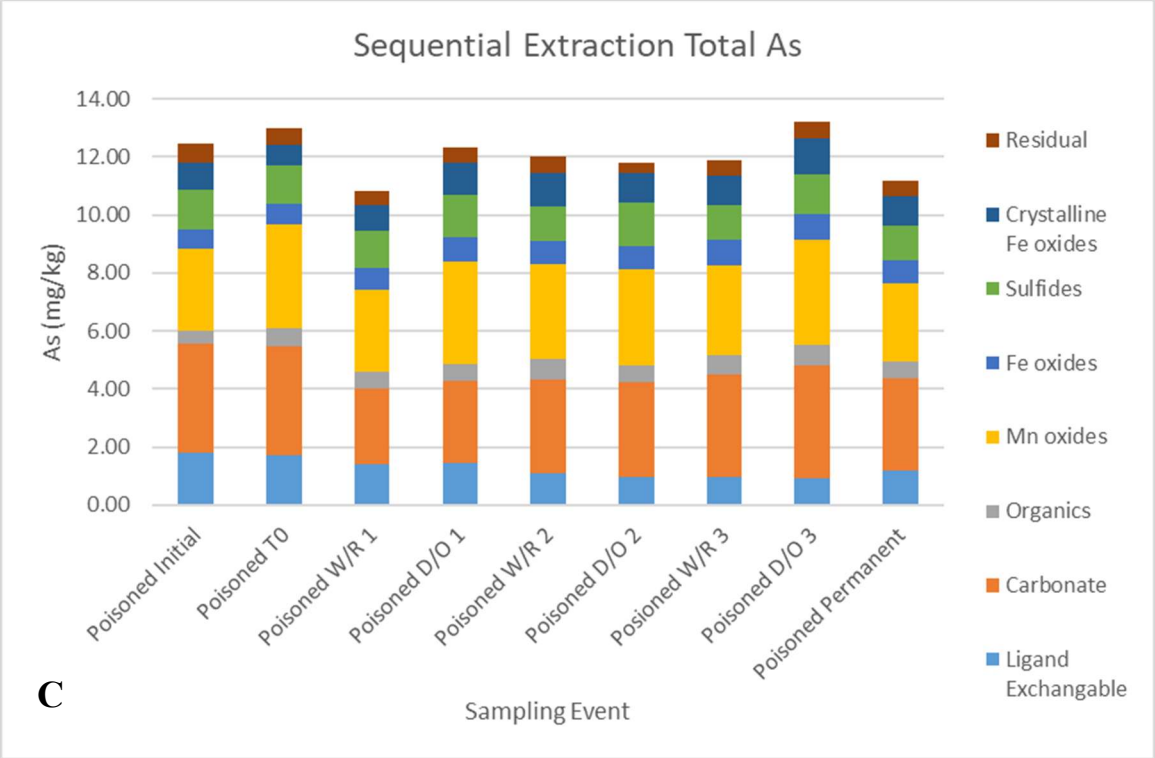

Fig. B-1. Arsenic associated with operationally defined sequential extraction steps for Biotic (A), Carbon-enhanced (B), and Poisoned (C) columns.

Fig. B-2. Carbon-enhanced and poisoned soil columns inundated with groundwater, capped, sealed, and placed in holding containers in anaerobic glovebag.

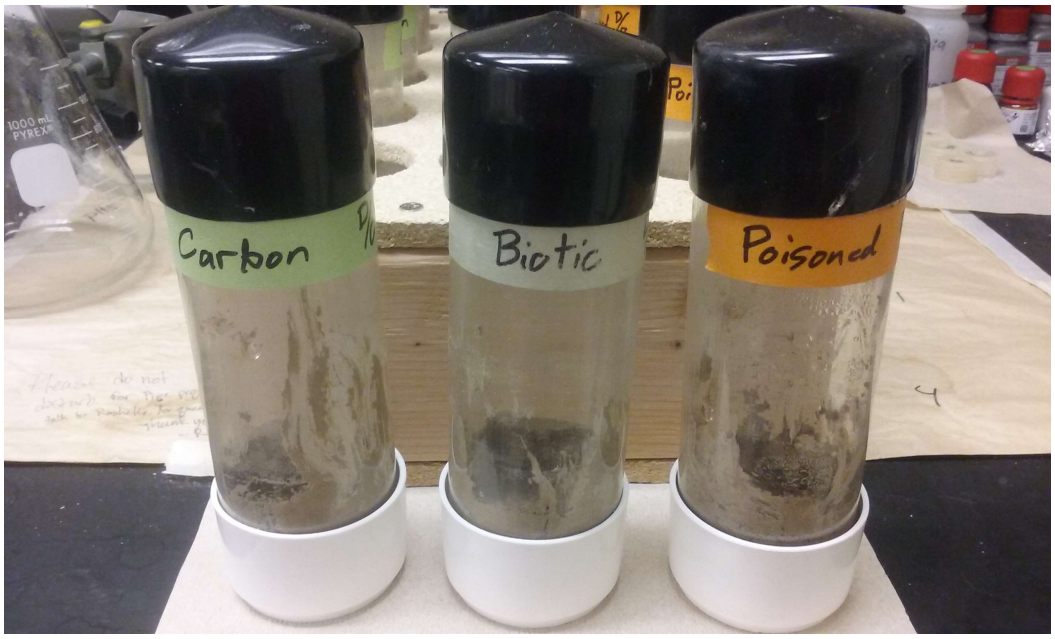

Fig. B-3. Carbon-enhanced, biotic, and poisoned soil columns unsealed, drained, and soil collected for sacrifice.

Fig. B-4. Poisoned and carbon-enhanced soil columns in anaerobic glovebag. Water in poisoned columns remained clear and soil remained light tan in color. Water and soil in carbon-enhanced columns turned dark green in color during first 56 days of column study (first reducing sacrifice).

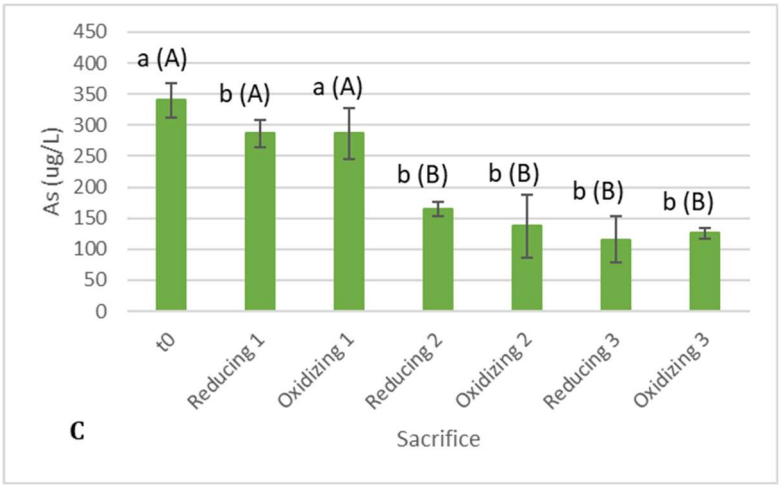

Fig. B-5. Arsenic concentrations in drainage water collected before reducing sacrifices for carbon-enhanced treatments. Error bars represent standard deviation. Values compared using one-way ANOVA. Values not connected by same letter are significantly different (α=0.05) by Tukey's honestly significant difference. Small letters reflect the comparison among treatments within a sampling event. Capital letters reflect the comparison across events within a treatment (Fig 25).

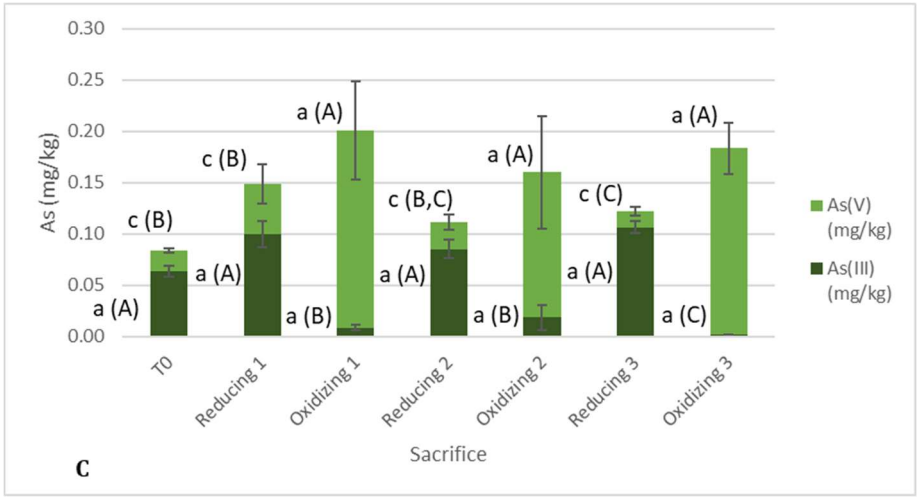

Fig. B-6. Arsenic speciation associated with pore water in carbon-enhanced column treatments. Error bars represent standard deviation. Values compared using one-way ANOVA. Values not connected by same letter are significantly different (α=0.05) by Tukey's honestly significant difference. Small letters reflect the comparison among treatments within a sampling event. Capital letters reflect the comparison across events within a treatment. (Fig. 26).

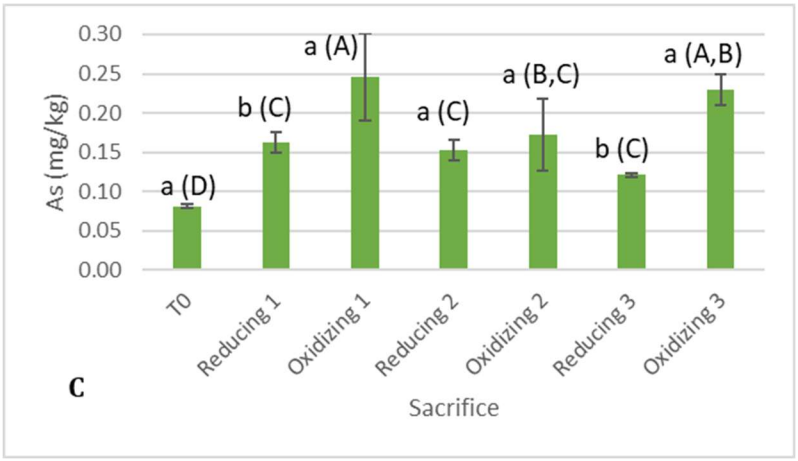

Fig. B-7. Pore water arsenic concentrations for carbon-enhanced treatments. Error bars represent standard deviation. Values compared using one-way ANOVA. Values not connected by same letter are significantly different (α=0.05) by Tukey's honestly significant difference. Small letters reflect the comparison among treatments within a sampling event. Capital letters reflect the comparison across events within a treatment. (Fig. 27).

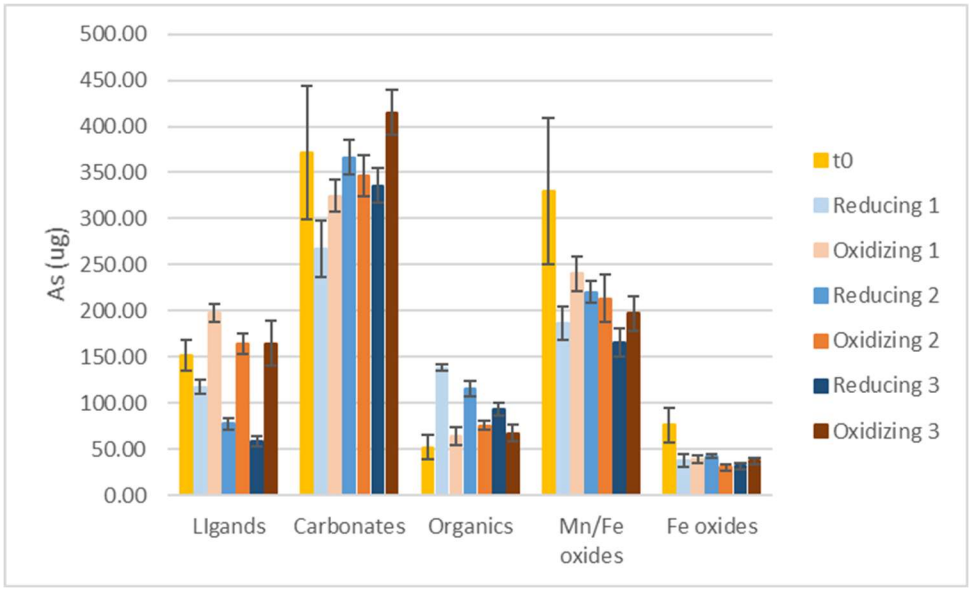

Fig. B-8. Mass of As associated with sequential extraction steps performed on column soil for each sampling event in carbon-enhanced columns. Error bars represent standard deviation

Table B-1. Mass of As associated with sequential extraction steps performed on column soil for each reducing and oxidizing sacrifice in carbon-enhanced columns with statistical analysis. Values were compared using one-way ANOVA. Values not connected by same letter for each sequential step are significantly different by Tukey's HSD.

Sequential Step	t0 (µg)	Reducing 1	Oxidizing 1	Reducing 2	Oxidizing 2	Reducing 3	Oxidizing 3
F1	152 B	117 C	197 A	77 D	164 B	58 D	165 B
F2	371 A,B	268 C	325 B,C	367 A,B	346 B	356 B,C	415 A
F3	52 E	138 A	64 D,E	116 B	76 C,D	93 C	67 D,E
F4	330 A	186 B,C	240 B	220 B,C	214 B,C	165 C	197 B,C
F5	76 A	37 B	39 B	42 B	30 B	31 B	37 B
F6	146 A	148 A	136 A,B	151 A	146 A	110 B	149 A
F7	88 B,C	96 B,C	105 A,B	118 A	95 B,C	80 C	116 A
F8	54 A,B	51 A,B	56 A,B	53 A,B	35 C	44 B,C	62 A

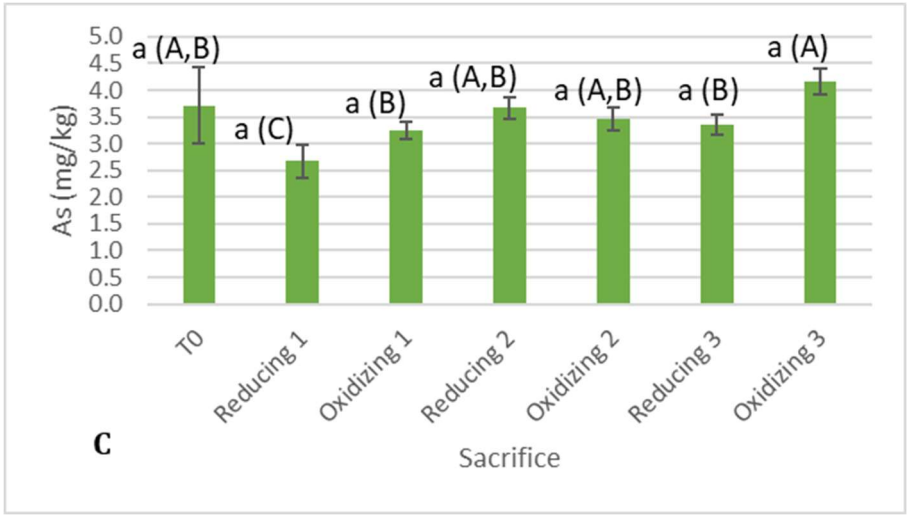

Fig. B-9. Total As concentrations associated with carbonate minerals for carbon-enhanced treatments. Error bars represent standard deviation. Values compared using one-way ANOVA. Values not connected by same letter are significantly different (α=0.05) by Tukey's honestly significant difference. Small letters reflect the comparison among treatments within a sampling event. Capital letters reflect the comparison across events within a treatment. (Fig. 30).

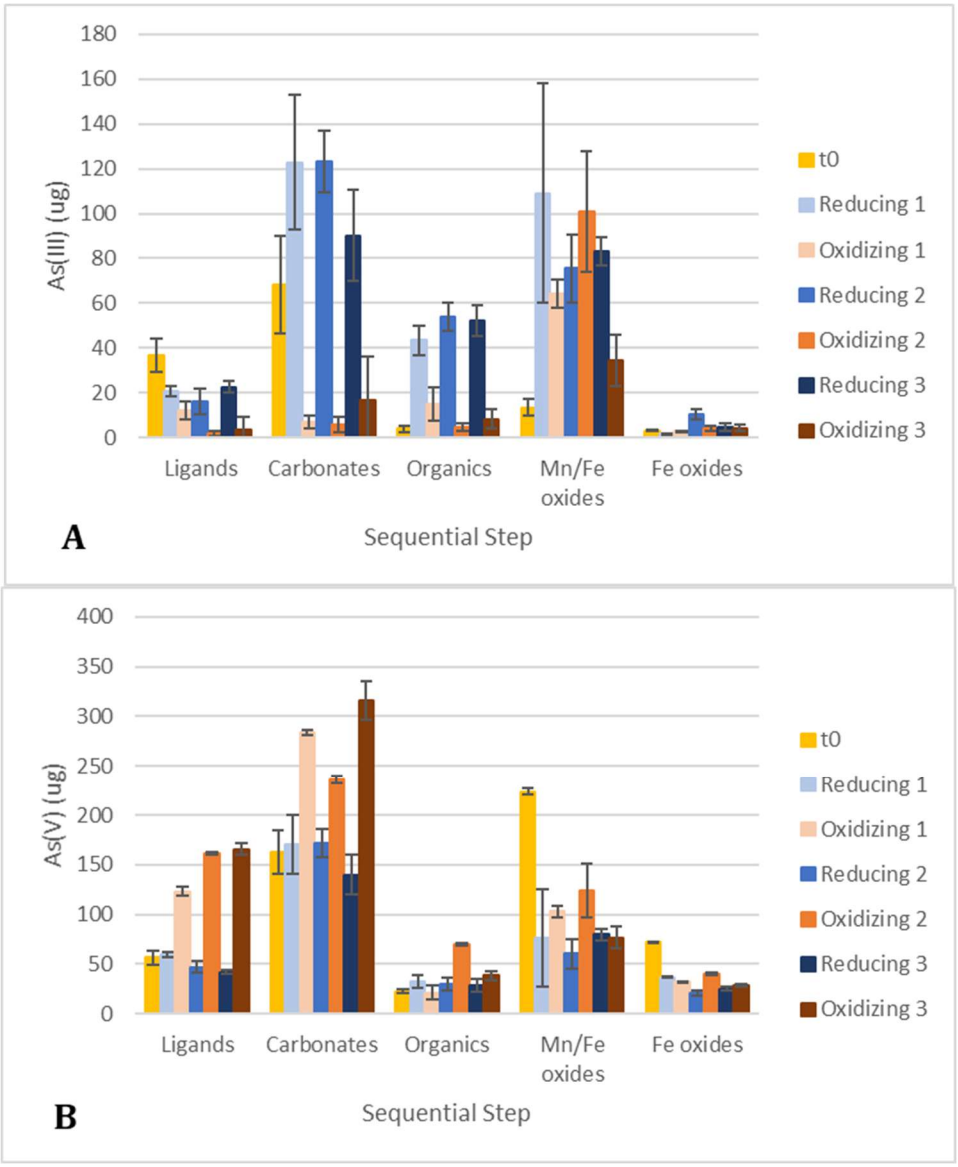

Fig. B-10. Mass of As(III) (A) and As(V) (B) associated with sequential extraction steps performed on column soil for each sacrifice in carbon-enhanced columns. Error bars represent standard deviation

Table B-2. Mass of As(III) and As(V) associated with sequential extraction steps performed on column soil for each sacrifice in carbon-enhanced columns with statistical analysis. Values were compared using one-way ANOVA. Values not connected by same letter for each sequential step are significantly different by Tukey's HSD.

As(III)							
Sequential Step	t0 (µg)	Reducing 1	Oxidizing 1	Reducing 2	Oxidizing 2	Reducing 3	Oxidizing 3
F1	37 A	21 B,C	12 C,D	16 B,C	2 E	23 B	3 D,E
F2	68 B	123 A	7 C	123 A	6 C	90 A,B	17 C
F3	4 C	43 A	15 B	54 A	5 B,C	52 A	8 B,C
F4	13 C	109 A	64 A,B	75 A,B	101 A	34 B,C	34 B,C
F5	3 B,C	2 C	3 B,C	10 A	4 B,C	5 B	4 B,C
F6	7 A	2 B	4 B	3 B	5 A,B	4 B	8 A
F7	5 A	6 A	1 A	1 A	5 A	3 A	5 A
As(V)							
Sequential Step	t0 (µg)	Reducing 1	Oxidizing 1	Reducing 2	Oxidizing 2	Reducing 3	Oxidizing 3
F1	56 C	59 C	123 B	47 C	162 A	42 C	166 A
F2	163 C	170 C	283 A	171 C	236 B	140 C	316 A
F3	23 C	33 B,C	21 C	30 B,C	70 A	29 B,C	38 B
F4	224 A	77 B	103 B	60 B	124 B	80 B	77 B
F5	72 A	37 B,C	32 B,C	21 C	40 B	25 B,C	28 B,C
F6	151 A,B	110 C	134 A,B,C	124 B,C	168 A	141 A,B,C	158 A,B
F7	76 A,B	57 B	61 A,B	72 A,B	92 A	72 A,B	80 A,B

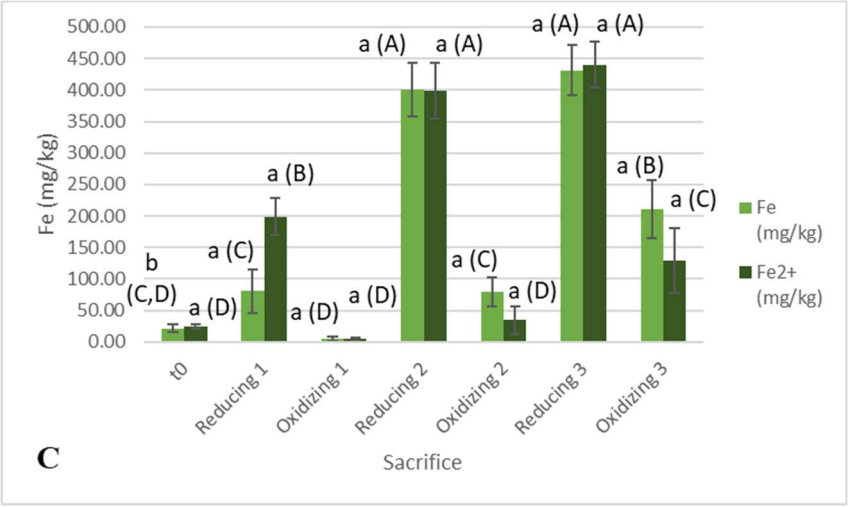

Fig. B-11. Fe concentrations associated with carbonate minerals (F2) in column soil for carbon-enhanced treatments. Error bars represent standard deviation. Values compared using one-way ANOVA. Values not connected by same letter are significantly different (α=0.05) by Tukey's honestly significant difference. Small letters reflect the comparison among treatments within a sampling event. Capital letters reflect the comparison across events within a treatment. (Fig. 34).

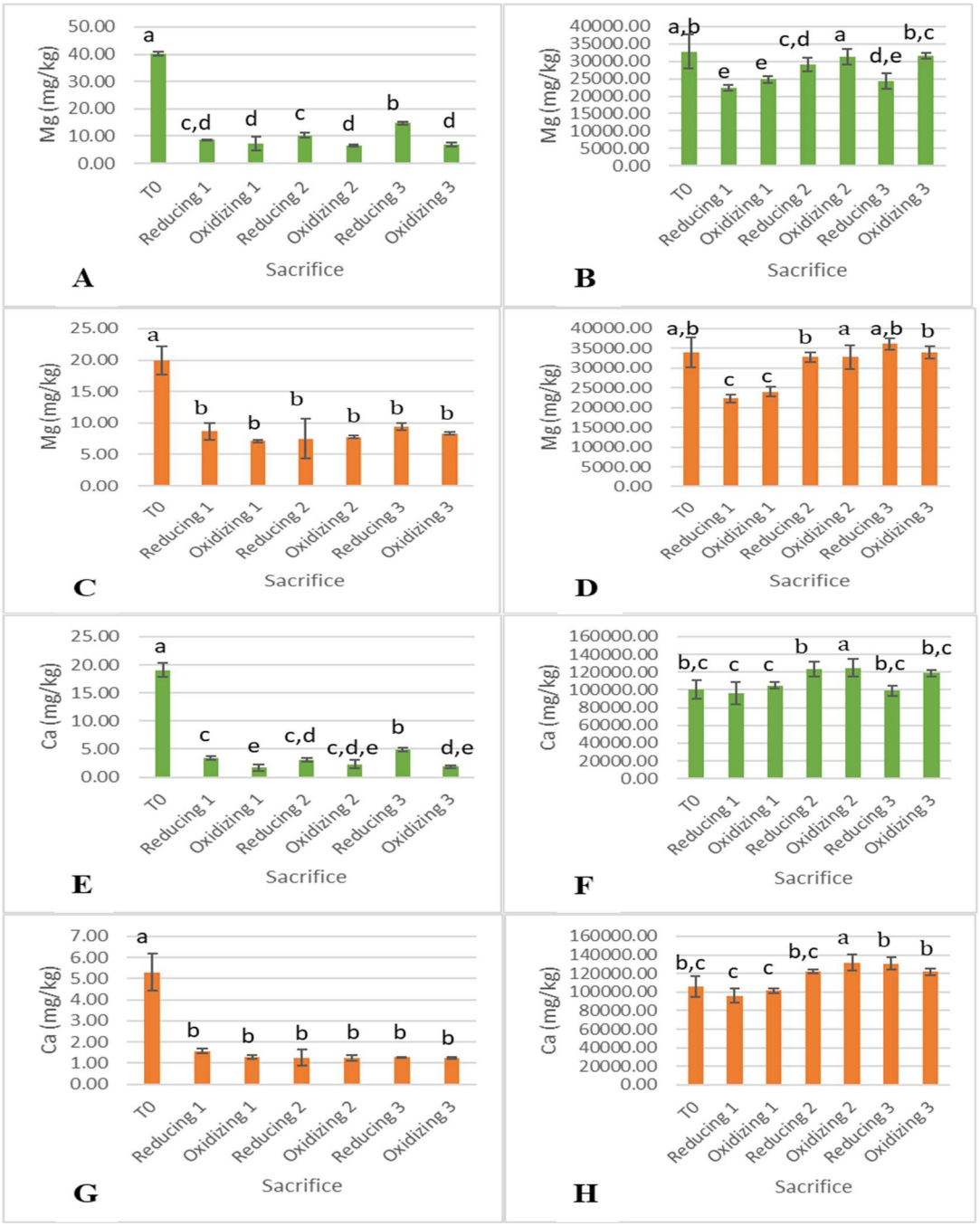

Fig B-12. Concentrations of pore water Mg (A), Mg associated with carbonates (B), pore water Ca (E), and Ca associated with carbonates (F) for carbon-enhanced columns and pore water Mg (C), Mg associated with carbonates (D), pore water Ca (G), and Ca associated with carbonates (H) for poisoned columns. Error bars represent standard deviation. Values compared by one-way ANOVA. Values in each treatment not connected by same letter are significantly different (α=0.05) by Tukey's honestly significant difference.